INFORMATION TO USERS

This manuscript has been reproduced from the microfilm master. UMI films the text directly from the original or copy submitted. Thus, some thesis and dissertation copies are in typewriter face, while others may be from any type of computer printer.

The quality of this reproduction is dependent upon the quality of the copy submitted. Broken or indistinct print, colored or poor quality illustrations and photographs, print bleedthrough, substandard margins, and improper alignment can adversely affect reproduction.

In the unlikely event that the author did not send UMI a complete manuscript and there are missing pages, these will be noted. Also, if unauthorized copyright material had to be removed, a note will indicate the deletion.

Oversize materials (e.g., maps, drawings, charts) are reproduced by sectioning the original, beginning at the upper left-hand corner and continuing from left to right in equal sections with small overlaps.

ProQuest Information and Learning
300 North Zeeb Road, Ann Arbor, MI 48106-1346 USA
800-521-0600

HYDRODYNAMIC BARRIERS FOR EFFECTIVE SITE REMEDIATION

Xiaopeng Zhao

A Thesis

In

Department of Building, Civil and

Environmental Engineering

Presented in Partial Fulfillment of the Requirements

For the Degree of Master of Applied Science at

Concordia University

Montreal, Quebec, Canada

September, 2002

ABSTRACT

Hydrodynamic Barriers for Effective Site Remediation

Xiaopeng Zhao

Conventional pump-and-treat (P&T) is an applicable component of many remedial systems. However, such a system will not be appropriate to achieve restoration in portions of many sites due to hydrogeologic and contaminant-related limitations. This includes the presence of significant accumulation of DNAPLs (denser-than-water nonaqueous phase liquids) trapped below the water table. Here, chemical enhancements to P&T shows some promise by mobilizing or dissolving the contaminants. However, this will make a portion of the injected chemicals and the contaminant to cross the boundary of the targeted site that causes the loss of chemicals and results in pollution migration to uncontaminated areas.

To confine the flow of the injected chemical to the target site, traditionally one sets up physical barriers around the boundaries of the site. In the present study, simple hydrodynamic principles related to image wells are used to provide hydrodynamic barriers around the site. Simple mathematical model and laboratory experiments were developed to assess the effectiveness of hydrodynamic barriers. The study shows that the degree of leakage of the chemicals injected into the target site can be controlled by the proper choice of the system of image wells set outside the target area. For more realistic systems, further study is needed to define its applicability.

Acknowledgements

I would like thank my advisor Dr. A.S.Ramamurthy for suggesting the research topic. I also want to thank Dr. D.Vo. for his interest and the encouragement he offered me.

Thanks will also give to the following:

1. L. Vo. Water resources lab technician. for the assembly of the lab experimental apparatus;
2. Ron Parisella. Environmental Engineering lab instructor. for his guidance with effluent analysis;
3. Rocco Lombardo. BCE technician. for his help on the sand analysis and compaction.

Table of Contents

LIST OF FIGURES

LIST OF TABLES

LIST OF ABBREVIATIONS

(L/D)NAPL	(Light/Dense) Non-Aqueous Phase Liquids
CQA	Construction quality assurance
TCE	Trichloroethylene
DOE	Department of Energy
EPA	Environmental Protection Agency
MOC	Method of characteristics
DSM	Deep soil mixing
VOCs	Volatile organic compounds
ADI	Alternating-direction implicit
SIP	Strongly-implicit procedure
PIC	Particle-in-cell

LIST OF SYMBOLS

K	aquifer transmissivity
L	length of target site
Q	flow of chemical to be used for the target site
R	number of recharge wells set within target area boundary (real sources)
S	storage coefficient(dimensionless)
T	the transmissivity tensor (L^2/t)
V	local groundwater flow velocity
W	width of target site
Φ	potential function
f_i	factor defining sources and sinks in the system (1 for source and –1 for sink)
m	absolute value of source or sink constant
n	number of recharge wells (sources) or extracting wells (sinks) in system
q	source or sink strength
s	groundwater ambient pressure gradient
u	velocity component in x direction
v	velocity component in y direction
x, y	rectangular coordinates of a position
x_i, y_i	rectangular coordinates of well locations in system
α	angle between V and x-axis
Φ	potential function

Ψ	stream function
ε	effective porosity of the aquifer, dimensionless
c	characteristic value
i	defining a well in system
(i, j)	matrix location of grid points
ρ_w	tap water density
ρ_s	salt solution density
d_p	mean particle diameter
ν_w	dynamic viscosity of Water

CHAPTER ONE

Introduction and Objectives

1.1 Introduction

Contaminated soil and groundwater can be remediated by a number of traditional methods. These include the pump and treat schemes, which rely on the aqueous mobilization or dissolution of the sorbed contaminant. This method is ineffective when the contaminant is hydrophobic as in the case of non-aqueous phase liquids (NAPLs). NAPLs have poor solubility (100ppm) and may also sorb well in the soil system. Recent technologies in site remediation include in situ flushing schemes. Here, a suitable surfactant is injected in place of water to free the strongly sorbed NAPLs and bring them to the surface with the help of extraction wells. The use of surfactants overcomes mass transfer limitations imposed by the resistance of hydrophobic compounds to conventional water flushing. Besides the use of surfactants, pump and treat schemes also involve other chemical amendments. These include the use of complexing agents and solvents to mobilize or dissolve the contaminant (Sabatini, et al, 1995 and Palmer and Fish, 1992) and thus assist in the decontamination of soil. Ideally, the existence of an aquitard below the contaminated zone is desirable, as it arrests the vertical movement of the injected chemical and the contaminant, if they are denser than water.

While treating the target site, a portion of the injected chemical and the contaminant may cross the boundary of the site that is being decontaminated. This migration results in the

loss of the injected chemical and also increases the potential for contaminating the zones outside the target site . Unlike hydrodynamic barriers, physical barriers are to be removed after site remediation is completed to restore the natural ground water flow. Physical barriers are expensive to build and dismantle.

The use of physical barriers to contain contaminated groundwater or to control the flow of groundwater has been analyzed in detail in the past (Knox 1983, Gupta 1993). Jandel and Tsang (1987) used hydrodynamic principles to obtain expressions for the boundary of the capture zone (dividing streamline) for a system of one or more extraction wells. Several novel methods to create efficient hydrodynamic isolation systems have been proposed and were found to be effective in the field (Ozbilgin and Powers 1984, Wilson 1984, and Keeley 1984). Gupta (1993) and Bedient et al (1994) provide excellent reviews of many pump and treat scheme models.

In the present study, a simple system of wells outside the target area is set up to act as image wells to the system of injection and extraction wells within the site. The resulting flow pattern provides a hydraulic barrier which confines the movement of the injected chemicals (surfactants) and the dislodged contaminant mostly to regions within the target site. Further, the image wells serve as monitoring wells after the clean-up task is completed.

1.2 Research objectives

To study the effectiveness of a hydraulic barrier enhanced chemical delivery system for improving the efficiency of a chemical enhanced remediation scheme such as the pump and treat or in-situ flushing system. To investigate experiments, two modules were studied for their ability to provide hydraulic barrier system to improve the hydraulic efficiency. To this end, the following procedures were adopted ,

1) Develop a simple mathematical model which can predict the effectiveness of hydraulic barriers using image wells. Analyse the performance of a few typical modular units for application in the pump and treat schemes and describe their characteristics such as the pattern of streamline , pressure distribution and leakage through the site boundary.
2) Develop and test a lab experimental unit to evaluate the effectiveness of the mo hydraulic barriers modules and, to provide a validation for some of the predictions made by the mathematical model.

CHAPTER TWO

Literature Review

As background for this study, this chapter introduces some information of remediation of NAPLS contaminated sites and various physical and hydraulic containment technologies.

2.1 NAPLs and Remediation Schemes

Although widely used for remediation of contaminated aquifers, it has now become obvious that pump and treat technology will not be able to reach the required contaminant concentrations in most aquifers by itself, even after a long operation time. This is quite true that at many sites where NAPLs (dense, non-aqueous phase liquids) was present (Richard,1996).

2.1.1 NAPLs

The awareness of NAPLs dates back over two decades, the pervasiveness of the problem has only recently become evident. The EPA, for example, reported in 1993 that in over 60% of sites where organic contamination has occurred the likely source is NAPLs and that 70% of all superfund sites with groundwater contamination have NAPLS . A majority of these non-superfund sites with a potential NAPL problem are manufacturing facilities, ranging from large multi-million dollar operations to small tool and die shops (Richard, 1996).

This group of groundwater contaminants includes LNAPLs (light non-aqueous phase liquids, comprised of petroleum products such as gasoline and diesel oil) which float on top of the groundwater and make them easier to characterize, map and remediate. DNAPLs also have been called "sinkers" and "toxic blobs", colorful descriptions which capture two of the most prevalent features of these compounds. DNAPLs are "sinkers" because they are heavier than water and sink until they hit an aquitard, a change in soil type or density. As a result, DNAPL movements are directed more by gravity than the flow of groundwater. If the base of the aquifer slopes in one direction, then the DNAPL will flow in the same direction seeking the lowest point. The direction of DNAPL movement may be counter to the groundwater flow, and therefore counter to the focus of traditional groundwater investigation programs.

In addition to DNAPLs and LNAPLs, there also are NNAPLs (neutrally buoyant non-aqueous phase liquids) which can be present at varying depths of the groundwater. As with DNAPLs, the exact characterization of each form of NAPL is determined by a combination of factors that include the compounds, release rates and site characteristics. Although all forms of NAPLs share low solubility points to varying degrees, only DNAPLs are heavier than water, which makes them very difficult to find and to effectively remediate.

2.1.2 Remediation Schemes

Progress has been made in efforts to actually clean up DNAPL contamination. Chemical enhancements to pump and treat and in-situ flushing was among those new cleanup procedures that show a certain promise.

Recognition that conventional pump-and-treat remediation often requires lengthy periods of time to achieve clean-up objectives encouraged professionals involved in site remediation to contemplate alternative methods of aquifer restoration. Some form of chemical enhancement for pump and treat will likely be an alternative considered for many waste-site cleanups. More details of researches in this field can be found in EPA/540/S-92/001 (Carl D. Palmer and William Fish ,1992) and Andre's thesis (Andre, 2001).

In-situ flushing is the injection or infiltration of an aqueous solution into a zone of contaminated soil/groundwater, followed by downgradient extraction of groundwater and elutriate (flushing solution mixed with the contaminants) and above ground treatment and discharge or re-injection. Flushing solutions include plain water sometimes augmented by surfactants, cosolvents, or other facilitators.

In-situ flushing enhances conventional pump and treat schemes through increasing the efficiency of a flushing pore volume, or accelerating natural flushing action. It has advantages that include the potential applicability to a broad range of contaminants and acceleration of site decontamination relative to the conventional pump and treat. Its limitation include the potential for spreading contaminants and consequent limited

regulatory acceptance, site geology setting limitation, and uncertainties involved in prediction of performance and clean up duration (Lauryn, 2000).

In-situ flushing is commonly applied to contaminated sites using surfactants or cosolvents as the primary flushing agents. Surfactants (surface-active-agents) are chemical compounds frequently used in detergents and food products that offer the properties of solution interfaces. Surfactants typically posses a hydrophilic (water loving) group, the "head" of molecule, and a strongly hydropholic (water fearing) group which is the "tail". The hydrophobic portion causes surfactants to exhibit high solubility in water, while the hydrophobic portion prefers to reside in a hydrophobic phase such as LNAPL or DNAPL. This enables surfactants to enhance the solubility of contaminants through miceller solubilization, the process by which aggregations of surfactant monomers form a micelle that the NAPL molecule can occupy(AATDF,1997) . The concentration of the surfactant needed to produce the formation is called the critical micelle concentration (CMC). The addition of a surfactant can also be used to enhance the mobility of the contaminant rather than the solubility by reducing the NAPL-water interfacial tension (AATDF,1997). This reduction results in the decrease of the capillary forces, that are responsible for the retention of residual and the formation of pooled NAPL, which subsequently restricts in contaminant mobility.

2.2 Overview of Subsurface Containment

Although no single remediation technique has yet proven itself to the effective in the treatment of all DNAPL contamination situations, considerable success has been achieved in the containment of the problem. Today, if a site is shown to have a DNAPL

problem, the first thing to do is determine the extent of the problem and then implement measures to contain and reduce the size of the contamination plumes. Often, portions of an aquifer can be restored to clean-up standards, even if the entire aquifer can not be cleaned up. These containment efforts usually include a pump and treat system or in some cases tile and drain systems (Love Canal, Niagara Falls, NY) which have been successful in the containment of DNAPL contamination.

Subsurface barrier can either by physical (impermeable walls, horizontal or vertical) or hydraulic. Hydraulic containment can be accomplished by controlling the direction of groundwater flow with capture zone or pressure ridges or by the use of physical barriers.

According to the 1996 Global Environment and Technology Foundation (GETF) market assessment, containment technology is "poised for significant, if not enormous growth." Underground containment barriers are an important method of limiting and/or eliminating the movement of contaminants through the subsurface. Subsurface barriers can maintain the volume of waste and reduce the potential for migration into the surrounding geologic media, or groundwater. In the past, containment has been used at sites where there was no other efficient and cost-effective option. However, subsurface barriers can be used in any number of situations where it is necessary to prevent the migration of contamination. Barriers are currently used for the containment of contaminated waste, as an interim step while final remediation alternatives are developed, and in coordination with treatment technologies. In many instances, subsurface barriers are able to effectively confine the contaminant for extended time periods and provide a cost-effective method of remediation.

There are many subsurface barrier technologies commercially available and others in various stages of development. The purpose and function of the containment system must be determined prior to designing and constructing the barrier. Site characterization is an essential part of choosing an appropriate barrier.

Rumer et al. (1996) suggests some factors that should be considered while designing a subsurface barrier. First, it is important to establish the barrier geometry—alignment, depth, and thickness. Second, a stress-deformation analysis should be performed on the surrounding area in order to assess the potential impacts of barrier construction. Third, compatibility testing must be done to select the most effective barrier materials and when necessary, appropriate mixture or combinations. Fourth, it is necessary to determine the most effective and feasible construction methods. Finally, construction quality assurance, along with monitoring, is a crucial component of subsurface barrier design.

Construction quality assurance (CQA) and construction quality control (CQC) are essential for the successful design, implementation, and performance of a subsurface barrier (Rumer et al., 1996, EPA 1998). The U.S. Environmental Protection Agency (EPA) defines quality control as "the contractor's observations, sampling, measuring, and testing to establish conformance to plans and specifications" (1987). Quality assurance, as defined by the EPA, is conducted by or for the project engineer and provides further confirmation that the construction complies with the specifications of the design. Quality assurance is not mandated by the EPA (Rumer et al., 1996).

Different types of subsurface barriers have different CQC criteria, however there are two primary concerns. First, the installed barrier must have a hydraulic conductivity equal to or less than that specified in the design (Rumer et al., 1995). The second concern is barrier continuity, which is difficult to assess; the methods available have had varying degrees of success. Additional information on CQA/CQC is available in many reposts (EPA 542-R-98-005); Quality Assurance and Quality Control for Waste Containment Facilities (EPA 600-R-93-182); Construction Quality Management for Remedial Action and Remedial Design Waste Containment Systems (EPA 540-R-92-073); and Construction Quality Control and Post-Construction Performance Verification for the Gilson Road Hazardous Waste Site Cutoff Wall (EPA 600-2-87-065).

There is currently no method of guaranteeing the continuity of a subsurface barrier (Sullivan et al., 1998). Discontinuities may occur during grout application/installation and joint formation. Cracking due to curing, settling, and wet/dry cycling may occur over time. Proper emplacement of a subsurface barrier is critical to ensure overall effectiveness of the containment system. Once a barrier is installed, verification and monitoring are crucial. At this time, there is no uniform method of monitoring the emplacement, long-term performance, or integrity of the barrier. The Department of Energy (DOE) has acknowledged this problem and incorporated different monitoring techniques into containment projects.

2.3 Established Physical Barriers

In pump and treat schemes, physical barriers such as grout curtains, slurry walls and sheet piling are installed through the unsaturated zone into saturated zone to divert uncontaminated soil & ground water around a site or limit the migration of contaminated ground water.

2.3.1 Sheet Piling

Sheet pile cutoff walls are constructed by driving vertical strips of steel, precast concrete, aluminum, or wood into the soil forming a subsurface barrier wall. The sheets are assembled before installation and driven or vibrated into the ground, a few feet at a time, to the desired depth. A continuous wall can be constructed by joining the sheets together. The joints between the sheet piles are vulnerable to leakage, and a number of patented techniques have evolved to seal them. In addition to different types of joints, a variety of sealants including grout, fly ash, and cement have been used to seal joints.

Table 2.1: Advantages and Disadvantages of Steel Sheet piles (Knox,1983)

Advantages	Disadvantages
1. Construction is not difficult; no excavation is necessary. 2. Contractors, equipment, and materials are easily available 3. Construction can be economical.	1.The steel sheet piling initially is not watertight. 2. Driving piles through ground containing boulders is difficult 3. Certain chemicals may attack the steel.

4. No maintenance required after construction. 5. Steel can be coated for protection from corrosion to extend its service life.	

While the technology is well understood, sheet pile walls had limited use in the United States and the United Kingdom. Private companies such as Waterloo Barrier Inc. have successfully adapted the general sheet pile barrier for containment uses. Waterloo Barrier Inc. has developed an unique method of sealing the joints between the sheet piles to reduce leakage, which has been a problem in the past.

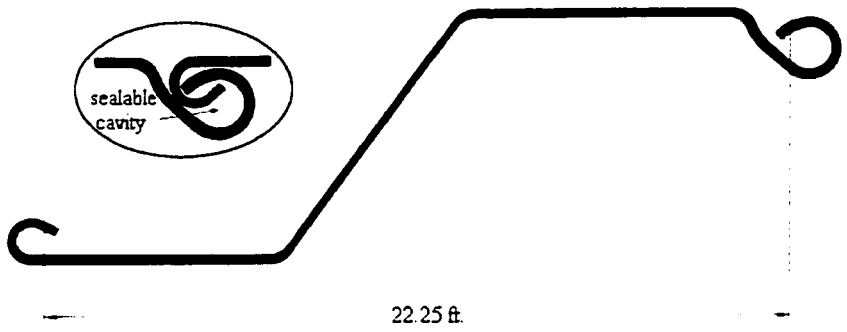

Figure 2.1: Waterloo Barrier™ Sealable Joint Steel Sheet Piling (WZ 75 profile) Waterloo Barrier Inc.

2.3.2 Grout Barriers (or Curtains)

Chemical grout, e.g., silicates, resins, and polymer systems, have been used for decades in conventional civil engineering problems such as excavation support; however, the development of chemical grouts for waste containment application is a relatively new field.

Grouting is the process that involves injecting a grout mixture at very high pressures (up to 5,000 – 6,000 pounds per square inch) and velocities (as great as 800 – 1,000 ft/s) into the pore spaces of the soil or rock. The jetted grout cuts, replaces, and mixes the soil with cementing material to form a column. Rotation of the drill rod, as it is being removed, will form a column. A panel is formed by leaving the drill rod in place (EPA, 1998). The soil structure is destroyed as grout and soil are mixed, forming a homogeneous mass. Jet grouting can be used in soil types ranging from gravel to clay, but the soil type can alter the diameter of the grout column. Soil properties also are related to the efficiency. For instance, jet grouting in clay is less efficient than in sand (Heiser et al., 1997).

Table 2.2: Advantages and Disadvantages of Grout System(Leslie Pearlman, 1999)

Advantages	Disadvantages
1. Versatile – jet grouting can stabilize a wide variety of soil types ranging from gravel to heavy clays (Mutch et al., 1997) 2. Soil heterogeneity has much less of an impact on wall placement than permeation grouting. 3. Installed at depths up to 150 – 200 ft 4.Jet grout unit is mobile, permitting drilling with rotation and percussion (Dwyer,1998) 5. Innovative equipment allows injection of multiple fluids or gases (Dwyer, 1998)	1. Difficult to ensure panel continuity (verticality is critical to ensure that gaps will not occur between panels) 2. Boreholes can become misaligned . 3. Presence of high water table and rapidly flowing ground water limits grout ability thr a. Extensive transport of contaminants b. Rapid dilution of grouts 4. Different soil types and densities affect ab to grout. 6. Procedure requires careful planning and pretesting.Methods of ensuring that all voids the wall have been effectively grouted are

– DTH percussion hammer – Multi-nozzle grout injection unit increases the efficiency of injection	not readily available.

Grouts are usually classified as particulate or chemical. Particulate grouts consist of water plus some particulate material which will solidify within the soil matrix. Chemical grouts usually consist of two or more liquids which will gel when they come in contact with each other.

2.3.3 Slurry walls

Slurry wall represent a technology for encapsulation an area to either prevent ground water pollution or restrict the movement of previously contaminated ground water. The technology involves digging a trench around an area and backfilling with an impermeable material.

For over 45 years, these walls have been used in the construction industry to contain and direct water, and as a result, the requirements and practices for designing and installing a slurry wall are well established. Slurry walls have been used for pollution control since 1970, and the technology is accepted and regarded as an effective method of isolating hazardous waste and preventing the migration of pollutants (Golder Associates Inc.,1994). Excavation under a slurry filled trench provides stability and prevents the trench from collapsing.

Slurry walls can either be placed up gradient from a waste site to prevent flow of ground water into the site, or placed around a site to prevent movement of polluted ground water away from a site. Usually, slurry walls will require a complementary technology such as surface capping or purge wells.

There are different materials, and combinations of materials, that can be used to construct slurry cutoff walls including soil-bentonite, cement-bentonite, and plastic concrete. The backfill and composite typically contain a mixture of materials such as cement, bentonite, fly ash, ground-blasted furnace slag, and clay. Other types of cutoff walls include mix-in-place, grout, and composite walls. Both organic and inorganic contaminants can have a negative impact on bentonite (in the wall and/or in the backfill). To help reduce this problem, additives can be used to alter the characteristics of the slurry wall. For example, additions of fly ash can potentially reduce the degradation of concrete by an alkali-silica reaction or sulfate attack.

Table 2.3 Advantages & Disadvantages of Slurry Trenches (Knox.1983)

Advantages	Disadvantages
1. Construction methods are simple. 2. Adjacent areas are not affected by ground water draw down. 3. Bentonite(mineral) will not dteriorate with age. 4.Leachate- resistant bentonites are available.	1. Cost of shipping betonite. 2. Some construction procedures are patented and require a license. 3. In rocky ground, over-excavation is necessary because of boulders. 4.Bentonite deteriorates when exposed to high

5.Low maintenance requirements. 6.Eliminate risks due to strikes, pump breakdowns, or power failures. 7.Eliminates headers and other above ground obstructions.	ionic strength leachates.

2.4 Innovative Barrier Technology

2.4.1 Frozen Barriers

Frozen barrier walls, also called cryogenic barriers, are constructed by artificially freezing the soil-pore water. As the moisture freezes, permeability decreases thereby forming an impermeable barrier. Once the wall is frozen, it remains impermeable and can prevent the migration of contaminants. When the barrier is no longer needed, the refrigeration system can be turned off, allowing the barrier to melt. In the past, this technology has been used for groundwater control and to strengthen walls at excavation sites.

The construction of a frozen barrier wall involves installing pipes called thermoprobes into the ground and circulating refrigerant (cryogenic) through them. As the refrigerant moves through the system, it removes heat from the soil and freezes the pore water. In arid regions, water can be injected into the soil to provide the moisture necessary to form the barrier or to repair the frozen wall. The thermoprobes can be placed in different configurations depending on the geologic media and the desired shape of the barrier. For

example, if the pipes are installed at a 45E angle along the sides of the area to be contained and installed vertically on the ends, a V-shaped barrier will be formed providing complete containment.

The choice of refrigerant is site and contaminant specific. For example, if the site is polluted with a low freezing point contaminant like trichloroethylene (TCE), a refrigerant such as liquid nitrogen may be required. Other possible refrigerants include calcium chloride brine and carbon dioxide. Alternative refrigerants can have a dramatic effect on the overall cost due to different efficiencies in their refrigeration cycles (Leslie Pearlman, 1999). In addition, friction or thermal resistance within the circulation systems can also reduce the efficiency.

Table 2-4 Advantages & Disadvantages of Frozen Barriers (Leslie Pearlman, 1999)

Advantages	Disadvantages
1. Environmentally safe 2. Lower risk and cost – Contaminated soil is not excavated – No by-products (Arctic Foundations website) 3. Contaminants are contained in situ with frozen soil as the containment medium 4. Thermoprobes may be installed in different positions to create a wall of almost any shape and size to fully contain contaminants 5. Can be used to contain a variety of materials including radioactive, heavy metal, and organic contaminants (DOE website)	1. No long-term data 2. Amount of energy and time to freeze the wall depends on the soil matrix (Layne Christensen Company information) 3. Drilling may be a constraint (EPA SITE website)

6. Easily removed by thawing	

2.4.2 In situ soil mixing

In situ soil mixing is a construction technology where the subsurface barrier is mixed-in-place. This method yields a smaller quantity of excavation spoils compared to external methods such as slurry walls.

Deep soil mixing (DSM), which was originally developed in Japan in the early 1960s, involves mixing an additive into the soil to produce a hard mass that acts as a barrier. The technology uses a special auger with a mixing shaft to simultaneously drill and inject the desired material, resulting in a column of soil and material. As the augers move through the earth, they loosen the soil, lift it into the mixing paddles, blend it with slurry, and inject it back out through the augers (Mutch et al., 1997). Possible slurry materials include bentonite, cement, lime, and additives (e.g., fly ash and slag that change the composition/durability of the material). DSM can be used to construct continuous walls by overlapping individual columns. Walls can be built up to 100 ft in depth.

In situ enhanced soil mixing (ISESM) is a modification of the deep soil mixing technology (DSM). ISESM is advantageous because it can include a number of treatment technologies (DOE website). The following list illustrates the types of treatment technologies that can be used in conjunction with DSM technologies:

- Soil mixing with vapor extraction combined with ambient air injection (vaporizes volatile organic compounds (VOCs)
- Soil mixing with vapor extraction combined with hot air injection
- Soil mixing with hydrogen peroxide injection (hydrogen peroxide oxidizes the VOCs)
- Soil mixing with grout injection for solidification/stabilization (the grout immobilizes the contaminant in solid form)

2.4.3 Geomembrane Composite Walls

Geomembranes were first used as vertical barriers in the early 1980s. They can be used alone or in conjunction with other containment systems. Although geomembranes are extremely impermeable when used in a composite wall, they can potentially provide an added level of protection. The permeability depends on the thickness of the geomembrane and the contaminant. While there are many kinds of geomembranes available, vertical walls are typically constructed of high density polyethylene (HDPE). Methods of installation include a trenching machine; vibrated insertion plate; slurry supported, segmented trench box; and vibrating beam (Rumer et al., 1996). There are different types of interlocks that can be used to connect the panels. The cost of HDPE ranges from \$10 – \$30/ft^2 (Mutch et al., 1997).

Long-term durability of HDPE is not yet known. However, under normal conditions, HDPE is expected to have a lifetime exceeding 300 years (Leslie Pearlman, 1999). The

Drexal University Geosynthetic Research Institute is studying eight factors that influence HDPE degradation: oxidation, chemical attack, hydraulic effects, ultraviolet radiation, nuclear radiation, biological attack, stress effects, and temperature effects (Rumer and Mitchell, 1996).

2.5 Hydraulic Barriers

Hydraulic containment is a design objective of nearly all pump-and-treat systems. Where restoration of soil/groundwater to health-based standards is the overall objective, the primary goal of containment must be to prevent farther spread of the contaminant plume during restoration efforts. Where NAPLs are present, containment using hydraulic and physical barriers might be the primary objective for cleanup efforts in the portion of the aquifer contaminated by free product and residual NAPL. In such situation a conventional pump-and-treat system might be used to restore the dissolved contaminant plume.

Hydraulic barriers using pumping generally require a series of injection wells are placed on the periphery of the plume, injecting at rates designed to produce both horizontal and vertical capture zones to prevent migration, while extraction is effective within the plume to remove the dissolved contaminants mass. This technology of ground water pollution control can be accomplished by controlling the direction of groundwater flow with capture zones (Jandel and Tsang,1987) or by using a pressure-ridge(Knox et al., 1984) . It is usually applied at DNAPL contaminated aquifer sites as a long term plume management strategy, or to temporarily contain the dissolved mass while other aquifer

restoration techniques are designed. A thorough knowledge of the hydrogeology is necessary for development of such a hydrodynamic control system(USEPA, 1990).

2.5.1 Horizontal and Vertical capture zones

Pumping wells provide hydraulic containment by creating a point of low hydraulic head to which nearby ground water flows. The portion of an aquifer where flow direction are toward a pumping well is called a capture zone. In an isotropic aquifer ,where hydraulic conductivity is the same in all directions, ground-water flow is perpendicular to the hydraulic head contours, also called equipotential lines. Figure2.3 show a pump-and-treat system is used with barrier walls to contain the ground-water contamination source areas.

A pumping well creates a zone of influence where the potentiometric surface has been modified. The capture zone is the portion of the zone of influence where ground water flows to the pumping well. The size and shape of a capture zone depend on the interaction of numerous factors, such as

- The hydraulic gradient and hydraulic conductivity of the aquifer.
- The extent to which the aquifer is heterogeneous or anisotropic.
- Whether the aquifer is confined or unconfined.
- The pumping rate and whether other pumping wells are operating.
- Whether the screened interval of the well fully or partially pentrates the aquifer.

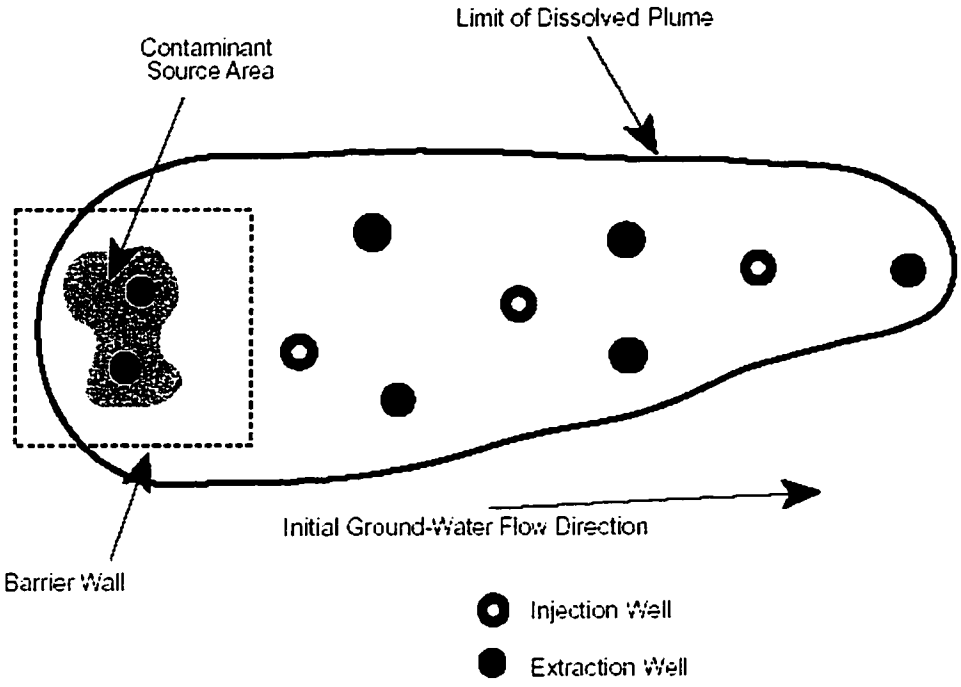

Figure 2.2. Plan view of a mixed containment-restoration strategy. A pump-and-treat system is used with barrier walls to contain the ground-water contamination source areas (e.g., where NAPL or waste may be present) and then collect and treat the dissolved contaminant plume (Cohen et al., 1994).

When the screened portion of a pumping well fully penetrates an aquifer, a two-dimensional analysis to delineate the horizontal capture zone is usually sufficient. When a pumping well only partially penetrates an aquifer, however, vertical capture zone analysis also is required to determine whether the capture zone will contain a contaminant plume.

2.5.2 Pressure ridge systems

Pressure ridge systems are produced by injecting uncontaminated water into the subsurface through a line of injection wells located upgradient or downgradient of a contamination plume. The primary purpose of a pressure ridge is to increase the hydraulic

gradient and hence the velocity of clean ground water moving into the plume, thereby increasing flow to recovery wells, which serves to wash the aquifer. Upgradient pressure ridges also serve to divert the flow of the uncontaminated ground water around the plume, and downgradient pressure ridges prevent further expansion of the contaminant plume. Typically, treated ground water from extraction wells within a contaminant plume supply the upgradient or downgradient injection wells used to create a pressure ridge.

2.5.3 Capture zone analysis and optimization modeling

Javadel and Tsang (1986) developed a useful analytical method for the design of recovery well systems, based on the concept of a capture zone. The capture zone for a well depends on the pumping rate and the aquifer conditions. Ideally, the capture zone should be somewhat larger that the plume to be cleaned up, so wells can be added until sufficient pumping capacity is provided to create a useful capture zone. However ,with more wells ,some contaminants may pass between the wells. Hence well spacing becomes an important parameter as well as pumping rate. The greater the pumping rate, the larger the capture zone ,so the closer the wells are placed, the better the chance of complete plume capture. Overall the method minimizes the pumping injection rates through a proper choice of well location and distance between wells.

Javandel and Tsang (1986) use complex potential theory as the basis for a simple graphical procedure to determine the pumping rate, the number of wells, and the distance between wells.

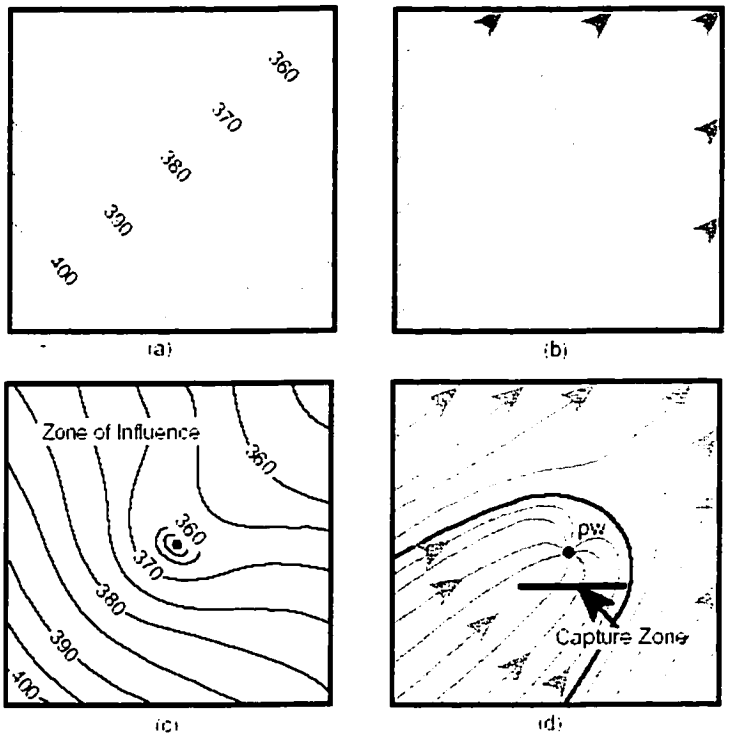

Figure 2.3. In an isotropic aquifer, ground-water flow lines (b) are perpendicular to hydraulic head contours (a). Pumping causes drawdowns and a new steady-state potentiometric surface within the well's zone of influence (c). Following the modified hydraulic gradients, ground water within the shaded capture zone flows to the pumping well (d). (Cohen et al., 1994, adapted from Gorelick et al., 1993).

The method requires type curves for one to four wells and values for two parameters, B is the aquifer thickness (assumed to be constant) and U the specific discharge or Darcy velocity (also assumed constant) for the regional flow system. The method involves the following five steps:

1. Construct a map of the contaminant plume at the same scale as the type curves. The edge or perimeter of the plume should be clearly indicated together with the direction of regional ground water flow.

2. Superimpose the type curve for one well on the plume, keeping the x-axis parallel to the direction of regional ground water flow and along the midline of the plume so that approximately equal proportions of the plume lie on each side of the x-axis. The pumped well on the type curve will be at the downstream end of the plume. The type curve is adjusted so that the plume is enclosed by a single Q/BU curve.
3. Calculate the single well pumping rate (Q) using the known values of aquifer thickness (B) and the Darcy velocity for regional flow (U) along with the value of Q/BU indicated on the type curve (TCV) with the equation $Q = B*U*TCV$
4. If the pumping rate is feasible, one well with pumping rate Q is required for cleanup. If the required production is not feasible due to a lack of available drawdown, it will be necessary to continue adding wells.
5. Repeat steps (2), (3) and (4) using the two-, three-, or four-well type curves in that order, until a single well pumping rate is calculated that the aquifer can support. The only extra difficulty comes from having to calculate the optimum spacing between wells using the following simple rules and to account for the interfacing among the pumped wells when checking on the feasibility of the pumping rates. The wells are always located symmetrically around the x-axis, as the type curves show.

2 wells	Q/(BU)
3wells	1.26Q/(BU)
4 wells	1.2Q/(BU)

The present analysis demonstrate that the capture with result of Javandel and Tsang (1986) actually generalizes to all gradient-wise-symmetric systems-i.e., systems in which

well locations and flow rates are symmetrical respecting a line perpendicular to background flow. Gradientwise-symmetric systems consist of "symmetric elements". each element being either a well on the symmetry line, or a pair of equal wells.

2.6 Application of the MOC Code

The USGS model was used to model ground water flow and chloride transport at the Conroe Waste site in Texas (Borden et al.,1984). The MOC model was first calibrated to the ground water flow field at the site. The study revealed that slight variations in hydraulic conductivity could play a significant part of recharge coming from the ponded source of contamination; thus, having a direct bearing on predicted and measured concentrations of the contaminants. The study concluded that uncertainty in aquifer parameters can preclude firm conclusions about the fate of contaminants in ground water. and highlighted the strengths and weaknesses of modeling with a limited database.

A detailed analysis of the performance of subsurface impermeable barriers for containing the movement of contaminated ground water was conducted by Knox (1983). The study, utilizing the MOC model, included examining the effects of hydrodynamic dispersion, the performance of the barrier in the presence of layered soils and when the barrier was fully penetrating but partially permeable.

Gupta (1993) utilized the USGS MOC numerical code to model the innovative application of barriers to access the effectiveness of hydraulic and impermeable barriers in improving the hydraulic efficiency of pump and treat systems which involve injection

of chemicals into the subsurface for remediation purposes. In the study, a revised estimate of trichloroethene (TCE) mass present in the aquifer was made by the method of moments. The results of the modeling study indicate that impermeable barriers are successful in decreasing the quantities of clean water from being pumped out while increasing the total mass of TCE extracted over the simulated time.

CHAPTER THREE

Theoretical Consideration

To model the effectiveness of hydraulic barrier produced by image wells for containing injected chemicals and contaminants in targeted site, this study involved application of the two-dimensional solute transport code developed by Konikow and Bredehoeft (1978). The following sections describe the general methods for handling two-dimensional groundwater flow problems including method of superposition, the method of images , and the general capabilities of the MOC to model flow regimes, delineate contaminant plumes and assess remedial activities.

3.1 Two- Dimensional Problems

3.1.1 Superposition

The differential equation for two dimensional steady flow in a homogeneous aquifer is

$$\frac{\partial^2 \Phi}{\partial x^2} + \frac{\partial^2 \Phi}{\partial y^2} = 0 \qquad (3.1)$$

where

Φ = potential function

x, y = coordinates

Because the equation is a linear and homogeneous differential equation, the principle of superposition applies. If two differential functions Φ_1 and Φ_2 are solutions of the Laplace's equation, then the function

$$\Phi(x, y) = c_1\Phi_1(x, y) + c_2\Phi_2(x, y) \qquad (3.2)$$

is also a solution. This approach can be applied to a system of multiple wells.

3.1.2 Method of Images

To solve problems of a well near a long body of water (river. canal. or lake) or a long straight impervious boundary (e.g. a mountain ridge or fault), a special application of superposition – method of images is introduced.

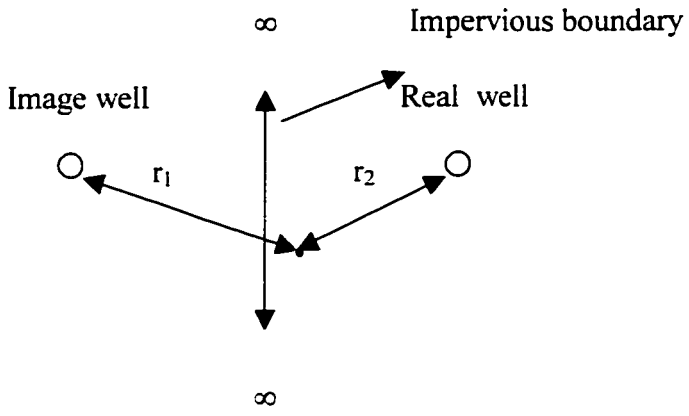

Figure3.1 Well near a straight impervious boundary

In case of a well near a long straight impervious boundary Figure3.1, one can replace the half-plane aquifer by a imaginary infinite aquifer with an imaginary well placed at the mirror image position from the real well. This represents the sink and sink problem and the solution for this case can be the equation

$$\Phi = \frac{Q}{2\pi}\ln(\frac{r_1 r_2}{R}) + \Phi_0 \qquad (3.3)$$

3.2 Introduction of MOC

The MOC is used to simulate solute transport in groundwater under varying boundary conditions, and is quite flexible in application to both one or two dimensional flow situations. The model computes changes in concentration over time caused by the

processes of convective transport, hydrodynamic processes of convective transport, hydrodynamic from fluid sources. The model couples the ground-water flow equation with the solute-transport equation. The model is based on a rectangular, block-centered, finite difference grid. It allows the specification of any number of injection or withdrawal wells and of spatially varying diffuse recharge or discharge, saturated thickness, transmissivity, boundary conditions, and initial heads and concentrations.

The following assumptions have been made in the development of the model and that must be carefully evaluated before applying the method to a field problem.

1.Darcy's law is valid and hydraulic-head gradients are the only significant driving mechanism for the fluid flow.

2.The defined sand box was saturated , porosity and hydraulic conductivity of sand(or aquifer) are constant with time, and porosity is uniform in space.

3.Gradients of fluid(s) density, viscosity, and temperature do not affect the velocity distribution.

4.No chemical reaction occur that affect the concentration of the solute, the fluid(s) properties, or the aquifer properties.

5.Ionic and molecular diffusion are negligible contributors to the total dispersive flux.

6.Vertical variations in the head and concentration are negligible.

7.The aquifer is homogeneous and isotropic with respect to the coefficients of longitudinal and transverse dispersivity.

When applying the model to a specific field problem, some assumptions may not be valid. In such case, the governing equation will have to be modified to account for the deviation of the appropriate factor or processes.

3.3 Theoretical background

The groundwater flow equation describing the transient two-dimensional areal flow of a homogeneous compressible fluid through a nonhomogeneous anisotropic aquifer can be written in the cartesian tensor notation as

$$\frac{\partial}{\partial x_i}\left(T_{ij}\frac{\partial h}{\partial x_j}\right) = S\frac{\partial h}{\partial t} + \mathrm{W} \qquad (3.4)$$

Where

T = the transmissivity tensor (L^2/t)

h = hydraulic head (L)

S = storage coefficient(dimensionless),

t = time, t

W = W (x,y,t) is the volume flux per unit area (L/t)

xi and xj are the Cartesian coordinates

Fluxes due to well pumpage, well injection, evapotranspiration, leakage into or out of the aquifer and rivers or lakes, are expressed as:

$$W(x,y,t) = Q(x,y,t) - \frac{K_z}{m}\left(\mathrm{H_S} - h\right) \qquad (3.5)$$

where

Q = rate of withdrawal or recharge (L^3/t)

K_Z = vertical hydraulic conductivity of the confining layer, streambed, or lakebed. L/t

m = thickness of the confining layer, streambed, or lakebed, L

H_Z = hydraulic head in the source bed, stream, or lake, L

The seepage velocity of ground water can be derived from Darcy's law:

$$V_i = -\frac{K_{ij}}{\varepsilon}\frac{\partial h}{\partial x_j} \qquad (3.6)$$

where

Vi = seepage velocity in the direction of x_i, L/t;

K_{ij} = hydraulic conductivity tensor,

ε = effective porosity of the aquifer, dimensionless

The equation used to describe the two dimensional areal transport and dispersion of a given nonreactive dissolved chemical species in flowing ground water was derived by Konikow and Bredehoeft(1978) :

$$\frac{\partial(Cb)}{\partial t} = \frac{\partial}{\partial x_i}\left(bD_{ij}\frac{\partial C}{\partial x_j}\right) - \frac{\partial}{\partial x_i}(bCV_i) - \frac{C'W}{\varepsilon} \qquad i, j = 1,2 \qquad (3.7)$$

Where,

C = concentration of the dissolved chemical species, M/L^3

D_{ij} = coefficient of hydrodynamic dispersion (a second-order tensor)

b = saturated thickness of the aquifer, L

C' = concentration of the dissolved chemical in a source or sink fluid, M/L^3.

The first term on the right side of equation 3.4 represents the change in concentration due to hydrodynamic dispersion. The second term describes the effects of convective transport, while the third term represents a fluid source or sink.

The dispersion coefficient related to the velocity of ground-water flow and to the nature of the aquifer can be derived by using Scheidegger's equation:

$$D_{ij} = \alpha_{ijmn} \frac{V_m V_n}{|V|} \qquad (3.8)$$

Where

α_{ijmn} = dispersivity of the aquifer, L

Vm,Vn= components of velocity in the m and n directions, respectively

|V| = magnitude of the velocity

For an isotropic aquifer the dispersivity tensor can be defined in terms of two constants. Longitudinal and transverse dispersivities of the aquifer (a_L and a_T, respectively) are related to the longitudinal and transverse dispersion coefficients by

$$D_L = \alpha_L |V| \qquad (3.9)$$

and

$$D_T = \alpha_T |V| \qquad (3.10)$$

The model is a miscible mass transport model that can handle both convective and dispersive transport. The final result of the simulations is that contaminant concentration are computed at the respective nodes along with chemical mass balances for each time step.

3.4 Mathematical model

The governing equations for ground water flow and solute transport are solved by numerical procedures. The region to be modeled is discretized into the required number of rectangular, block centered, finite-difference cells in a grid. Nodes are defined at the center of each cell. Boundary conditions, aquifer parameters such as saturated thickness and transmissivity, and initial values of head and solute concentration are designated at the nodes of the grid. An implicit finite-difference form of equation 3.4 is solved numerically by using either an alternating-direction implicit (ADI) or strongly-implicit procedure (SIP) procedure.

In the ADI scheme for two-dimensional areal flow of ground water, one of the second derivative of the head is expressed in terms of known values at the "k" time level. The other second derivative is then expressed implicitly in terms of unknown values at the "k+l" time level. In a grid consisting of "n" nodes in the x direction and "m" nodes in the y direction, it is then possible to solve one line at a time (solving for all values of yon that line) marching in the direction of increasing equations with (m-l) unknowns. Thus, instead of solving a single system of (n-l)(m-1) equations, the problem is reduced to that of solving (m-l) equations (n-l) times; to go from the k to k+ 1 time level, which is a

supposedly easier task. The equations also form a tridiagonal matrix system which expedites solution.

To remove numerical instability , the ADI method involves alternating the direction in which the solution is carried out. Thus in successive time steps, the second derivatives previously expressed explicitly are expressed implicitly and vice versa. For simple problems, the ADI method gives very rapid convergence, while the advantage decreases when a complex problem is attempted. On the other hand, the SIP method for solving the ground water flow equation does not depend upon the complexity of the problem. For heterogeneous and anisotropic aquifers, the SIP method is much faster and involves fewer numerical difficulties than ADI or the line successive over relaxation method (Remson et al., 1971; Trescott et al., 1976).

The SIP method has also been called" an approximate factorization technique" .The method is called strongly implicit because it is related more closely to a "direct" method of solving the equations such as Gaussian elimination (Remson et al., 1971). The SIP procedure is described conceptually as a solution procedure for a system of equations with a coefficient matrix [A] , which is difficult to solve directly; and for which a modified matrix [C] = [A] + [B] is found that can be easily solved. The necessary condition is that the matrix [C] should be in some sense close to [A] , so that the modified matrix will form an acceptable basis for an iterative technique (Remson et al., 1971).

3.5 Method of characteristics

The method of characteristics is used solve the solute-transport equation. It is a particle-in-cell (PIC) method and is applied in a particle tracking scheme ,as shown in Figure3.2 . Because the governing partial differential equation (3.6) for solute transport is nonlinear, the solution is obtained indirectly by solving an equivalent system of ordinary differential equations. When transport is dominated by convection, the solute transport equation may closely approximate a hyperbolic partial differential equation and be highly compatible with the method of characteristics (Konikow and Bredehoeft, 1978) .

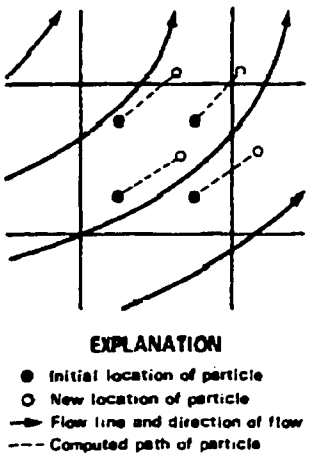

Figure 3.2 Part of hypothetical finite-difference grid showing relation of flow field to movement of points.

The ordinary differential equations are obtained by rewriting the transport equation as:

$$\frac{\partial C}{\partial t} = \frac{1}{b}\frac{\partial}{\partial x_i}\left(bD_{ij}\frac{\partial C}{\partial x_j}\right) - V_x\frac{\partial C}{\partial x} - V_y\frac{\partial C}{\partial y} + F \qquad (3.11)$$

where

$$F = \frac{C\left(S\frac{\partial h}{\partial t} + W - \varepsilon\frac{\partial b}{\partial t}\right) - C'W}{\varepsilon b} \qquad (3.12)$$

In the MOC procedure, changes with time in properties of the fluid, such as concentration, may be described either for fixed points within a stationary coordinate system as successive fluid particles pass the reference points; or for reference fluid particles as they move along their respective paths past fixed points in space. In the USGS model, the later is adopted system of coordinates. Thus, the rate of change concentration associated with fluid movement, expressed as dC/dt (which is called the material derivative of concentration) is tracked, and expressed as:

$$\frac{dC}{dt} = \frac{\partial C}{\partial t} + \frac{\partial C}{\partial x}\frac{\mathrm{dx}}{\mathrm{dt}} + \frac{\partial C}{\partial y}\frac{\mathrm{dy}}{\mathrm{dt}} \qquad (3.13)$$

The material derivation of position is defined by the velocity components in the x and y directions. By comparing equation 3.13 to equation3.11, the characteristic equations for the x and y components of velocity and for the concentration are obtained, The solutions to the system of equations are given as:

$$x = x(t)\ ;\ y = y(t)\ ;\ \text{and}\ C = C(t) \qquad (3.14)$$

These are called the characteristic curves for the solute transport equation.

3.6 Particle tracking

The solution to the transport equation is obtained numerically by introducing a set of moving points than can be traced within the stationary coordinates of the finite-difference grid. The moving points or particles represent the center of gravity of a specified amount of heat or solute, and each corresponds to one characteristic curve. Values of x, y, and C are obtained as functions of t for each curve. The average concentration results from the number of particles located in each cell at that time in relation to the fluid volume within the cell. The moving points simulate convective transport because the concentration at each node of the grid will change with each time step as different points having different concentrations enter and leave the area of the cell. The changes in concentration caused by hydrodynamic dispersion, fluid sources, divergence of velocity , and changes in saturated thickness are calculated using an explicit finite-difference approximation and expressed as:

$$\Delta C_{i,j,k} = \Delta t\left[\frac{1}{b}\frac{\partial}{\partial x_i}\left(bD_{ij}\frac{\partial C}{\partial x_j}\right)+\mathrm{F}\right] \qquad (3.15)$$

The explicit numerical solution of the solute-transport equation has a number of stability criteria associated with it. The time increment required to solve the flow equation is limited in size by the smallest time step calculated for any individual node in the entire grid. A second criterion is that the change in concentration in a source node cannot exceed the difference between the source concentration and the concentration in the aquifer. A third criterion essential for stability of the numerical solution is the maximum distance the particle is allowed to be convected. For accurate computation of

concentration changes caused by convective transport, it is required that marker particles be uniformly spaced and move along continuous paths.

For a given velocity field and grid, a restriction is placed on the size of the time increment to assure that the distance between successive time steps does not exceed certain critical cell distances which are related to the size of cell by a fraction 'γ' called CELDIS(cell distance). At no-flow boundaries , neither water or solute is allowed to flow across the boundary. Sometimes it is possible for a particle to be convected across the no-flow boundary during a particular time interval. Figure 3.3 shows such a possible situation when a particle moving along a curvilinear path will be convected across the impermeable boundary. In this instance, the particle is relocated inside the aquifer by reflection across the boundary. This causes it to be reloated closer to the true flow line.

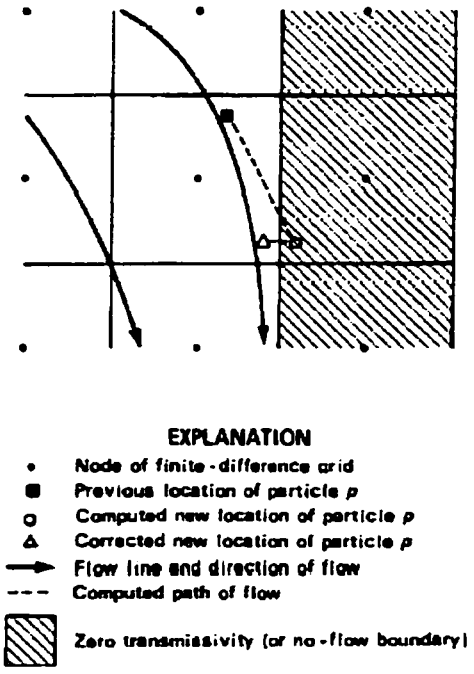

Figure 3.3 Possible movement of a particle near an Impermeable no flow boundary(from Konikow and Bredehoeft,1978).

3.7 Boundary conditions

Appropriate boundary and initial conditions can be specified in MOC model. These can be either constant-flux type(well withdrawals or injection) or constant head boundaries (recharging rivers, leaking aquifer etc.) .

A constant-flux boundary can be used to represent aquifer underflow, well withdrawals, or well injection. A no-flow boundary is a special case of a constant-flux boundary. No-flow boundaries are designated by setting the transmissivity equal to zero at appropriate nodes, thereby precluding the flow of water or dissolved chemicals across the boundaries of the cell containing that node.

A constant-head boundary in the model can represent parts of the aquifer where the head will not change with time, such as recharge boundaries or areas beyond the in fluence of hydraulic stresses. In this model constant-head boundaries are simulated by adjusting the leakage term at the appropriate nodes. This is accomplished by setting the leakance coefficient (K_Z/m) to a sufficiently high value (such as 1.0 s^{-1}) to allow the head in the aquifer at a node to be implicitly computed as a value that is essentially equal to the value of $H_{,,}$ which in this case would be specified as the desired constant-head altitude. The resulting rate of leakage into or out of the designated constant-head cell would equal the flux required to maintain the head in the aquifer at the specified constant-head altitude.

3.8 Mass balance

Mass balance computation are performed both for the solute being modeled and for groundwater. The calculations are based on the principal of conservation of mass, which requires that the net inflow and outflow of mass from the grid (or net flux) be equal to the

accumulated mass (or change in mass stored) in the grid. Mass balance errors are computed using the following equation:

$$E = \frac{100.0(M_f - \Delta M_S)}{M_0 - M_f} \qquad (3.16)$$

where

E = mass balance error, calculated as a percent

M_f= net mass flux (M^3/t)

M_0 = initial mass of solute present(M^3/t) and

ΔM_s = change in mass stored in the section of aquifer modeled in the finite-difference grid (M^3/t)

3.9 Mass transfer processes

The MOC solute transport code is capable of simulating many of the mass transfer and exchange processes relevant for contaminant transport modeling. The solute transport equation considers first-order, irreversible, linear and nonlinear equilibrium-controlled sorption, and equilibrium –controlled ion exchange. These processed are incorporated into the general transport equation, the modified form of which then becomes:

$$\frac{\partial C}{\partial t} + \frac{\rho_b}{\varepsilon}\frac{d\bar{C}}{dt} = \frac{1}{b}\frac{\partial}{\partial x_i}\left(bD_{ij}\frac{\partial C}{\partial x_j}\right) - V_i\frac{\partial C}{\partial x_i} + \frac{W(C - C')}{\varepsilon b} - \lambda C - \frac{\rho_b}{\varepsilon}\lambda\bar{C} \qquad (3.17)$$

where

λ = decay rate constant (l/t)

$\bar{C}$ = concentration of the solute sorbed (or exchanged) on the porous medium (MM^{-1}), and

C' = concentration of the solute in the source fluid (M/L^3)

The decay term on the right side of the above equation commonly represents radioactive decay, but can also represent chemical decomposition or biodegradation. It is assumed that the solute and the sorbed mass decay at the same rate. Linear sorption is represented in the model by the following relationship:

$$\bar{C} = K_d C \qquad (3.18)$$

where

K_d = distribution coefficient

If the reaction is assumed to be instantaneouse and revercible, the retardation factor is constant and can be calculated according to :

$$R_f = 1 + \frac{\rho_b K_d}{\varepsilon} \qquad (3.19)$$

Nonlinear sorption is incorporated into the solute transport equation for which the slope $\frac{d\bar{C}}{dC}$ is not constant but depends on the solute concentration. Two types of isotherms (Freundlich and Langmuir) are considered in the code. For Freundlich sorption isotherms, the sorbed concentration is related to the aqueous concentration by the relationship:

$$\bar{C} = K_f C^n \qquad (3.20)$$

where

K_f = Freundlich sorption equilibrium constant

n = Freundlich exponent

The retardation factor is a function of the concentration and expressed as:

$$R_f(C) = 1 + \frac{\rho_b}{\varepsilon} n K_f C^{n-1} \qquad (3.21)$$

For the Langmuir sorption isotherm, the porous media is considered to have a maximum sorptive capacity expressed by the relation:

$$\bar{C} = \frac{K_f Q C}{(1 + K_f C)} \qquad (3.22)$$

where

K_f = Langmuir sorption equilibrium constant

Q = the maximum sorption capacity of the media

At high concentration, the slope of the isotherm approaches zero as the media does not absorb any more solute.

Retardation is incorporated in the particle tracking and dispersion calculations explicitly. This means that as each particle is convected along a characteristic curve , its velocity is retarded using a linearized retardation factor computed explicitly for each time step using the call concentration from the previous time step. Changes in concentration resulting from dispersion are then calculated. The retardation factor for dispersion and source calculations is computed from the half-step cell concentrations. These are the average of the cell concentration at the end of the previous time step and the new cell concentration after accounting for convection and decay only. Thus , the maximum concentration from either the initial condition or from the source is used to compute a minimum retardation factor. The minimum retardation factor is the then used with the maximum flow velocity value to determine the time-step size for particle moves. The minimum retardation factor is recomputed for each pumping period (Goode and Konikow, 1989)

CHAPTER FOUR

Modeling of Hydrodynamic barrier

The goal of this study was to assess the effectiveness of hydrodynamic barrier for improving the containment efficiency of chemical enhanced pump and treat system utilized in NAPL contaminated site. To model the innovative techniques being studied, a mathematical model was developed to evaluate the effectiveness of hydrodynamic barrier. A defined site ABCD was developed in the study (Figure 4.1).

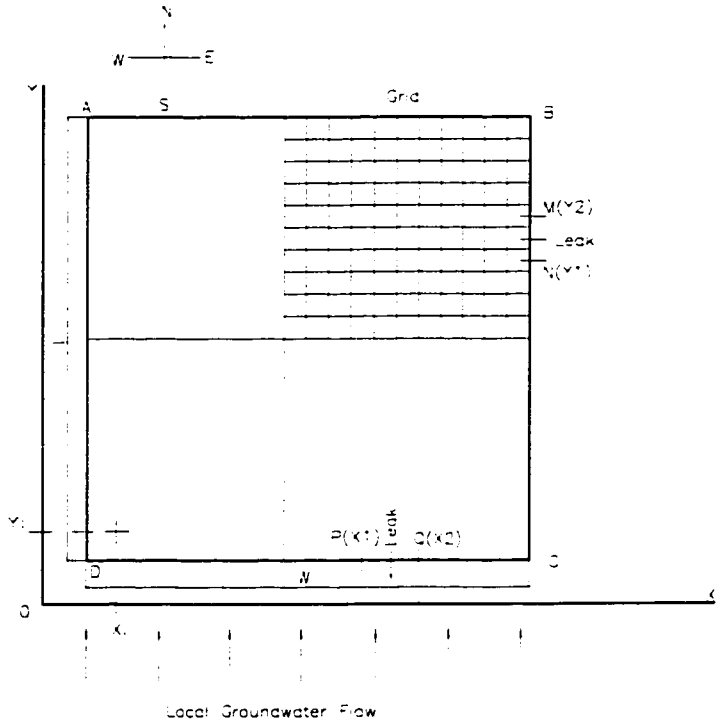

Figure 4.1 Site ABCD

4.1 Theoretical Consideration

Consider the module A system of the pump and treat scheme consisting of 2 injecting and 2 extracting wells in a contaminated site ABCD of length L and width W (Fig. 4.1). Let

the region outside ABCD be free of the contaminant. Assume that the flow is steady, 2-dimensional and laminar in the aquifer, which has a unit depth. Further, let the contaminant distribution in the site be homogenous. It is required to limit the movement of the injected surfactants and the released contaminant to regions within the site boundary ABCD. To this end, provide 8 additional image wells outside ABCD as in Fig. 5.6. Let Q/2 be the strength of each of the wells and let dQ be the total liquid flow leakage out of the site ABCD through various sections of its boundary.

The equations governing the flow of water in the soil matrix is linear and the streamline pattern for a system of wells shown in Fig.5.6 can be easily obtained by the principle of superposition, since the streamline pattern for each individual well is known (Valentine, 1969). In a phreatic aquifer, superposition is justified as an approximation (Bear, 1979).

Consider a point at the Southwest corner of ABCD as the origin. While getting the streamline pattern for the well system, the effect of the shift in the origin for each well can be easily incorporated. A system of discharge and recharge wells (sources and sinks) is designed with different well arrangements (modules A and B) to control the leakage of surfactant [chemical] and the contaminant outward from the target area through sections of the boundary ABCD.

4.2 Governing equations

Consider a source (Fig. 4.1) of strength q at a point (x_i, y_i). The source constant is $m = q/2\pi$ and the corresponding stream function for the source is,

$$\Psi_i = f_i \, m \tan^{-1} \frac{(y - y_i)}{(x - x_i)} \tag{4.1}$$

where, $f_i = 1$ for the source and -1 for the sink.

For a system of n sources and n sinks, having the same strength, one can write,

$$\Psi = \sum_{i=1}^{2n} \Psi_i \tag{4.2}$$

The velocity component u in the x direction for this system is,

$$u = \frac{\partial \Psi}{\partial y} = \sum_{i=1}^{2n} f_i m \frac{(x - x_i)}{(x - x_i)^2 + (y - y_i)^2} \tag{4.3}$$

and the velocity component v in the y direction for this system is,

$$v = -\frac{\partial \Psi}{\partial x} = \sum_{i=1}^{2n} f_i m \frac{(y - y_i)}{(x - x_i)^2 + (y - y_i)^2} \tag{4.4}$$

Our interest is in the chemicals and the released contaminant leaking out of boundary ABCD.

Along CB fixed at x = W, the leakage dq through strip MN of width $y_2 - y_1$ (Fig. 4.1) is,

$$dq = u dx = d\Psi = \sum_{i=1}^{2n} f_i m \tan^{-1}\left(\frac{y - y_i}{x - x_i}\right) \tag{4.5}$$

Care was taken to consider the exiting flow only. For this contribution, the velocities that are in the right positive direction (left to right) are considered. They can be identified by the positive sign of $d\psi/dy$ for strips along the boundary CB. A simple computing program was used to determine the flows exiting from the boundaries. A typical value of dx=dy= L/100 was used for the computation. Thus along CB:

$$q_{CB} = Leak_{MN} = \sum_{i=1}^{2n} f_i m \tan^{-1}\left(\frac{y-y_i}{x-x_i}\right)\Big|_{y_1}^{y_2} \tag{4.6}$$

The procedure was repeated for the boundary DA. Along the boundaries such as AB and DC, y is fixed. Considering DC, the leakage out of the strip PQ is

$$dq = -vdy = d\Psi = \sum_{i=1}^{2n} f_i m \tan^{-1}\left(\frac{y-y_i}{x-x_i}\right) \tag{4.7}$$

As in the previous case, only flow exiting from the site to the surrounding area is considered to calculate the leak. Thus along DC:

$$q_{DC} = leak_{PQ} = \sum_{i=1}^{2n} f_i m \tan^{-1}\left(\frac{y-y_i}{x-x_i}\right)\Big|_{x_1}^{x_2} \tag{4.8}$$

If there is local groundwater flow of considerable magnitude in the region, it can also be included in the flow system. Let the flow of natural groundwater be parallel and steady. Further, assuming that its velocity V is at an angle α (Fig. 4.1) to the x-axis, the expression for the stream function of the combined system comprising of n sources, n sinks and groundwater flow can be written as follows:

$$\Psi = \sum_{1}^{2n} f_i m \tan^{-1}\frac{(y-y_i)}{(x-x_i)} + V(y\cos\alpha - x\sin\alpha) \tag{4.9}$$

Here, V = -Ks, where K is the aquifer transmissivity and s is the groundwater ambient pressure gradient [Valentine, 1969].

Also, the corresponding potential function can be expressed as follows.

$$\Phi = \sum_{1}^{2n} \tfrac{1}{2} f_i m \ln\left[(x - x_i)^2 + (y - y_i)^2\right] + V(x\cos\alpha + y\sin\alpha) \qquad (4.10)$$

For simplicity, the well system is analyzed without any local ground water flow. As stated earlier, its contribution can be easily incorporated, if its flow rate and orientation are known.

The chemicals used for cleaning the target site will be injected at a flow rate of Q through the recharge wells (real sources) set within the boundary ABCD. If there are R real sources, the strength of each real well will be m, where,

$$m = \frac{q}{2\pi} = \frac{Q}{2\pi R}$$

The stream function ψ for the well system can be rewritten in terms of Q, R and W as follows,

$$\Psi = \frac{Q}{2\pi R}\left[\sum_{1}^{2n} f_i \tan^{-1}\left(\frac{y - y_i}{x - x_i}\right)\right] \qquad (4.11)$$

The corresponding potential function Φ is given below.

$$\Phi = \frac{Q}{4\pi R}\left[\sum_{1}^{2n} f_i \ln[(x - x_i)^2 + (y - y_i)^2]\right] \qquad (4.12)$$

Also, the pressure head h at any point is related to Φ. Thus, following Valentine (1969),

$$\Phi = -Kh \qquad (4.13)$$

and,

$$d\Phi = -Kdh \qquad (4.14)$$

4.3 Grid system

For the purpose of analysis, a rectangular grid system (Fig. 4.1) is superimposed on the target site boundary ABCD of width W and length L. In some cases, a larger grid size of 1.4L x 1.4W is chosen to include a small portion of the flow area outside the target site. Let AD denote the North direction (Fig. 4.1). The distances between grid points are 0.05W (East-West) and 0.05L (North-South).

4.4 Streamline pattern

Equation (4.11) directly provides the values of Ψ at all grid points. These were used to develop the streamline pattern for the flow system since the streamlines denote the locus of fixed Ψ values.

4.5 Pressure head distribution

The Φ values were obtained at all the grid points using Equation (4.12). Using this information, the differences of the Φ values ($d\Phi$) between adjacent grid points were computed. These differences were transformed to differences in pressure head (dh) between the corresponding adjacent grid points (Equation10b). Let A be the grid point (1,1) and let its adjacent grid point (Fig. 4.1) to the right along AB be (1,2). For this configuration,

$$d\Phi\big|_{1,1to1,2} = \Phi_{1,2} - \Phi_{1,1}$$

Hence, the differential pressure head between these two grid points is,

$$dh\big|_{1,1to1,2} = -\frac{1}{K} d\Phi\big|_{1,1to1,2}$$

After computing the dh values between all the adjacent grid points of the grid, a pressure head of 10 units was arbitrarily chosen at the North-West corner of the grid (i = 1, j = 1). Using this reference pressure head value and the known values of the pressure head differences between adjacent grid points, the pressure head at all other grid points were computed. Finally, for a non-dimensional presentation, all the pressure head values were normalized by the value of the pressure head at the grid center. It may be added that K need not be specified while dealing with a non-dimensional representation.

4.6 Velocity distribution

To develop the velocity vector plots, the values of u and v at all grid points were obtained using Eqs. (4.3) and (4.4).

4.7 Well system modules

For purposes of illustration, only two specific well modules are studied in detail. Fig. 5.6 shows a simple system of wells termed as module A. It has two real wells injecting the chemicals (surfactants) into the site and two extracting wells removing the unused chemical and the released contaminant. Fig. 5.7 denotes a group of four module A units with c/W = 0.01. Since increased values of c/W limit the number of individual modules that can be used in a given site, c/W = 0.01 was chosen. The value of W/L was arbitrarily

chosen to be 1.416. The disposition of the wells indicates that sites with W/L = 0.706 and W/L = 1.416 [=1/0.706] have similar flow characteristics.

4.8 Analysis

Sample calculations are provided in Appendix B. The figures referred to below are found at the end of this section.

4.8.1 Factors affecting leakage

Fig.4.2 shows that the presence of image wells reduces the leakage considerably for module A, the 4 modules A system too drastically reduces the leakage when image wells are present. The effect of varying the parameters L/W and c/W in the basic module A is shown in Fig.4.3.

Figs. 5.8 to Fig. 5.10 denote module B and two of its variations set in the same target site. For the module B system, Fig. 4.2 indicates that the leakage out of the site continuously decreases as the number of modules increases. In a subsequent section, it will be shown that leakage is primarily through the end modules and this supports the fact that addition of more intermediate modules for the basic module B decreases the leakage more.

In reality, to suit the non-homogeneity of contaminant distribution, the performance of different well system configurations should be studied to arrive at the optimal configuration that is site specific. Also, in actual practice, the performance of the system will be closer to the theoretical prediction of leakage, if there is an aquitard just below the zone of contamination. When the natural ground water flow in the aquifer is considerably

large, one should include a suitable stream function denoting the uniform flow in Equation(4.2) to include its contribution to the total stream function. Reynolds numbers near a well will be quite high and this may lead to deviations of the actual values of velocity and pressure from theoretical predictions in the vicinity of wells. The main flow characteristics of the wells are the distributions of the pressure head and velocity. These can be found after knowing the locations and strengths of the wells.

4.8.2 Flow characteristics

The flow characteristics of a few selected well modules are shown in Figures. 4.4 to 7.

4.8.3 Module A well systems

Figures. 4.4a, 4.4b and 4.4c show the streamline pattern, pressure head distribution and velocity vector plot for the 4 modules A system (Fig.5.7) in which the natural groundwater contribution is absent. As expected, the streamline pattern, pressure head distribution and velocity vector plot for the 4 modules A system display the expected diagonal symmetry of flow. The velocity vector plot [Fig. 4.4c] includes a small area outside the target site. The flow distribution is nearly even, except in the regions at the center of each of the 4 individual modules and the site center (Fig. 4.4c). Fig. 3c clearly shows that only a small quantity of water from the image wells will enter the site through the boundaries, since at the boundaries, the velocity components normal to the site boundary ABCD (Fig. 4.1) are very small. The leakage of chemicals ($\Delta Q/Q = 8.3\%$) to regions outside the site boundary is also restricted to the regions near the 4 corners A, B,

C and D and the small gaps between the extraction wells located near x/W = 0.5 (Fig. 4.4c).

The data of the non-dimensional pressure head distribution (Fig. 4.4b) can be converted to true values of the pressure head to plot the free surface line, when the reference pressure data is known at any location in the site. Clearly, the decontamination of the site will not be quite effective in the small region around the centers (Fig. 4.4a) of the 4 individual modules and the site center where the pressure gradients are small. This can be partly remedied in some cases by discontinuous pumping, if the residual contaminant is sufficiently mobile. Alternatively, the well system can be redesigned to remove the contaminant from the center of each of the 4 modules (quarter regions) of the site.

4.8.4 Module B well systems

Figs. 4.5, 4.6 and 4.7 show the effect of using the module B systems with 4, 12 and 16 real injecting wells, respectively. Leakage out of the site (Fig. 4.4) for the basic module B system (Fig. 5.8) is mostly confined to regions near the 4 corner injecting wells (sources) and the total leakage is 21.6% (Fig. 4.2). Hence, for the basic module B, adding one or two additional intermediate modules between its end modules (Figs.5.9 and 5.10) should improve its performance. Figs. 4.2 show that $\Delta Q/Q$ = 13.6% for the 3 modules B system and $\Delta Q/Q$ = 9.9% for the 4 modules B system, respectively. Fig.4.8 shows the variation of $\Delta Q/Q$ for the module B unit and its variations. As mentioned earlier, the leakage out

of the site for all the module B units is mostly confined to regions near the 4 injecting wells (sources) at the corners (Figs. 4.5c, 4.6c and 4.7c).

Moreover, the possibility of reducing the leakage further in a large site is suggested by the above observations. For instance, consider the use of the 4 modules B system (Fig. 5.10) for decontamination of a site. For this system, addition of a single water module B at each of the system (not shown) will improve the performance as the resulting 6 modules system with its image system can effectively further reduce the leak to very small values.

4.9 Summary

1. The use of image wells in combination with real wells can reduce the leakage of chemicals and surfactants out of the site boundary.
2. For large sites, where the module B system or its variations are used, addition of pure water well system modules at the ends can reduce the leakage further.

The effectiveness of the proposed system in the field is closely related to the assumptions on which the analysis is carried out. The reduction in the amount of chemicals (surfactants) needed to clean up a site by pump and treat scheme is considerable.

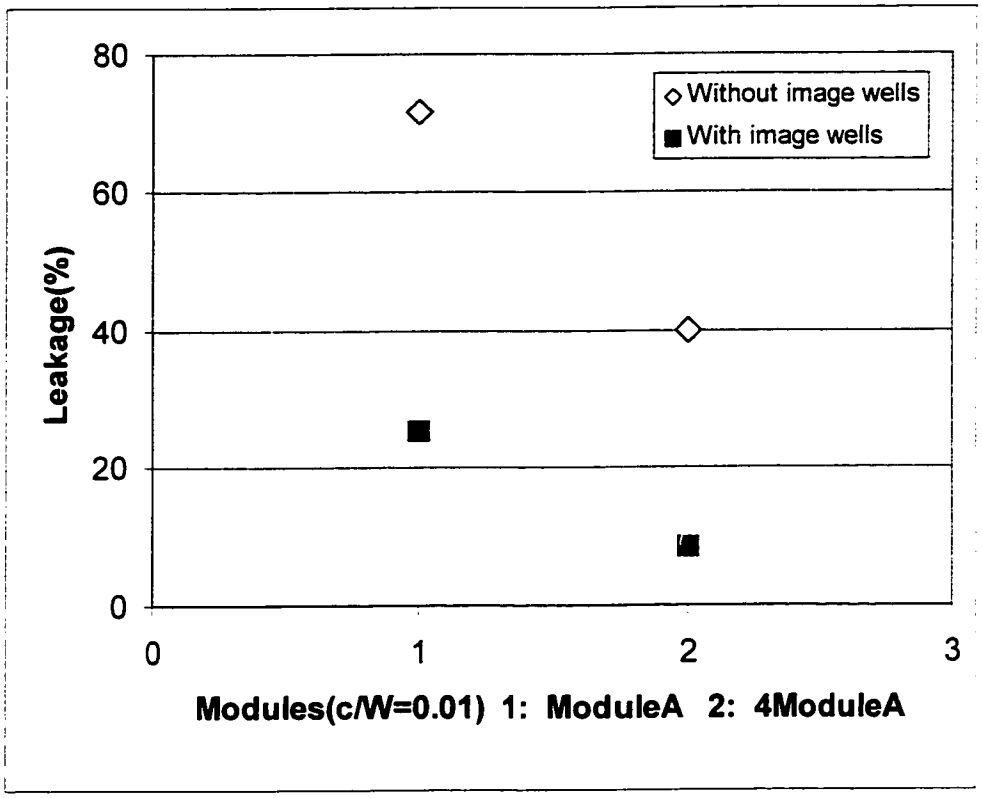

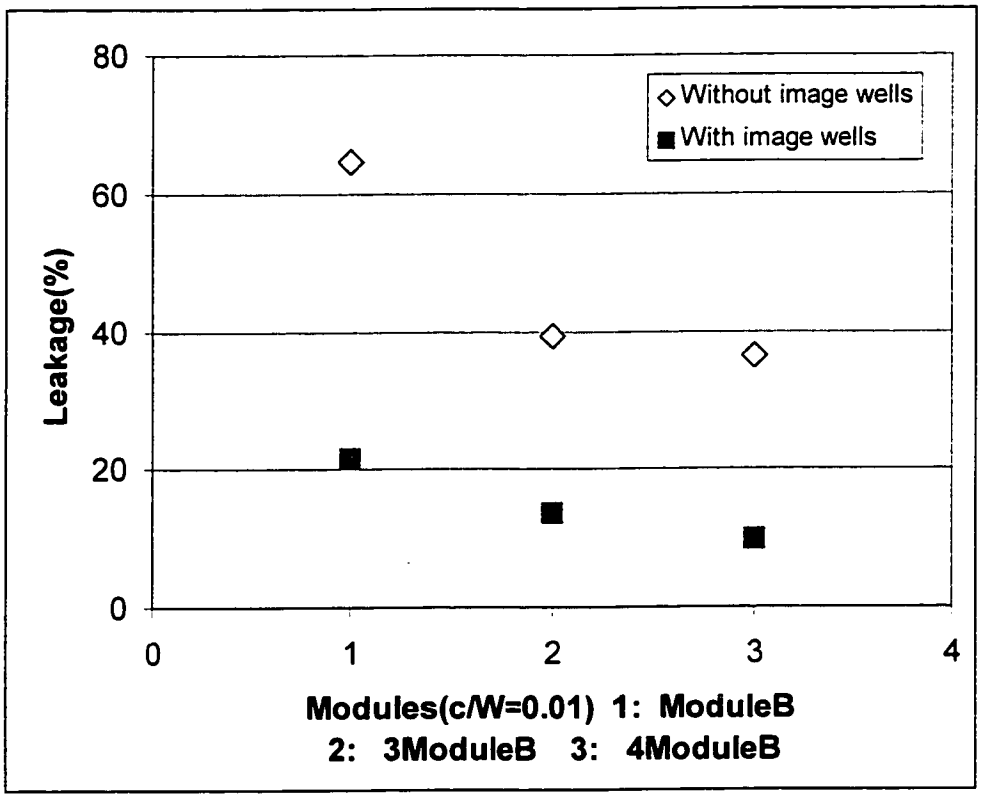

Figure 4.2 Modules & calculated leakage at c/W=0.01

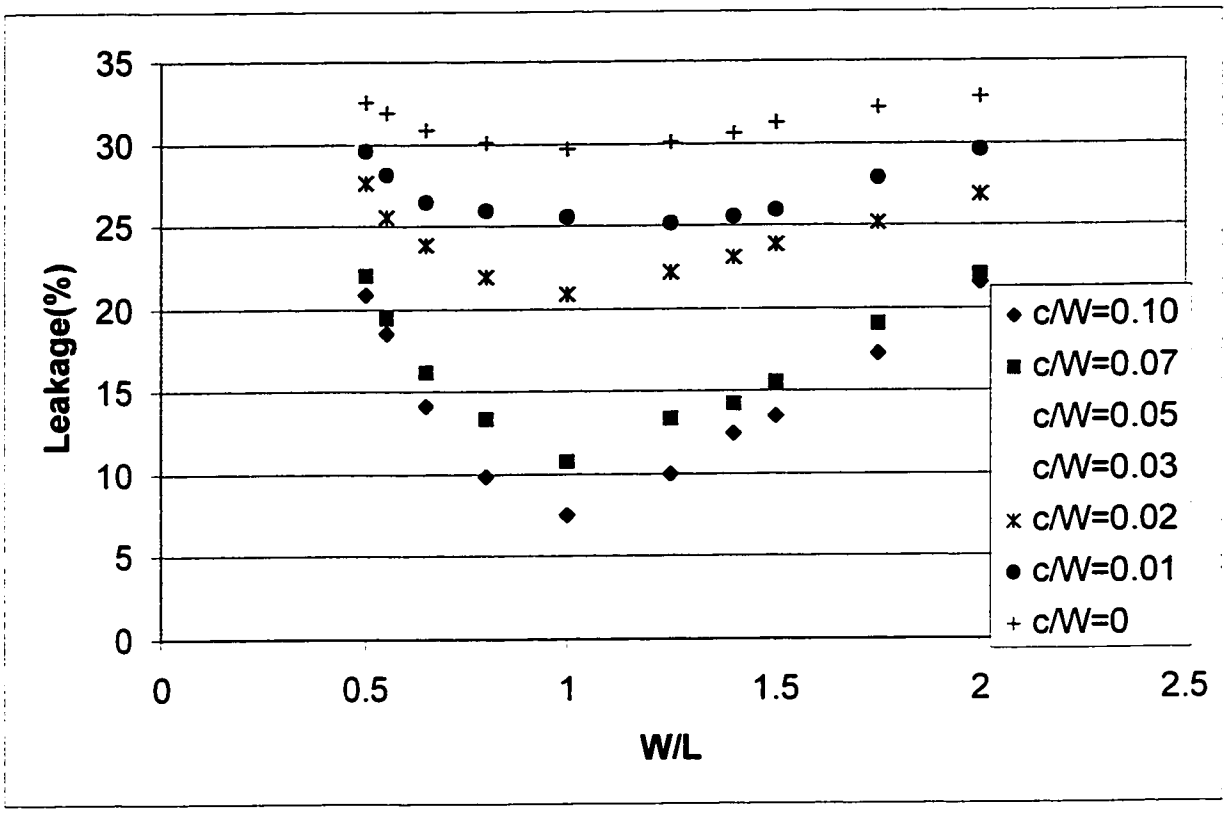

Figure 4.3 Module A : Leakage variation with W/L and c/W

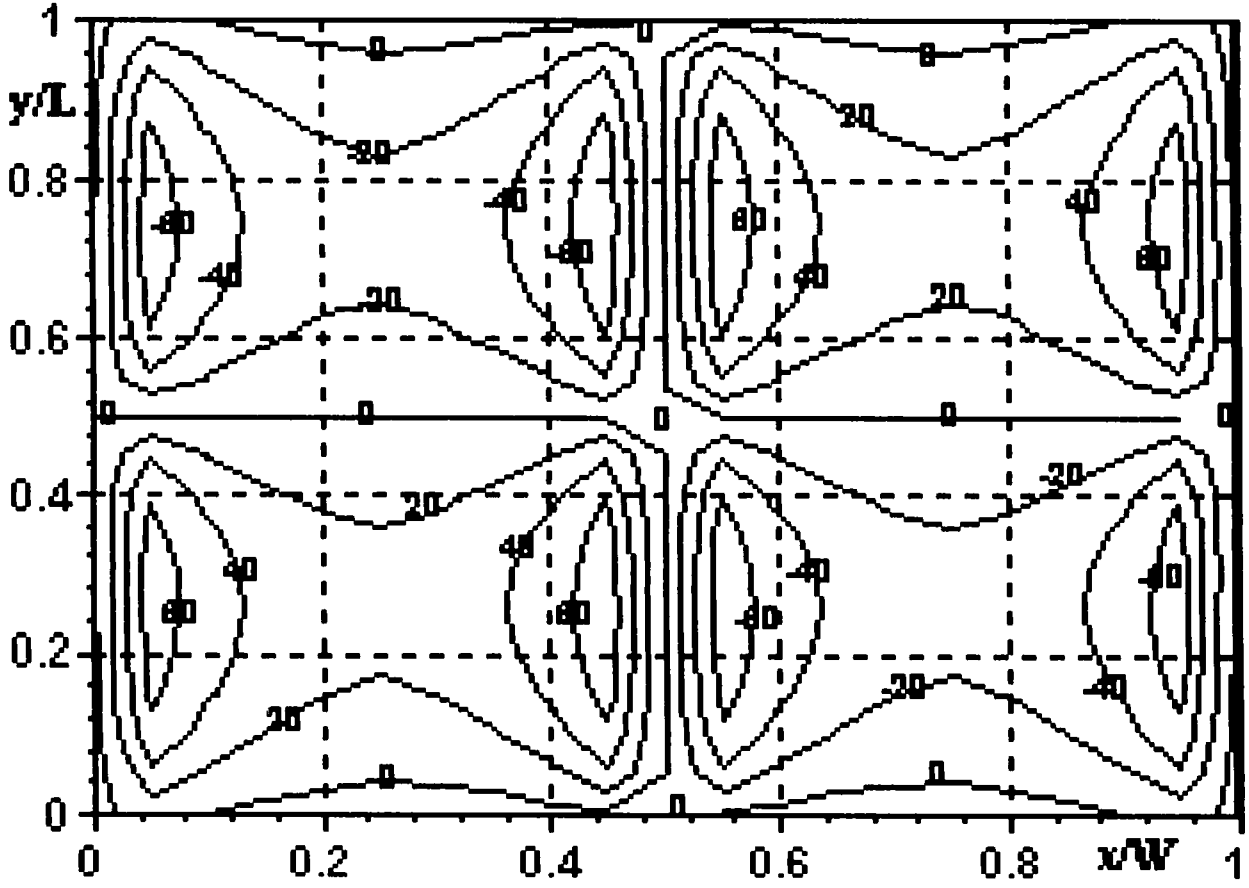

Fig. 4.4a: Flow Characteristics for 4 Modules A with Image Wells - Streamlines

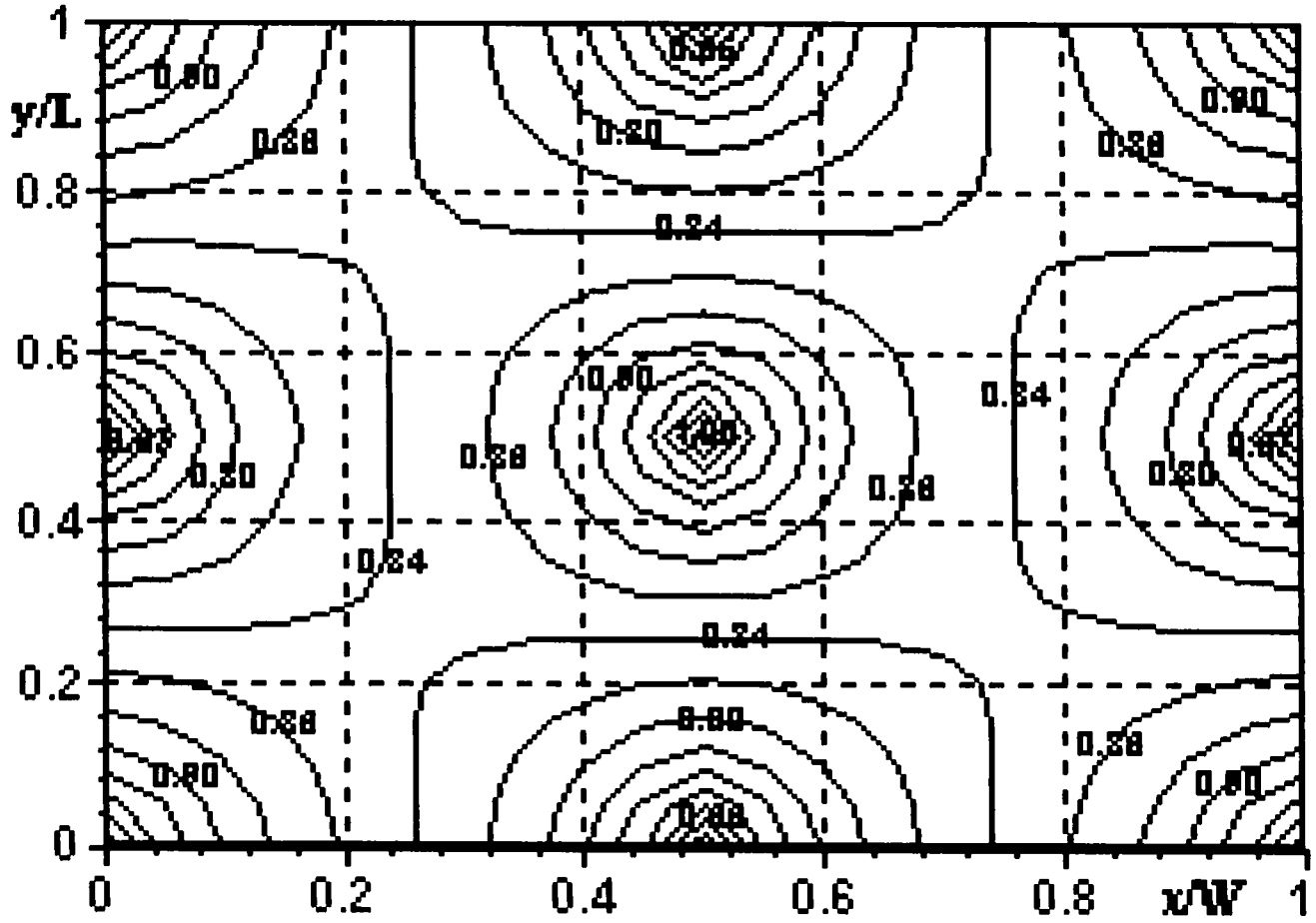

Fig. 4.4b : Flow Characteristics for 4 Modules A with Image Wells - Pressure Head Distribution

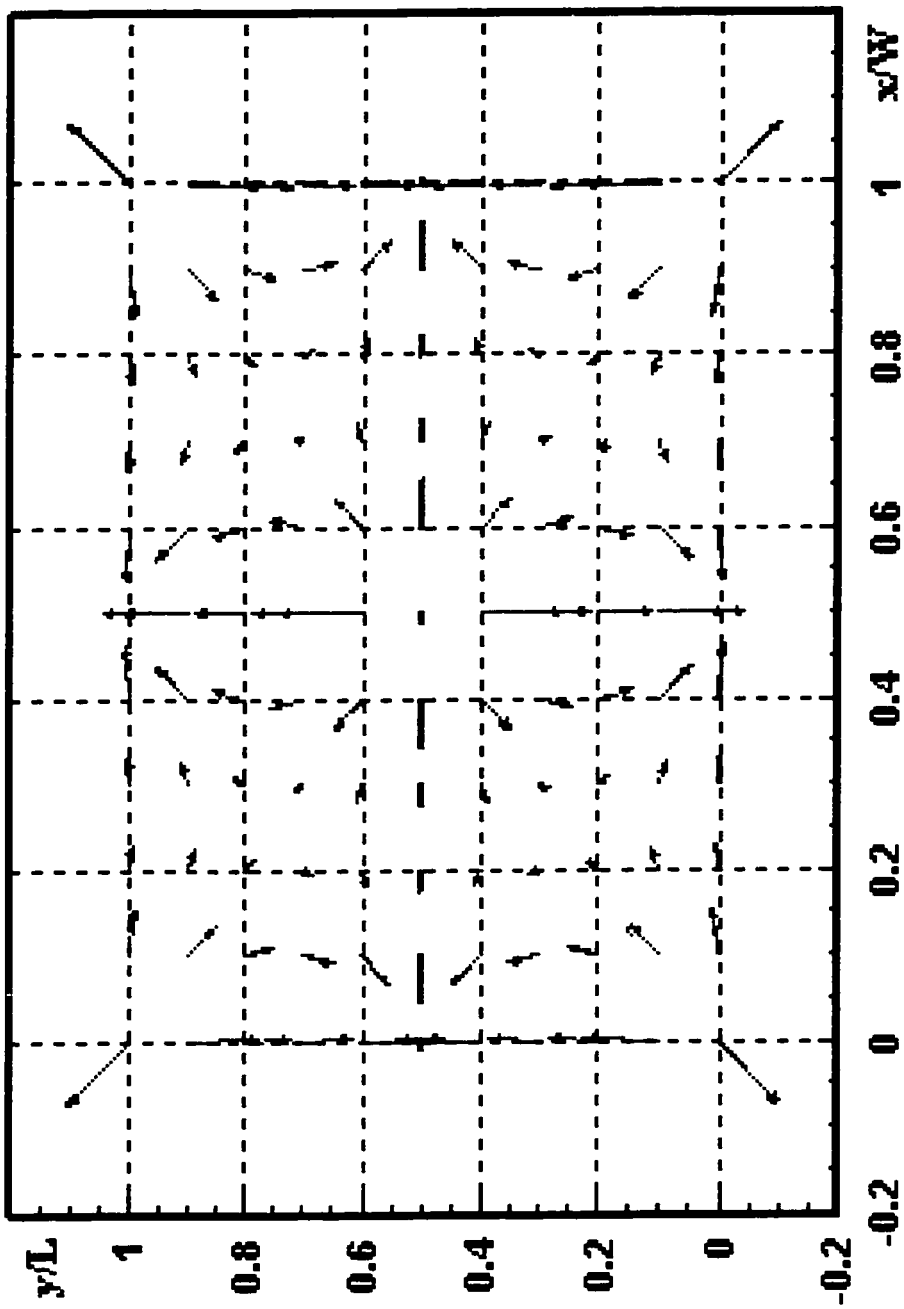

Fig. 4.4c: Flow Characteristics for 4 Modules A with Image Wells – Velocity Vector Plots

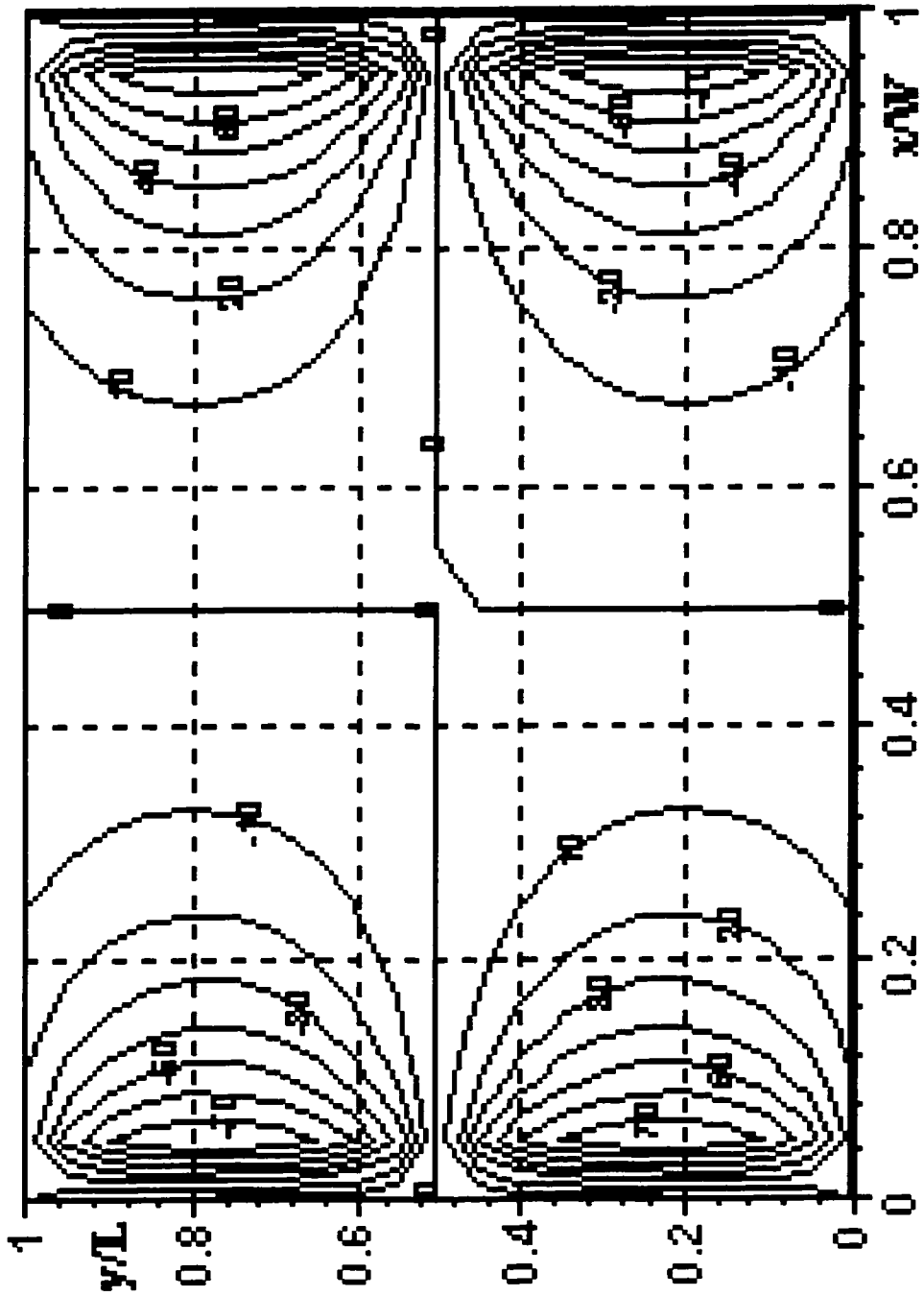

Fig. 4.5a: Flow Characteristics for Module B with Image Wells- Streamlines

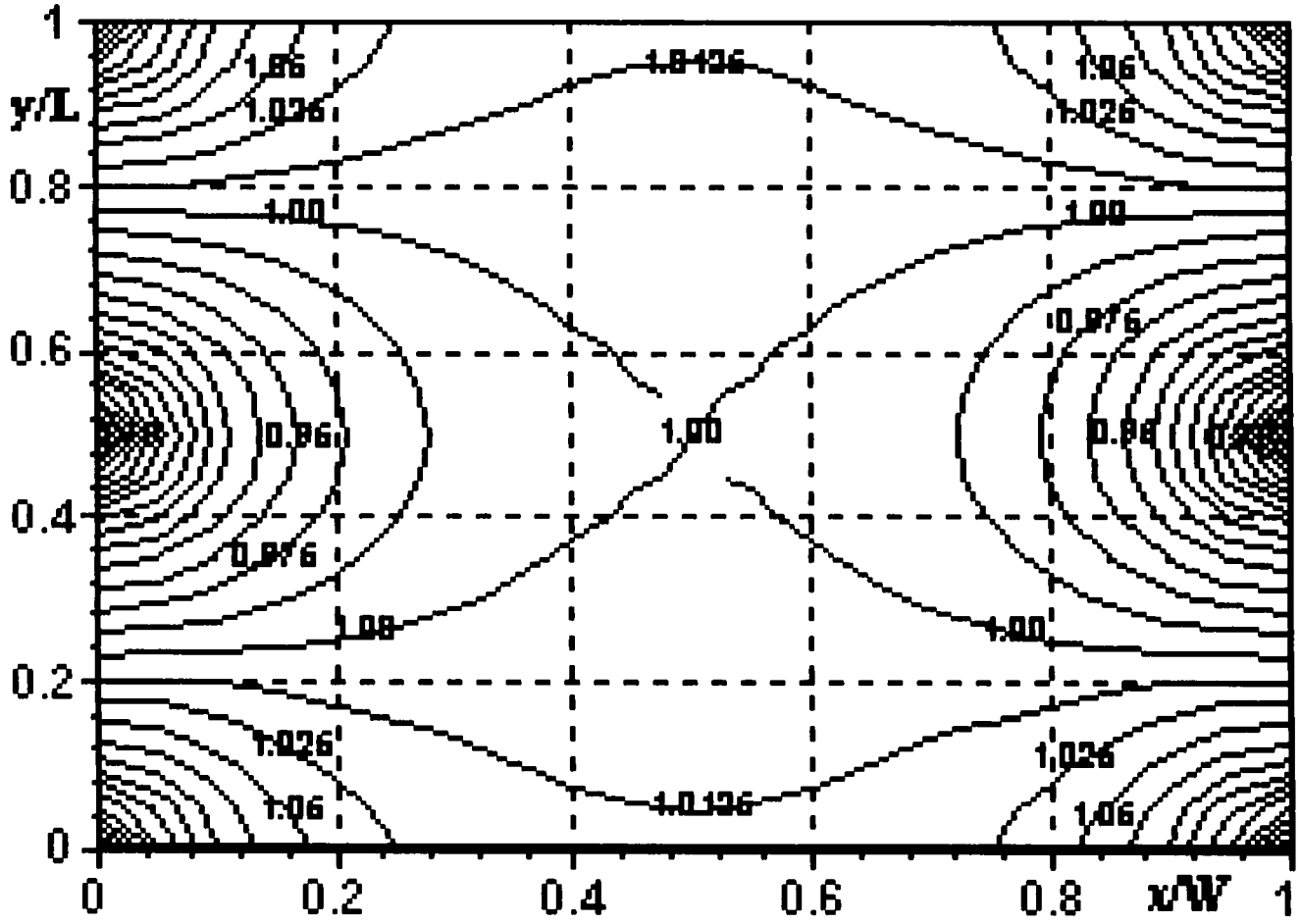

Fig. 4.5b : Flow Characteristics for Module B with Image Wells - Pressure Head Distribution

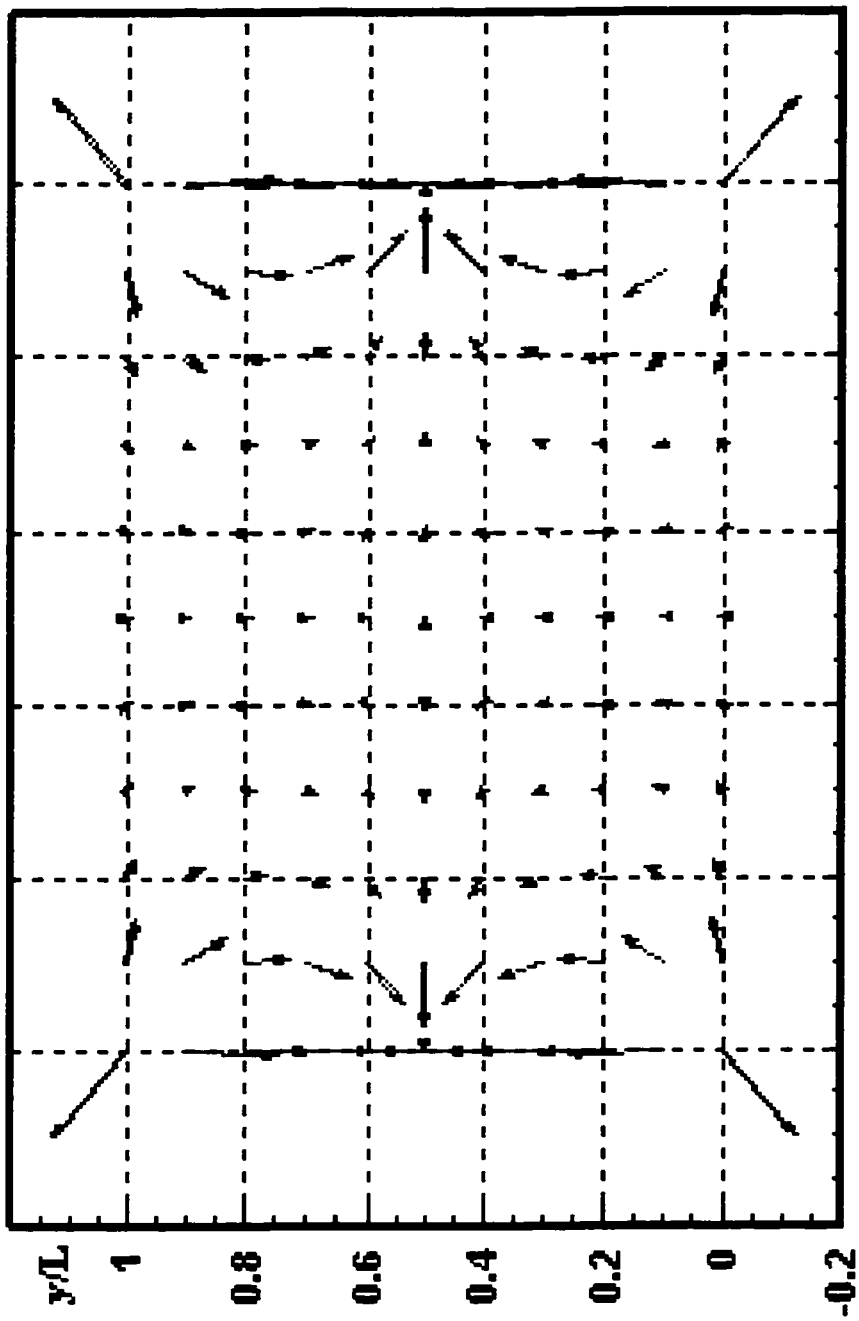

Fig. 4.5c: Flow Characteristics for Module B with Image Wells - Velocity Vector Plots

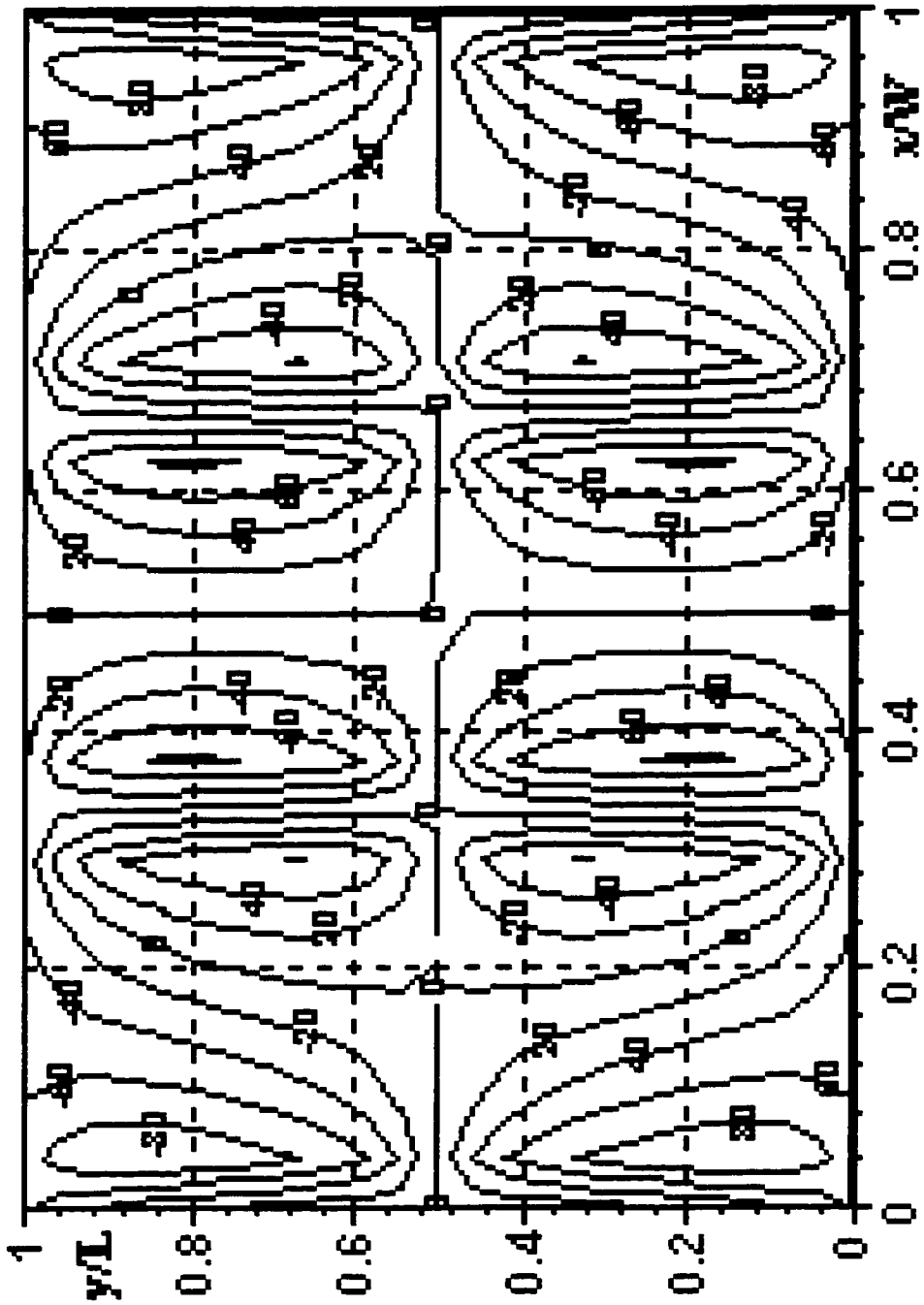

Fig. 4.6a: Flow Characteristics for 3 Modules B with Image Wells - Streamlines

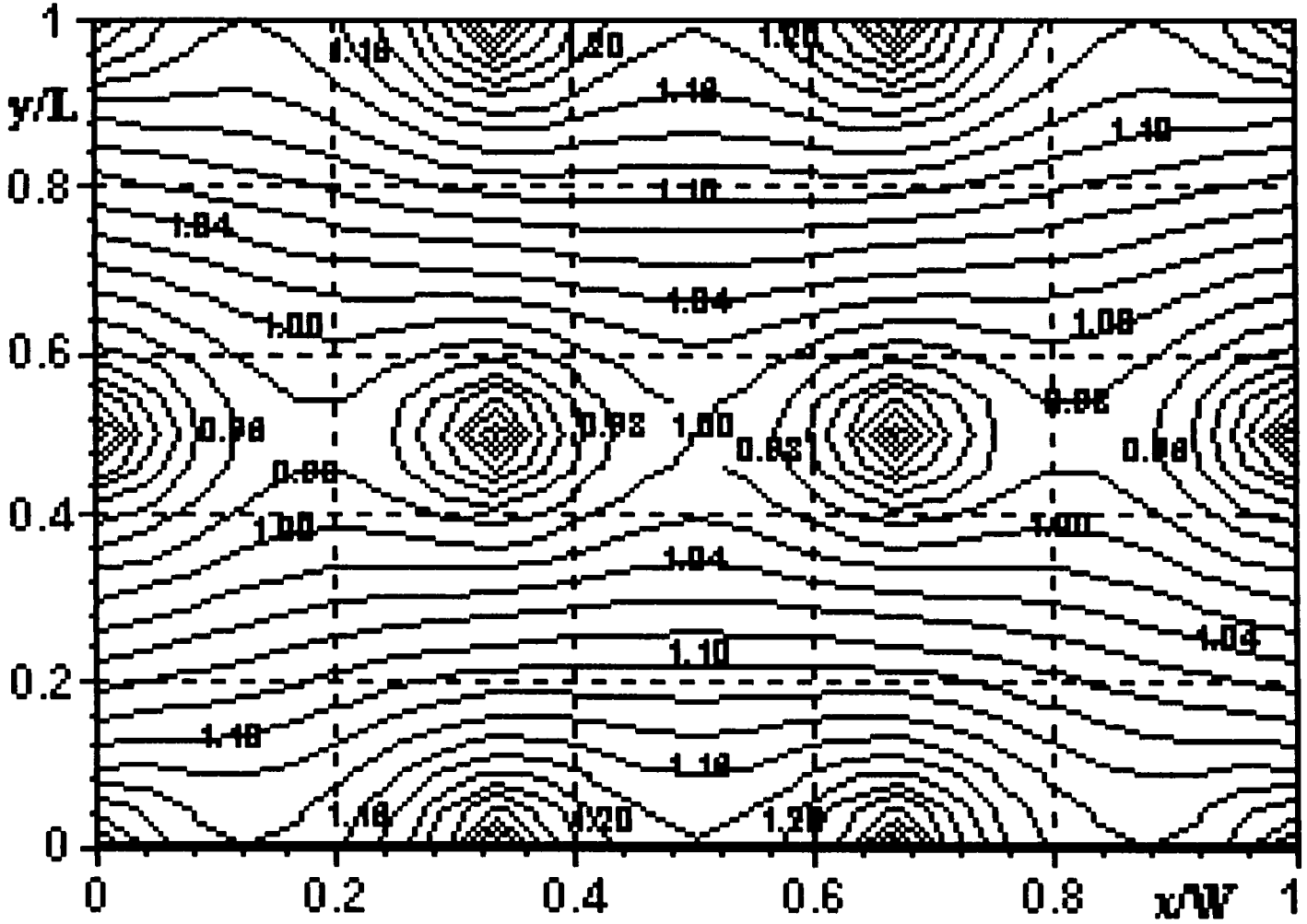

Fig. 4.6b : Flow Characteristics for 3 Modules B with Image Wells - Pressure Head Distribution

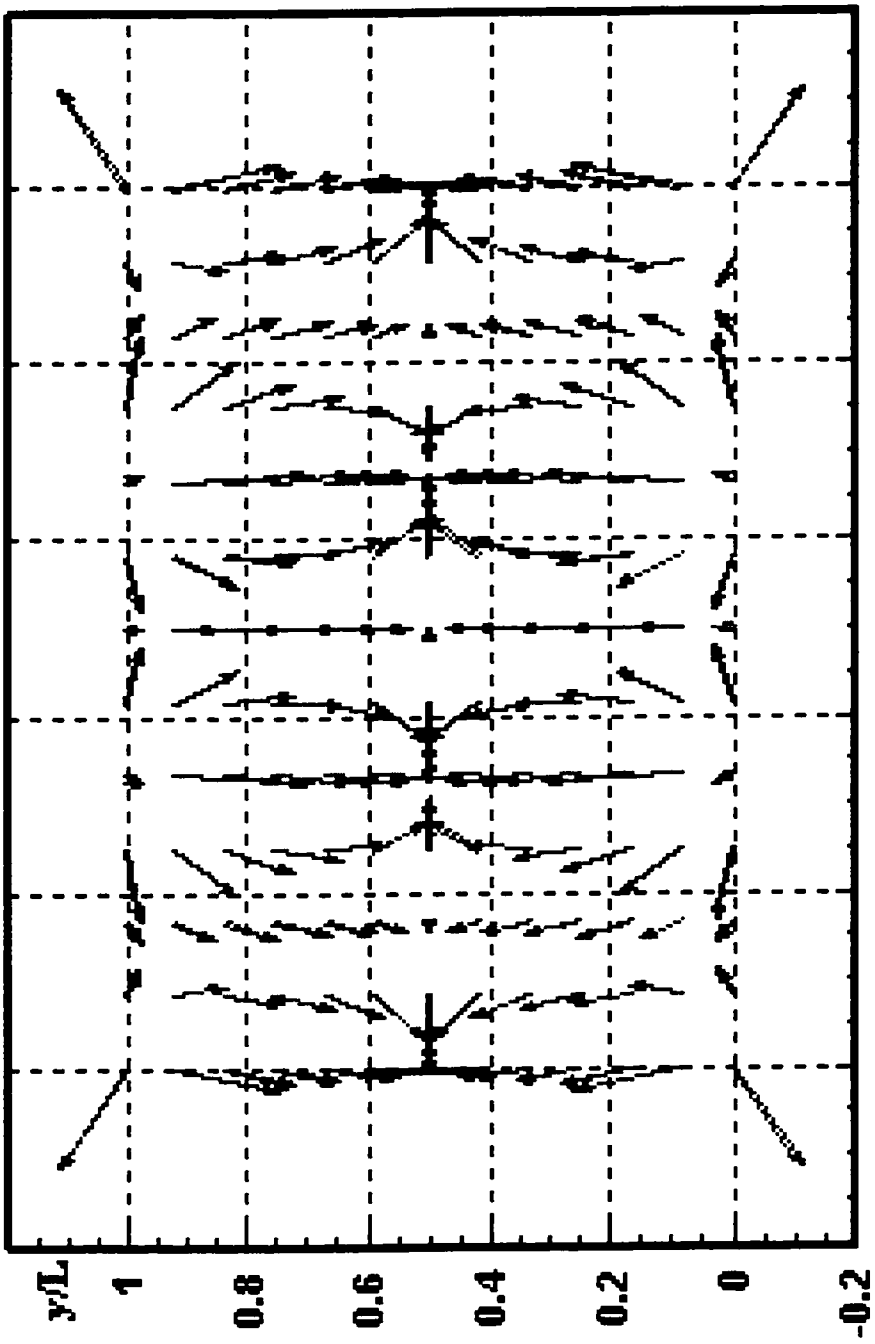

Fig. 4.6c: Flow Characteristics for 3 Modules B with Image Wells - Velocity Vector Plots

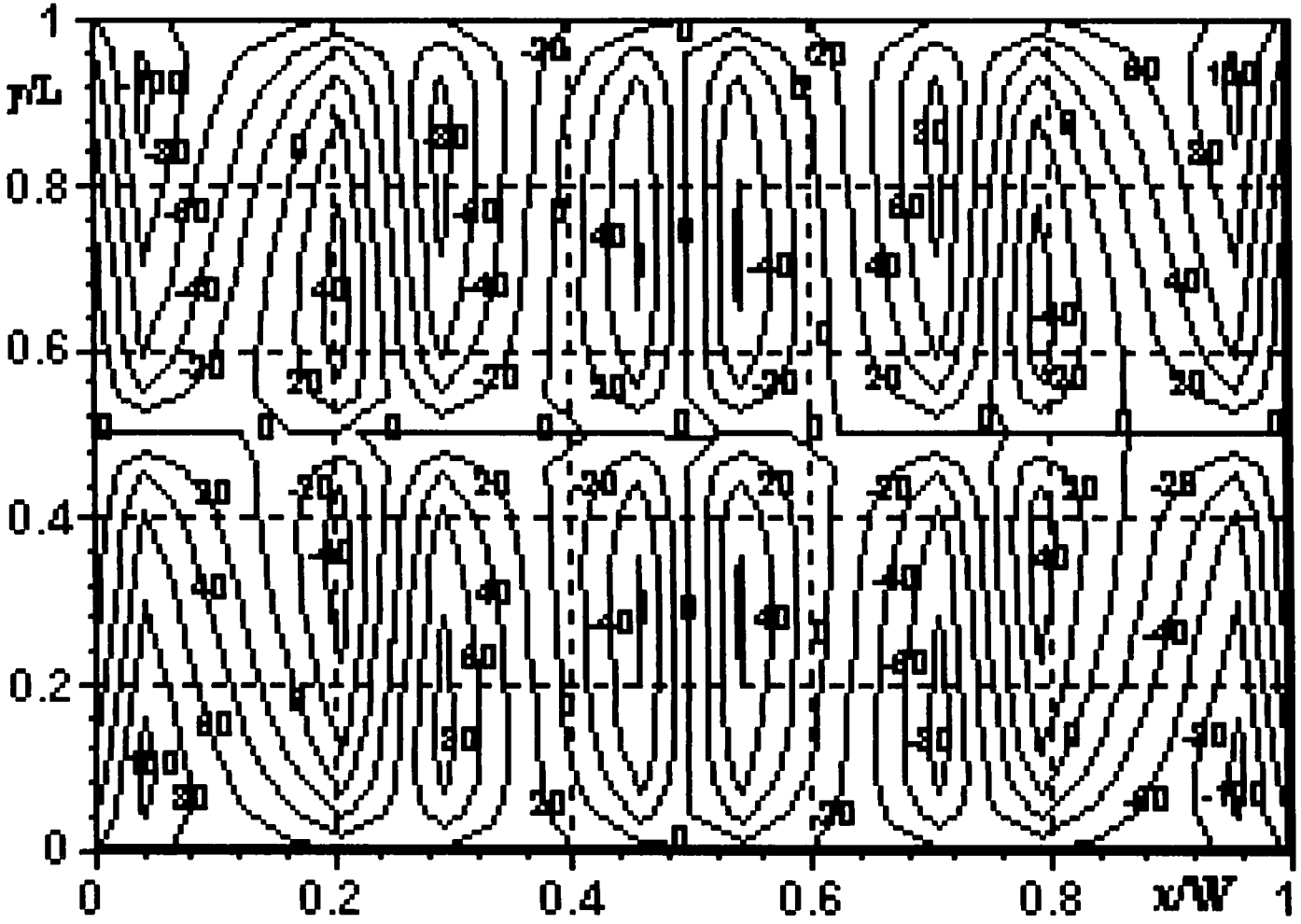

Fig. 4.7a: Flow Characteristics for 4 Modules B with Image Wells - Streamlines

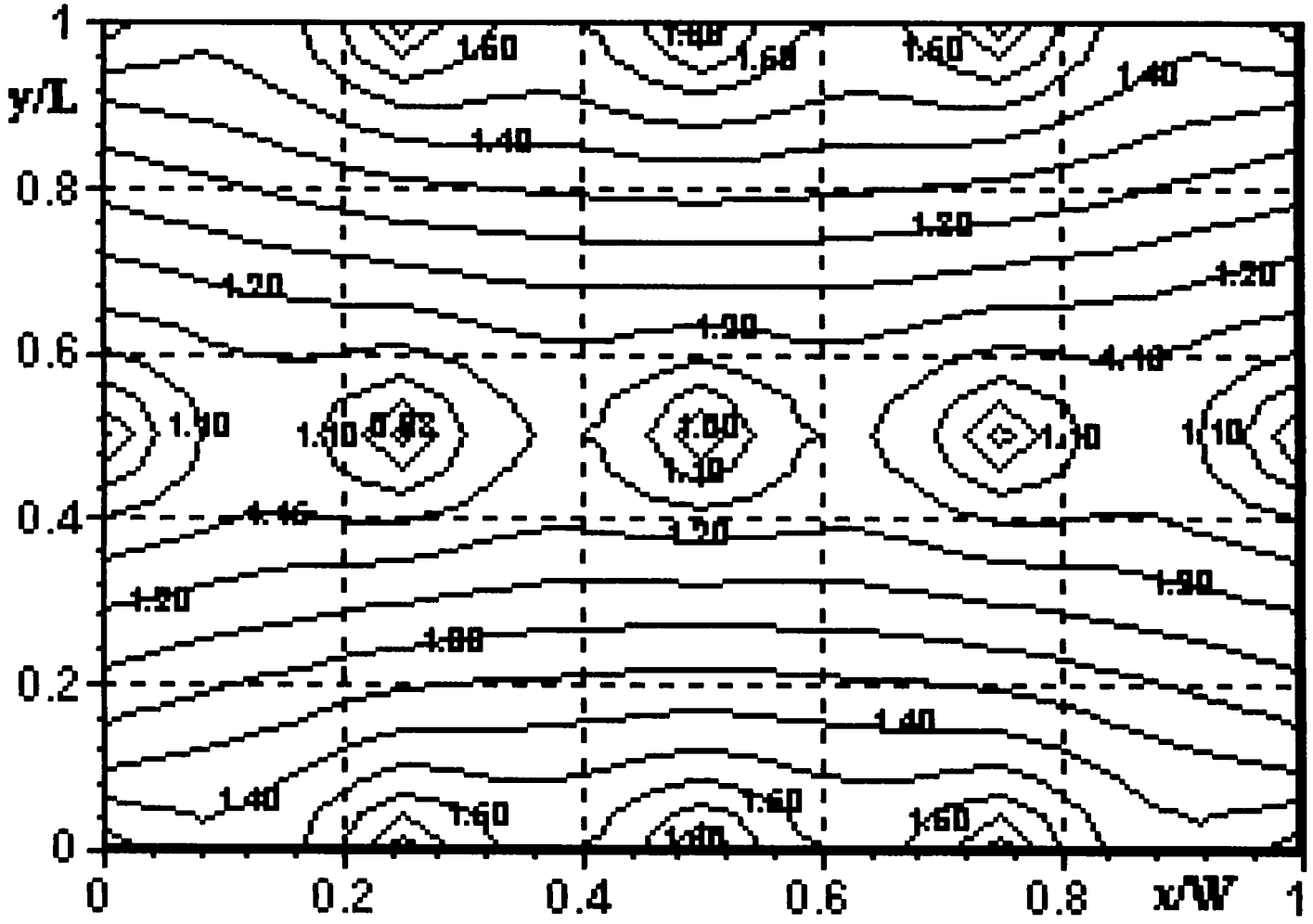

Fig. 4.7b : Flow Characteristics for 4 Modules B with Image Wells - Pressure Head Distribution

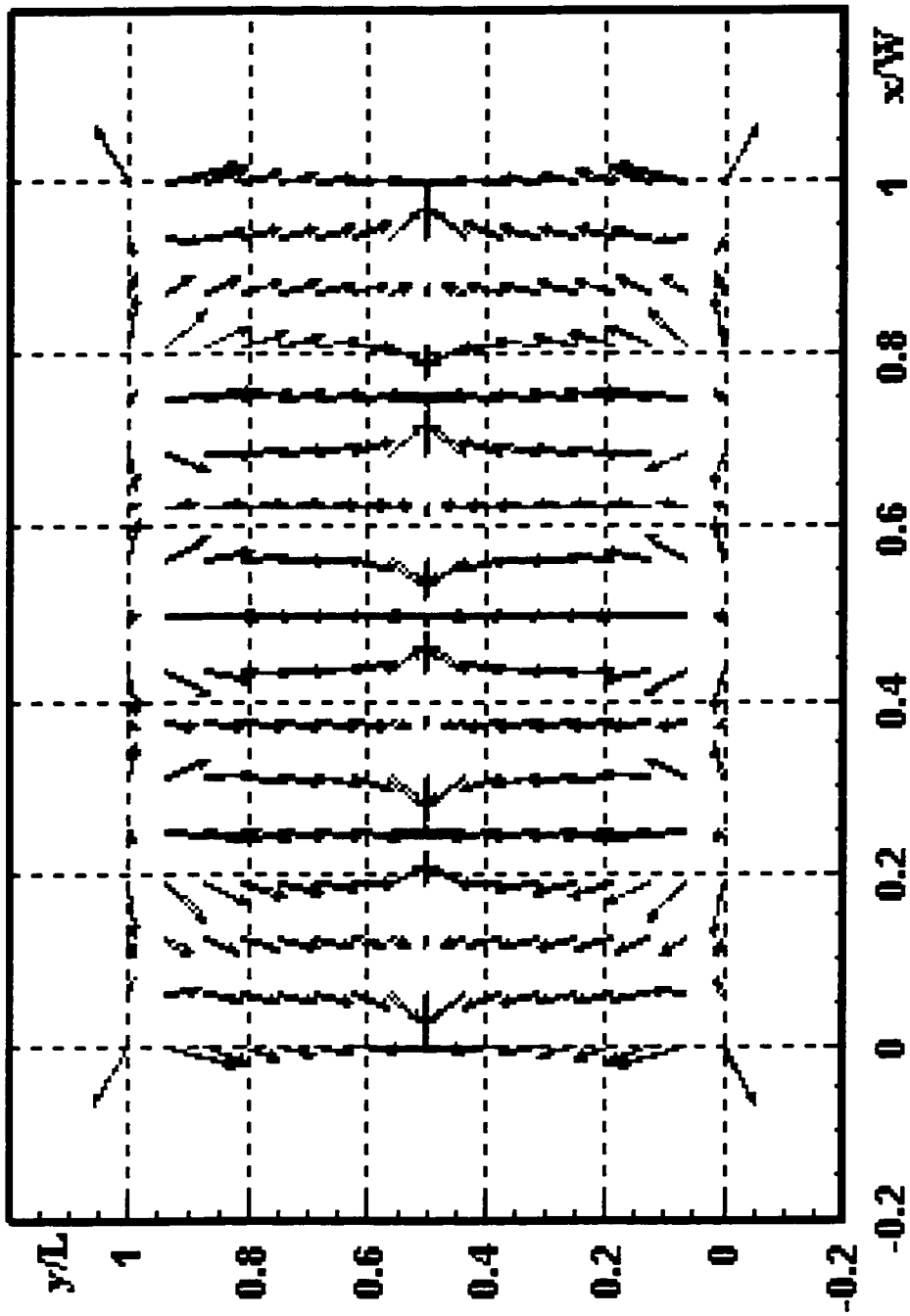

Fig. 4.7c: Flow Characteristics for 4 Modules B with Image Wells - Velocity Vector Plots

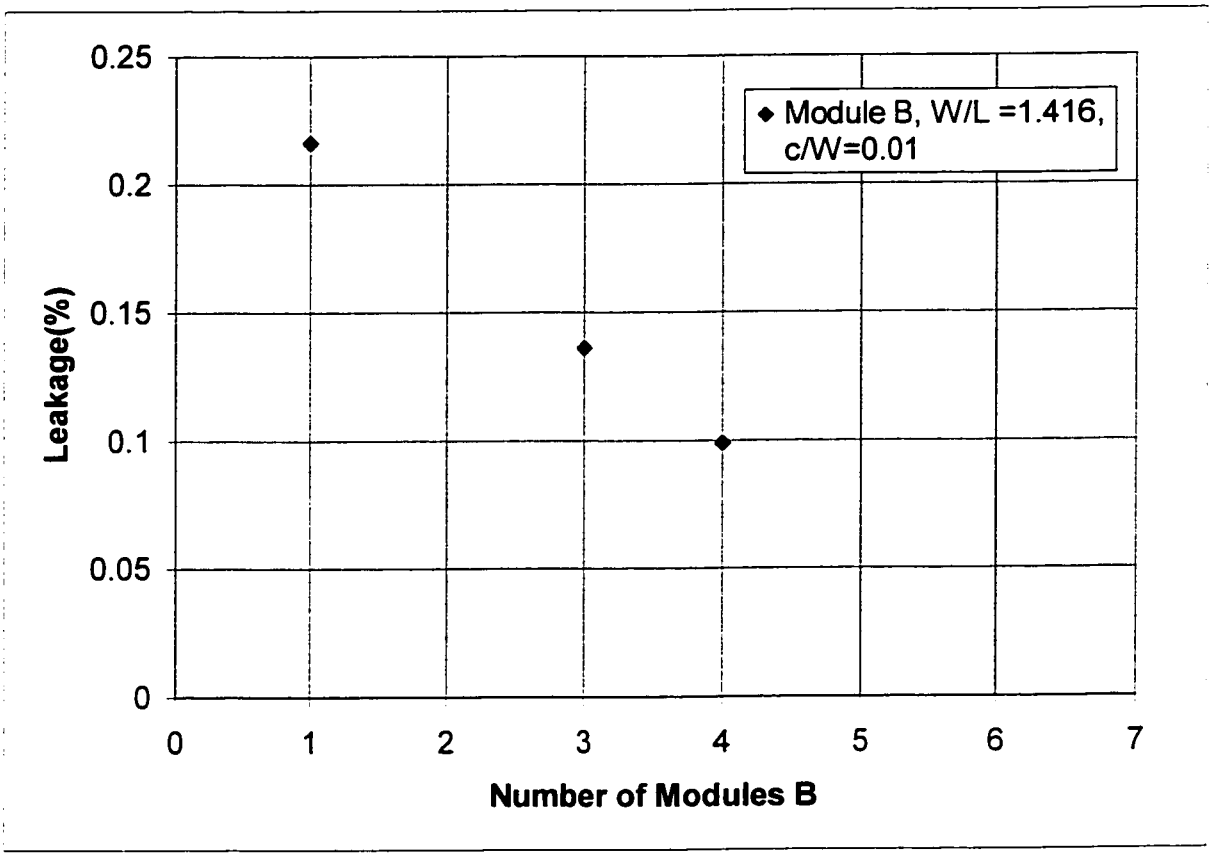

Fig. 4.8 Variation of leakage (%) with the number of modules B

CHAPTER FIVE

Experimental equipment and Conditions

To evaluate the effectiveness of the hydrodynamic barriers produced by image wells and to verify predictions in Chapter four, a lab demonstration unit (Fig.5.1) was designed and installed at the Water Resource Lab.

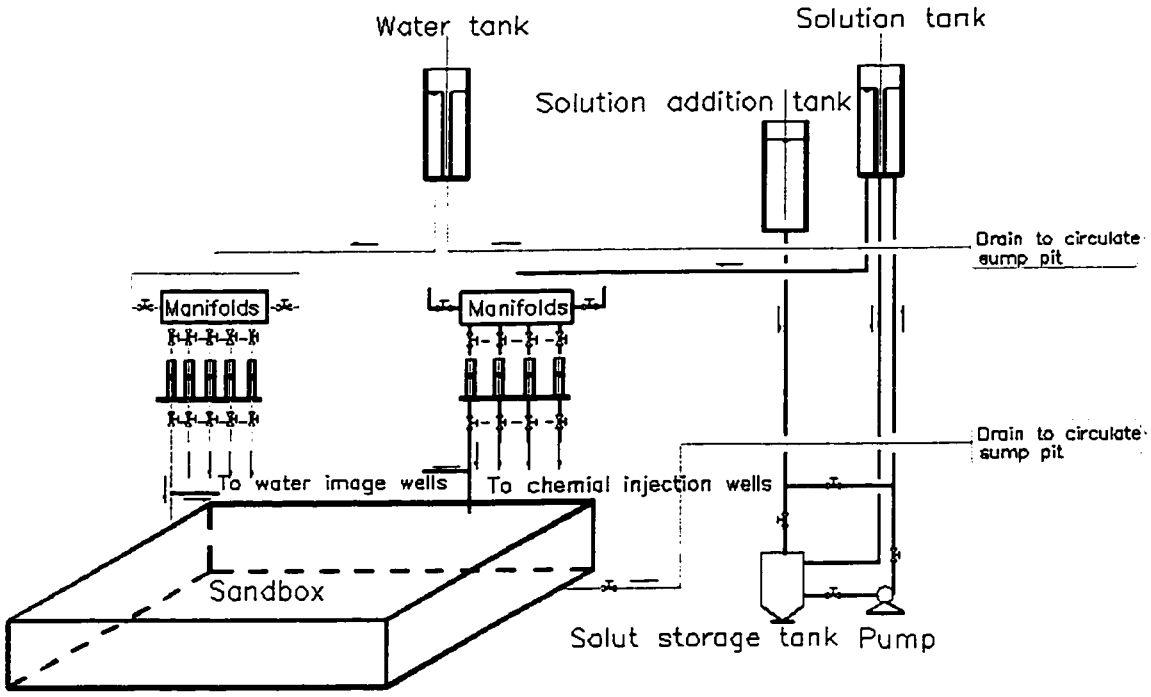

Fig5.1 Lab demo unit scheme (without wells in place)

The system design for the experimental apparatus must consider the following factors: volume and flow direction for both chemical (salt solution) and water, homogeneous flow to each injection point, as well as a means to monitoring and control the system accurately. The unit and its main components were described below.

5.1 Soil Media Characteristics

Ottawa sand was selected as soil in this study for its uniform mineral composition, low particle porosity, and for its extremely low content of fractional organic carbon. The sand was produced by Ricci Bros, Sand Company Inc. and was purchased from Sial Inc, Canada of Montreal with particle sizes from 0.71 mm(mesh # 24) to 2.36mm (mesh # 8) and mean partial size of 1.5mm was adapted. Prior to use, the sand was sieved to remove particle size finer than 0.71mm and coarser than 2.36mm and to produce grading curves. Figures of sieving procedure and result of sand size distribution were provided below.

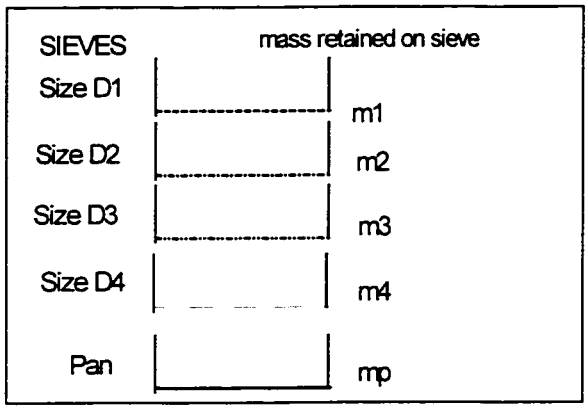

Fig. 5.2 Sieving procedure

The sand was then thoroughly washed with tap water for three times and last half hour each to remove colloidal material and to compact the space.

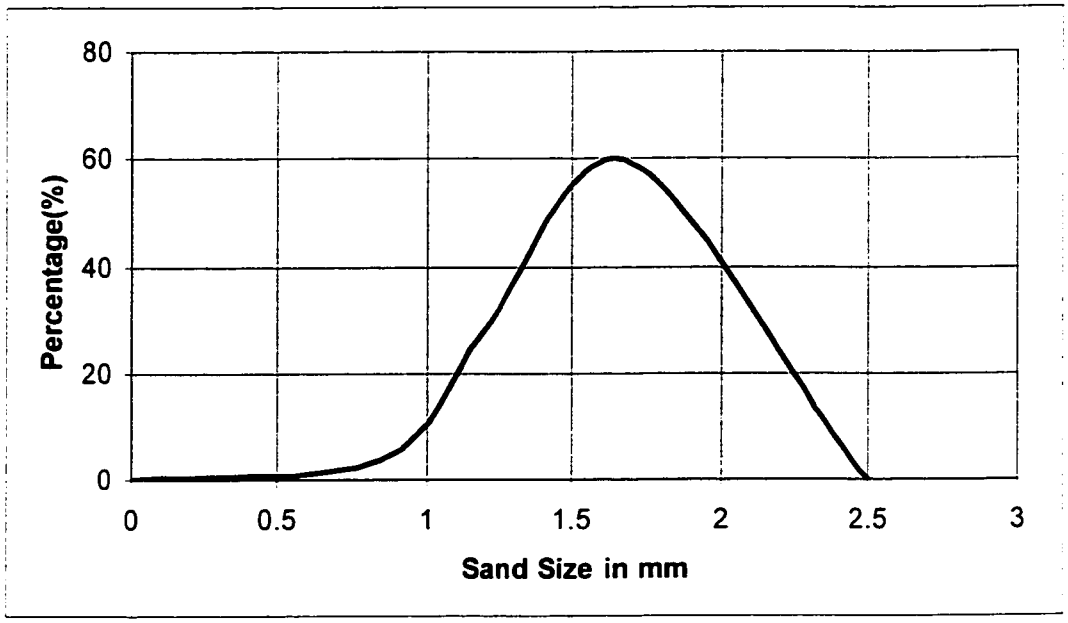

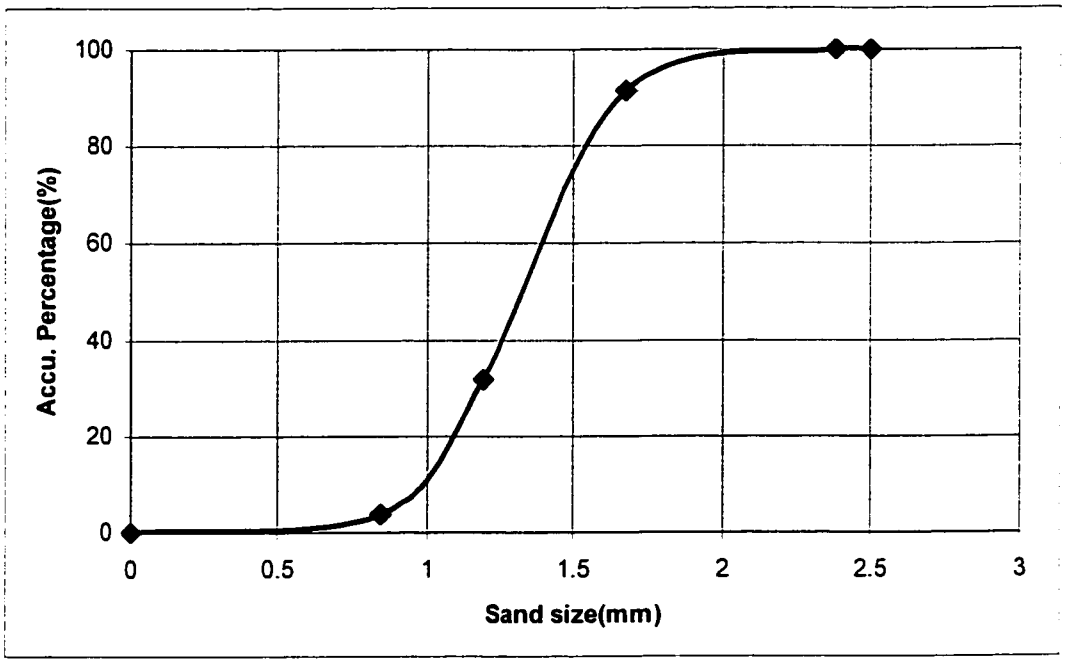

Figure 5.3 Sand size distribution

5.2 Sandbox

A rectangular shape box , noted as sandbox, was made of steel(1/4 " thick) to contain soils-sand. It is 610mm long, 806mm wide and 100mm high. There holes on sandbox to

serve as source and sink points. Figure 5.4 provides details on sandbox and brass tubes to plug in those holes.

The sandbox was horizontally placed on the table after fully packed with Ottawa sand with an enhanced compaction procedure.

5.3 Chemical

Table salt solution was selected as chemical because of it's nonreactive property. It was injected to sandbox through the wells. In the experiments, the salt solution was produced with concentration of 0.1N .

5.4 Packing

The sandbox was packed using an enhanced standardised procedure by putting the sandbox on a vibrator . Since the packing uniformity increases with layer thinness, thin 5 cm layers was employed and each layer was vibrated for 2 hours .

5.5 Instruments

The instruments used in the experiments were the following:

1. A precision lab use balance to weight salt to make solution, minimum unit – 0.1g;
2. A digital conductivity meter, Fisher Scientific.

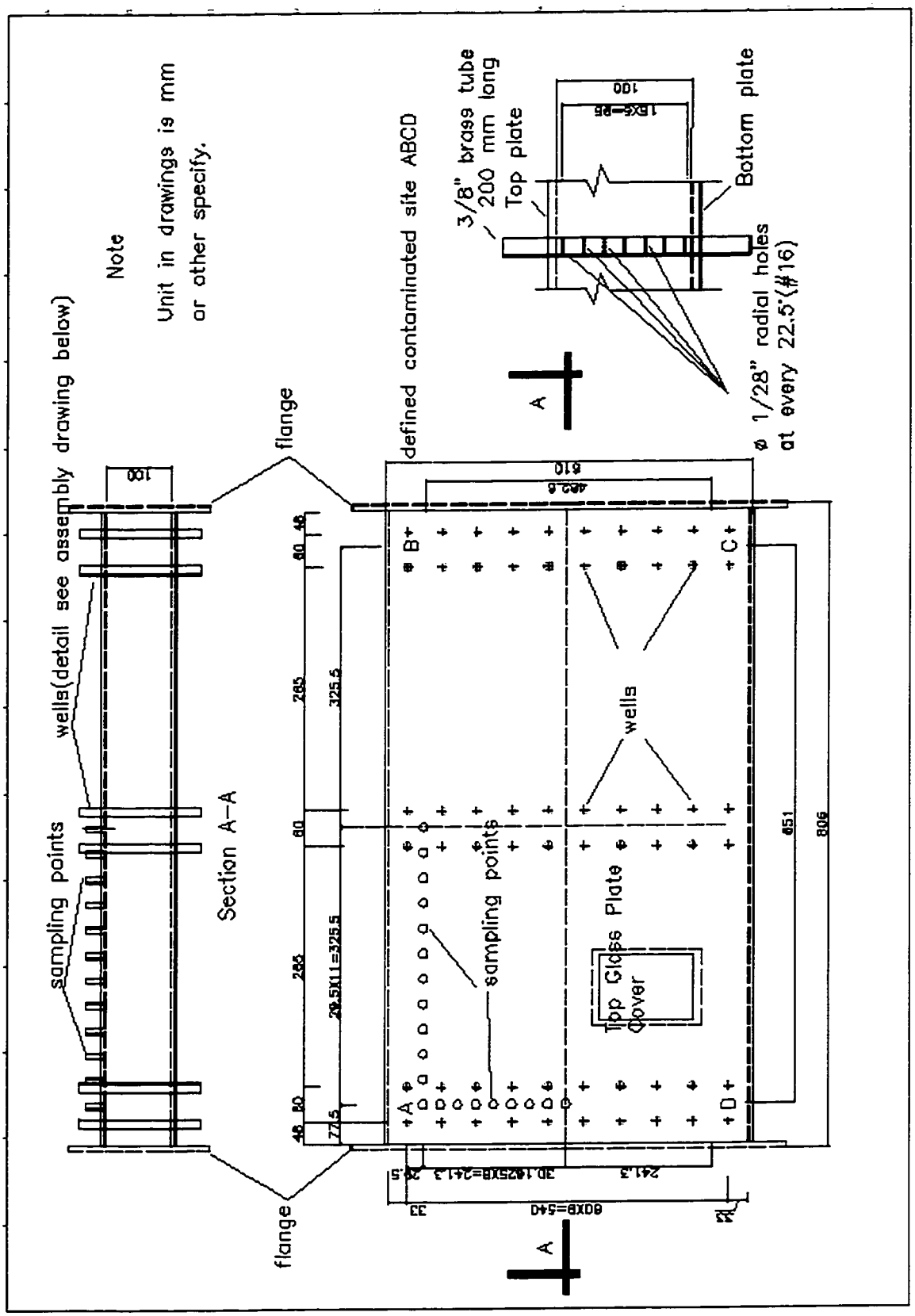

Fig. 5.4 Sandbox for tests

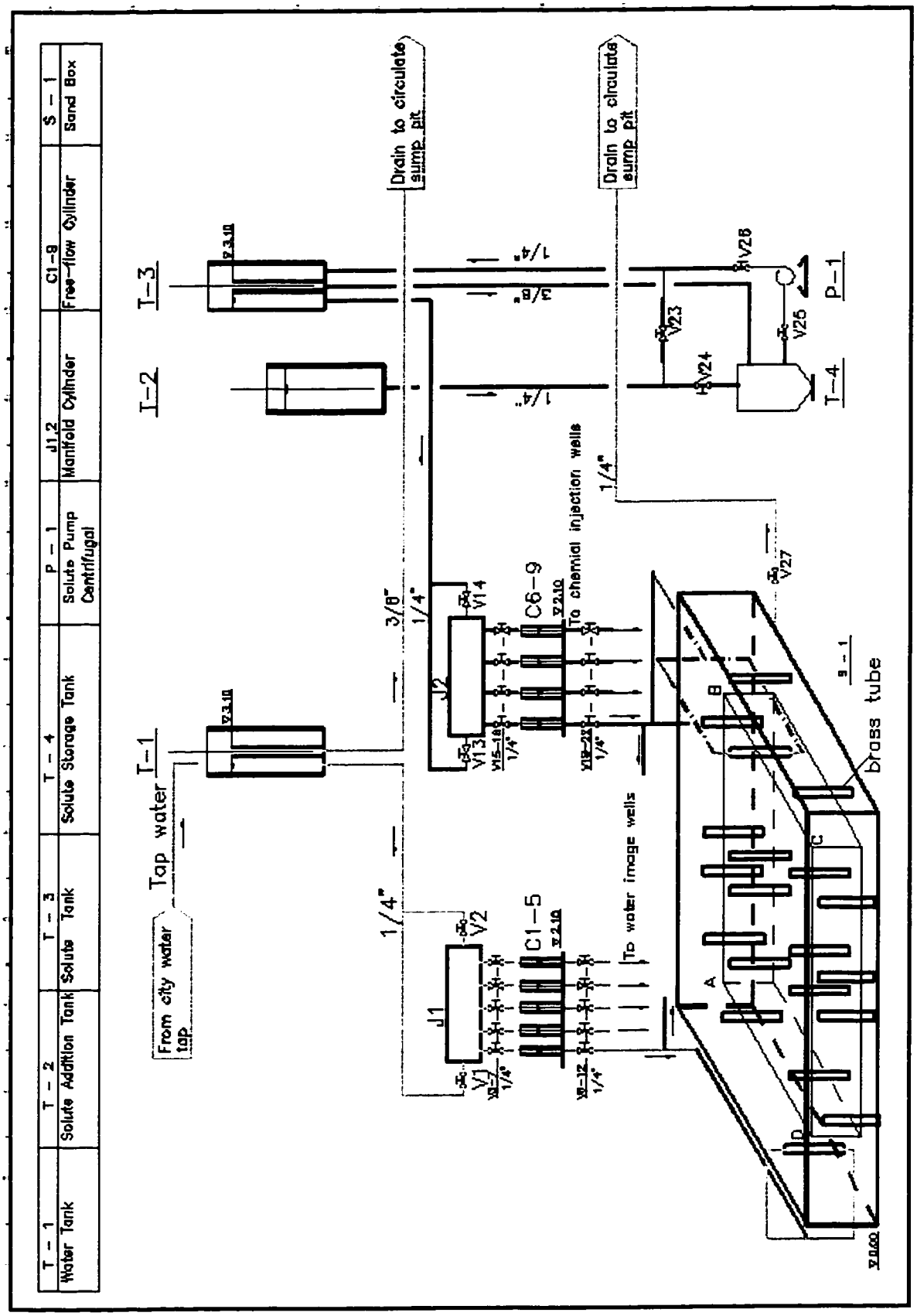

Fig. 5.5 Well and piping and system

5.6 Experimental Method

To provide a homogeneous flow to each injection point as well as a means to monitor and control the system accurately, a simple piping apparatus was developed and is shown in Figure 5.5.

5.6.1 Water

Water was supplied directly from the city water pipe which reached tank T-1 with a flow rate close to 2L/min . To keep a constant water head, an overflow tube was installed in the center of the tank. The connections for modules were described below.

During the experiments, water first flows from T-1 to conjunctional cylinder J1 with a design flow rate Q (L/min) adjusted by valve V1 and V2. With the help of valve V3-7 (the number of valves used depends on module-wells evolved), the same flow rate was achieved after each valve which flows freely to cylinder C1-5. Water in each cylinder then flows to two or four symmetric wells in the sandbox (Figure5.6.5.7.5.8.5.9 and 5.10), valve V8-12 were used as fine adjustors to ensure that no overflow and air entrapment occurred during the experiments.

5.6.2 Salt solution

Before the start of the experiments, the 0.1N salt solution was made and stored in the tank T2,T3,T4 (Figure5.5). During the experiments, brine stored in tank T-4 was pumped P-1 to solute tank T-3, to keep a constant water head. An overflow tube was installed in

center of the tank to drain overflow back to T-4. By closing the valve V23 and open valve V24, brine stored in T-2 flows to T-4 .

During the experiments, brine first flows from T-3 to conjunctional cylinder J2 with a specified flow rate controlled by valves V13 and V14. With the help of valve V15,V16,V17,V18, the same flow rate was achieved and flow freely to cylinder(s) C6-9 (number in use is as same as valve). Brine in each cylinder then flows to two or four symmetric wells in sandbox (Figure5.6,5.7,5.8,5.9 and 5.10). Valves V19-22 provided adjustment to flow to ensure no overflow and air entrapping occurring during the experiments.

5.6.3 Water saturation

The sandbox was initially saturated with tap water from city water pipe through tank T-1. The injected water was controlled at the low flow rate of 0.5l/min and outlet valve V27 was opened gradually to provide complete saturation and to ensure the thorough removal of air from the sandbox. To ensure no air was entrapped after saturation, the outlet was kept 50mm higher than top surface of the sandbox.

5.6.4 Connections

To provide the lab experimental condition corresponding to each module, specific piping connections were provided. The number of wells used depends on the module type chosen. To supply equal flow to image wells , the flow from the water tank (T-1 in figure 5.5) was fed to conjunctional cylinder (J1) , which in turn provided equal flow to the

image wells. Similar arrangement was done for the flow of salt solution. Total flow to the manifold cylinders –J1and J2 was adjusted to provide same effluent for each tube from both J1and J2.

Inside the contaminated site ABCD (Figure5.6,5.7,5.8,5.9 and 5.10) , real sources with same marked number were connected , so were image sources outside ABCD. Each sink was individually connected to drain. For all connected wells, the top and bottom of brass tube were connected to provide homogeneous flow via small holes.

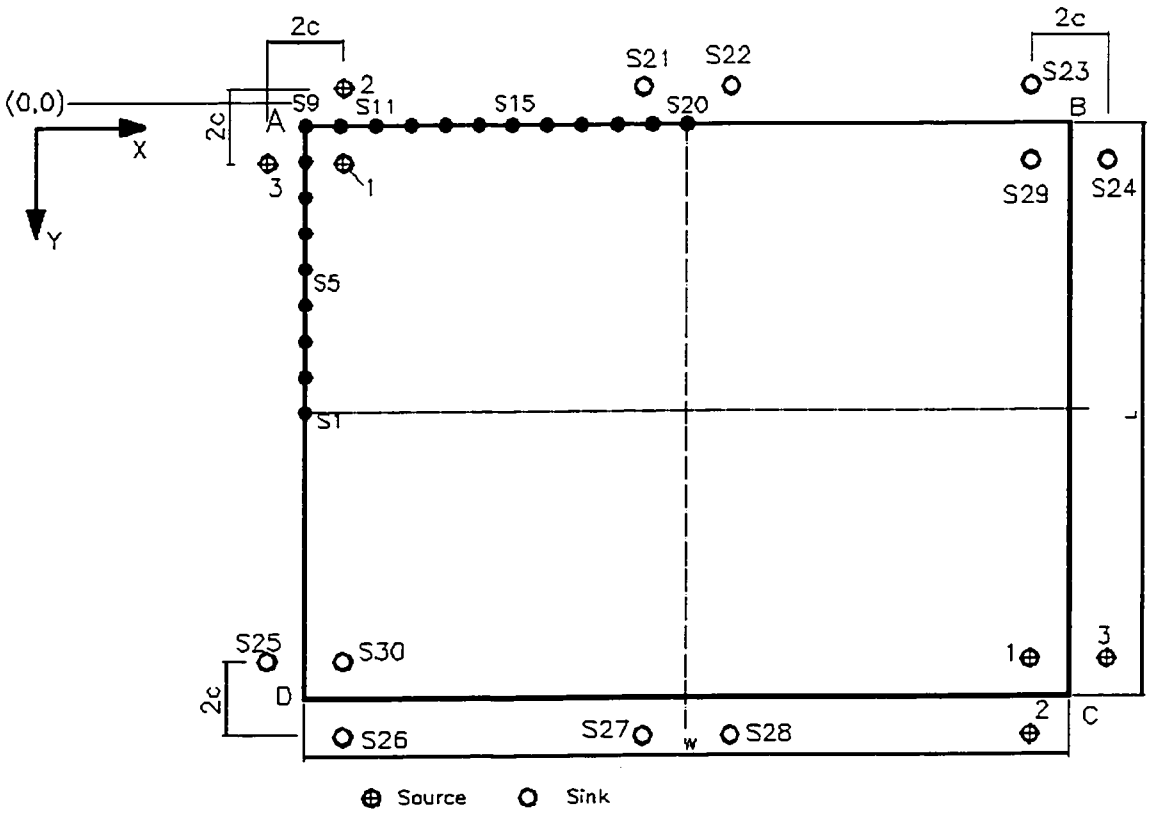

Fig. 5.6 Module A unit

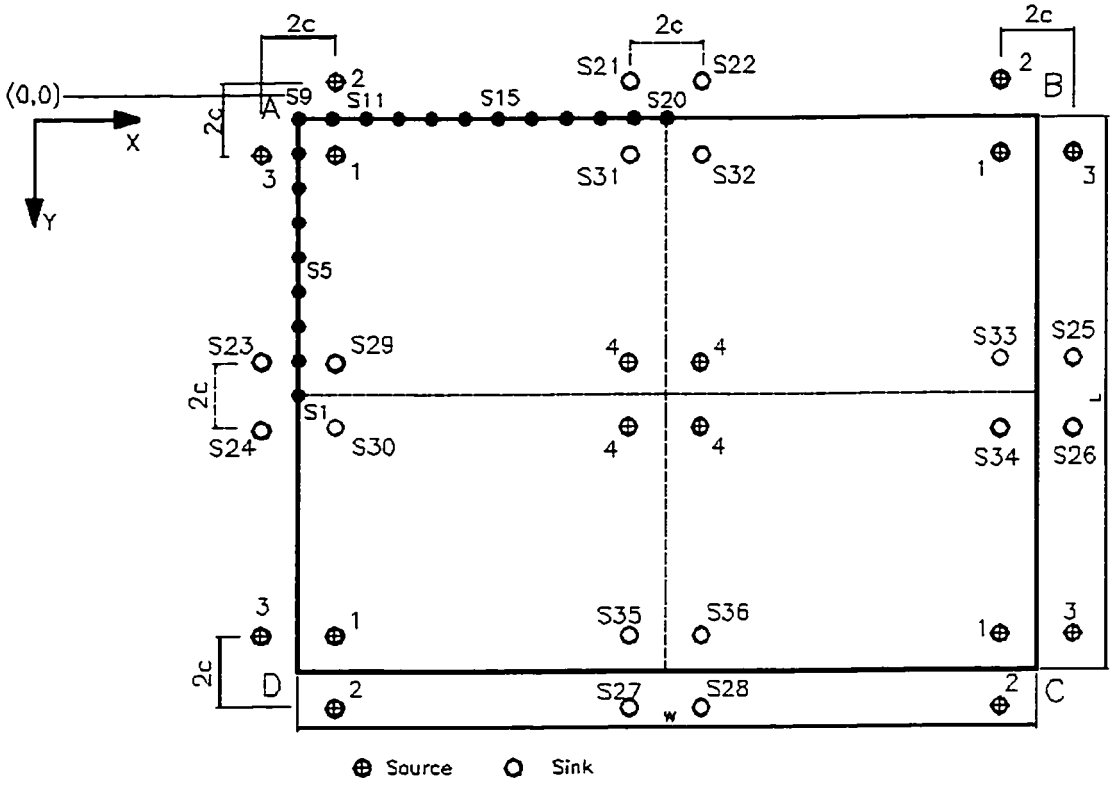

Fig.5.7 4-module A unit

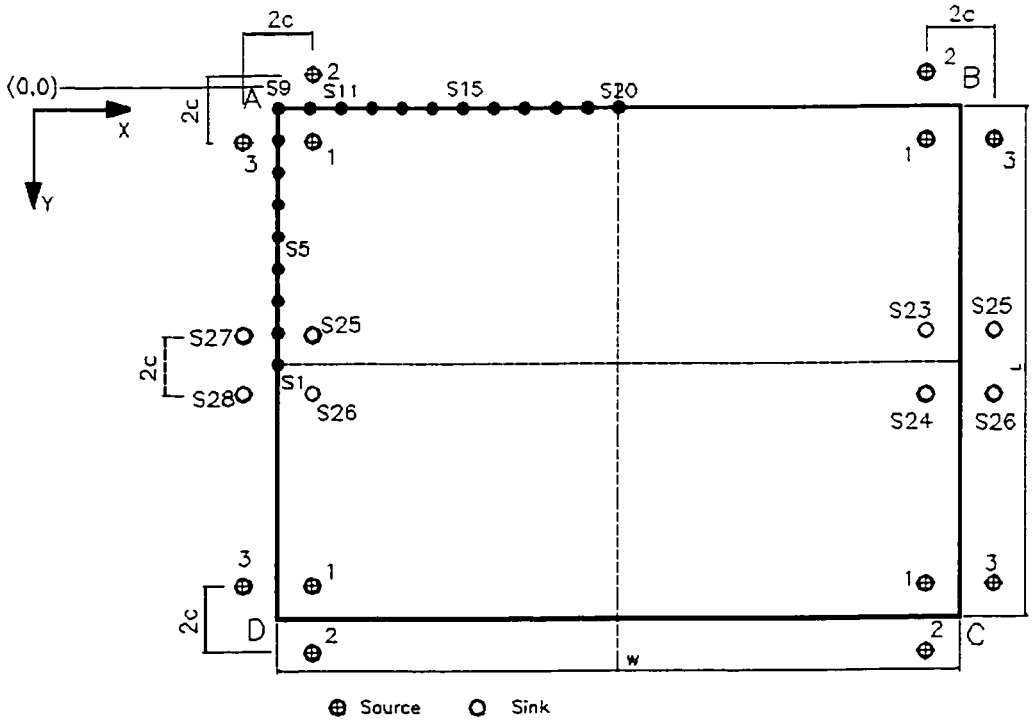

Fig.5.8 Module B unit

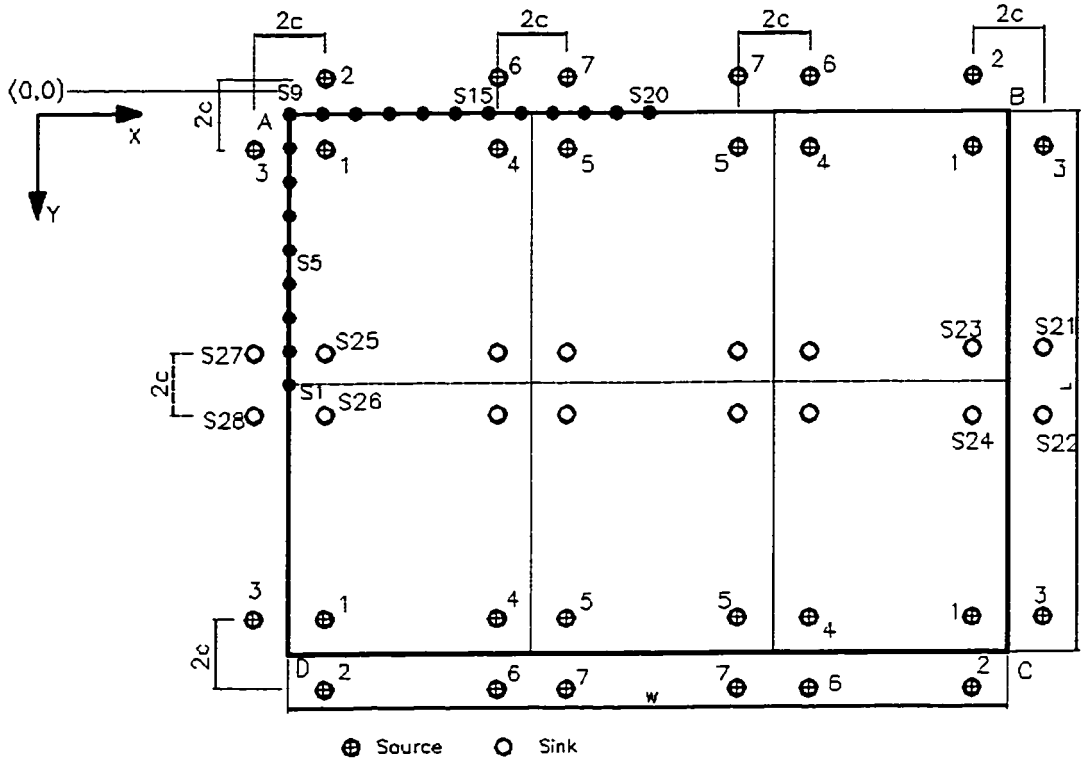

Fig.5.9 3 module B unit

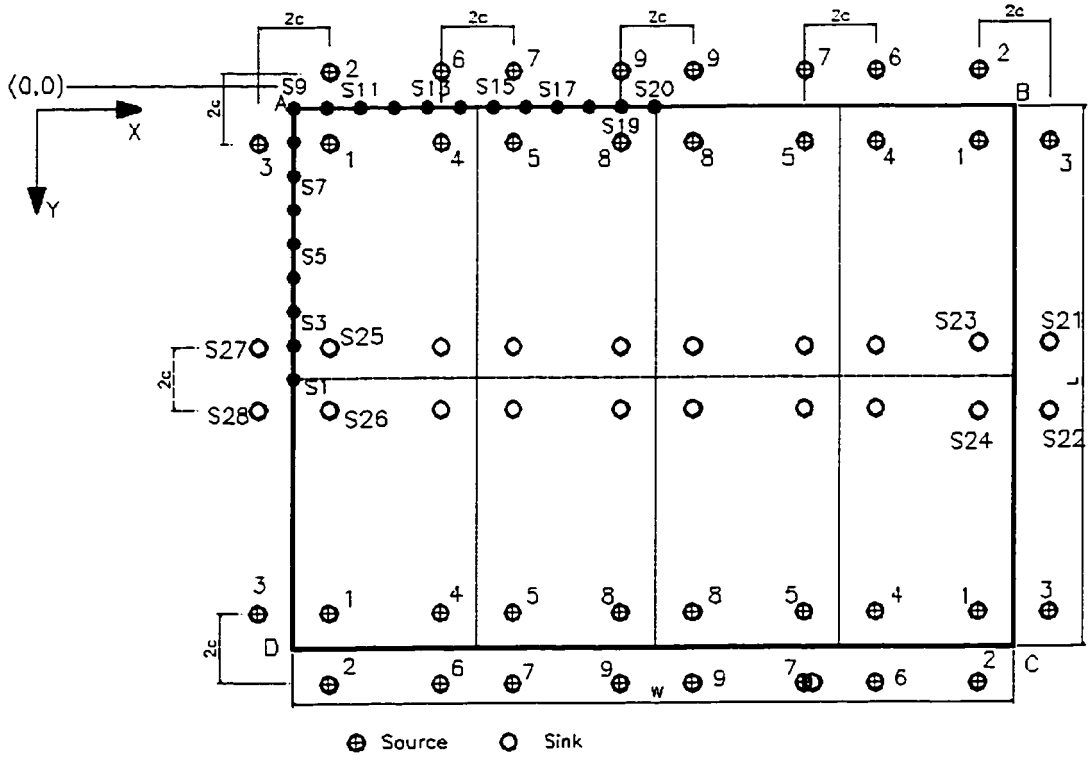

Fig. 5.10 4 Module B unit

5.7 Sampling

After the sandbox was fully saturated with water (5.7.3) for each module, the valve system was adjusted to provide the derived inflow to and from the wells. After running the system for 30 minutes, 15 ml of sample was collected from each sampling point – marked with capital letter S in Fig.5.6 –10. Following factors were measured,

1. Ambient temperature;
2. Water temperature;
3. TDS (total dissolved solids) of samples.

In experiments of module B, 3moduleB and 4 Module B , the flow rate of each image sink (S21,22,27,28) were measured to computer leakage using mass balance .

Between experiments, sand in the sandbox was thoroughly washed by injecting tap water through whole section for 1 hour. Five samples were taken from points locates in both center and four corners of the sandbox to measure its TDS (total dissolved solids) which indicates whether or not the sandbox was reset to "original" condition- that is TDS of those samples were as nearly same as that of tap water. If this is not the case, washing was continue.

CHAPTER SIX

Results and Analysis

6.1 Parameters

The parameters and their range in the experiments are provided in Table 6.1 .

Table 6.1 : Parameters for the experiments T = 20 °C ± 1 °C

Parameter	Symbol	Value	Units
Tap water density	ρ_w	1000	$kg \cdot m^{-3}$
Salt solution density	ρ_s	1050	$kg \cdot m^{-3}$
Sandbox cross sectional area	A	6.22×10^{-2}	m^2
Mean particle diameter	d_P	1.5×10^{-3}	m
Dynamic viscosity of Water	ν_W	1.003×10^{-6}	m^2/s

6.2 Hydraulic Conductivity

Estimation of the bulk hydraulic conductivity (K) of the soil matrix was an essential first step in characterizing the site and subsequently in determining the expected flux for the treatment system. Hydraulic conductivity testing is usually carried out using falling head and static head methods .

Estimation of hydraulic conductivity from grain size can also be undertaken using Hazen's formula:

$$K = C\, d_{10}^2 \qquad (6.1)$$

where:

d_{10} = the effective grain size diameter in centimeter and is defined as the value where 10% of the particles are finer and 90% coarser by weight;

C varies from 100 to 150 cm/s depending on the material; and,

K = hydraulic conductivity in cm/s.

Representative samples collected from commercial sand yielded laboratory measured effective grain sizes of 0.071 and 0.236 cm. Substituting the average value of 0.1 cm into the formula and using a value of 140 (pure sand) for C, yields hydraulic conductivities of 2.56 cm/s. This calculated value was more in keeping with expectations and was thus considered a reasonable approximation of hydraulic conductivity.

Static water level method was applied in lab testings. These tests were performed by measuring the static water level upstream and downstream of the sandbox . Water flow rate was maintained at a constant value across the measurement sections. Darcy law yields,

$$Q = -KA\frac{dh}{ds} \qquad (6.2)$$

Where

Q = the flow rate

A = the gross area of flow path

$\frac{dh}{ds}$ = the piezometric gradient along the flow path

K = hydraulic conductivity

Thus,

$$K = -Q\frac{ds}{Adh}$$

Measured Q is 2.25L/min - 37.5 cm^3/s , A = 622 cm^2, Ds is 59.1 cm and measured dh is −1.4 cm,

$$K = -Q\frac{ds}{Adh} = 2.53 \text{ cm/s}$$

This matches well with what is calculated by the Hazen formula .

6.3 Reynolds number

The expressions used in Chapter 4 and the whole experiments are valid only for laminar flow. Darcy's law and the calculation and Darcy velocity are valid for Reynolds number(N_R) close to 1(Bedient et al. 1994) or in the adaptive range of 1-10 . Darcy velocity(q_A) is defined here as the flow rate through the sandbox cross section, which is expressed as : q_A = Q/A. For flow in porous media, the dimensionless Reynolds number can be expressed as follows:

$$N_R = \frac{q_A d_P}{\nu_W} \qquad (6.3)$$

Darcy's law is valid for most ground water systems. However, the Reynolds number should be calculated for the highest flow rate (3.6L/min) which occurs in the 4 module B experiment. Using the information provided in Table 6.1, N_R at 3.6L/min is 1.44. This is slightly above the normal laminar range and is the adaptive range.

6.4 Results

The data tables compiled for the modules are located in Appendix B. Experimental procedures and sampling points for each module are provided in Chapter 5.

6.4.1 Boundary conditions

Figure 6.1 to Figure 6.5 show the measured TDS of samples along the X and Y axis(from corner A) includes both with and without image wells conditions for each module.

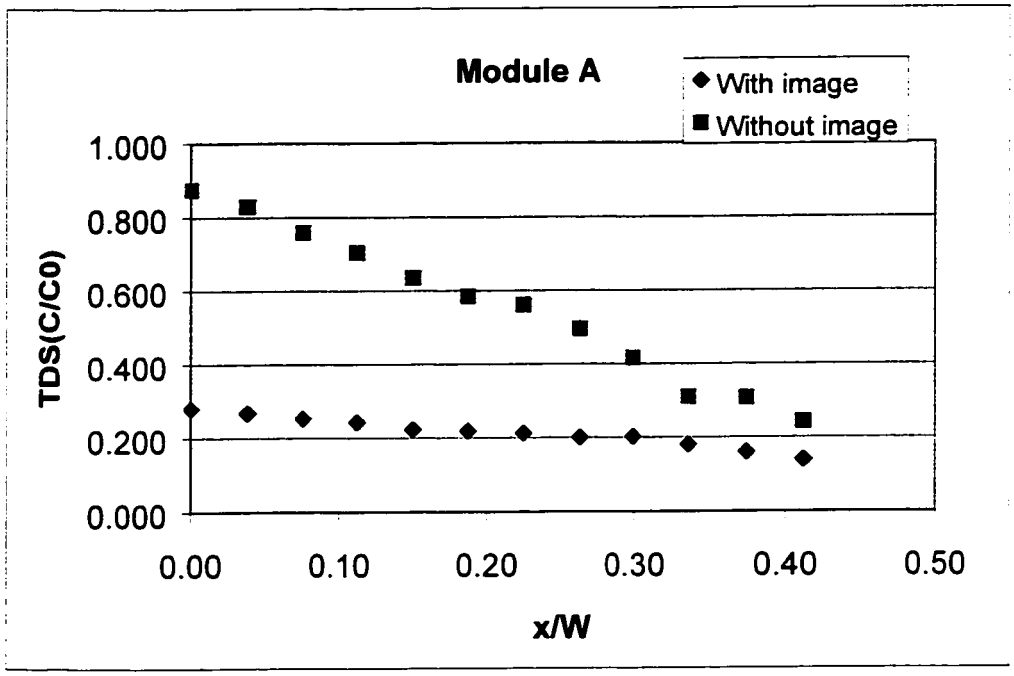

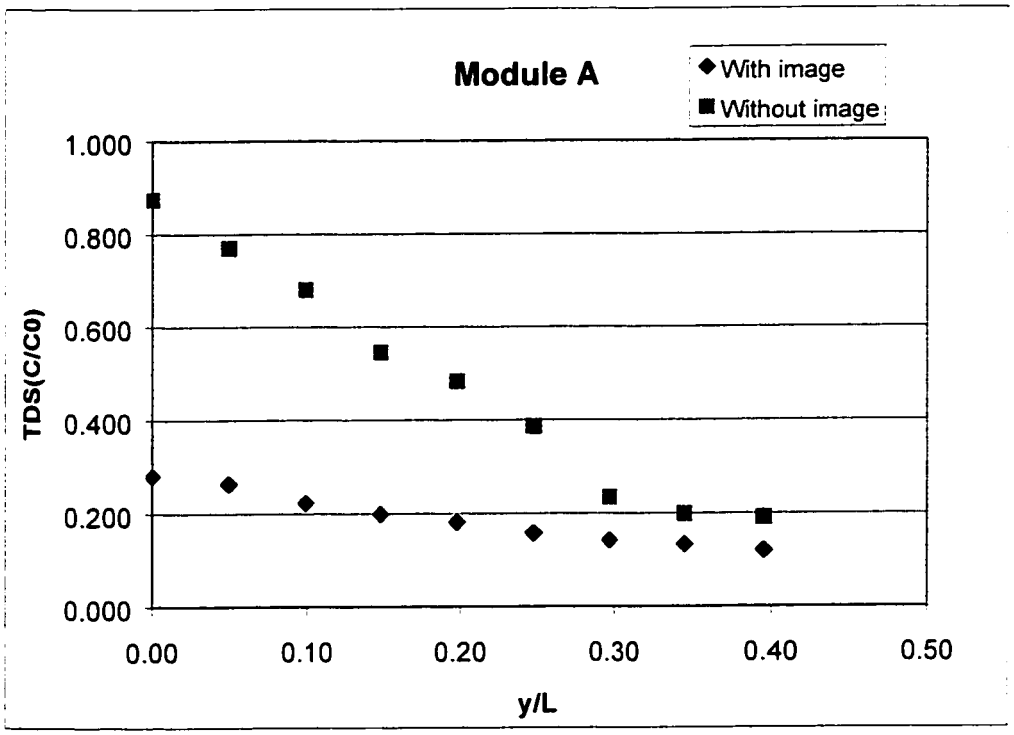

Figure 6.1 Module A variation of TDS (C/C_0) along the boundary

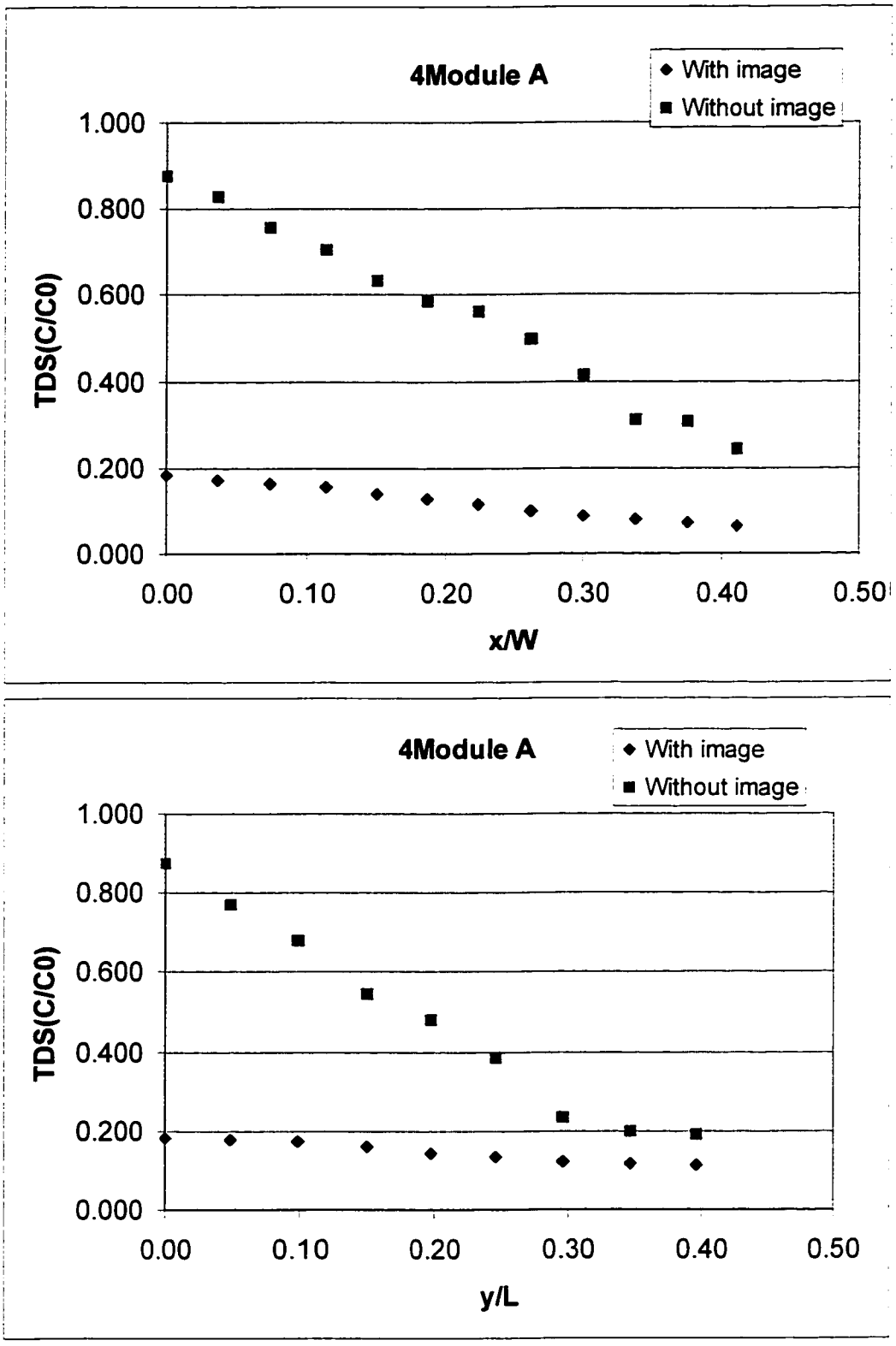

Figure 6.2 4Module A Variation of TDS (C/C_0) along the boundary

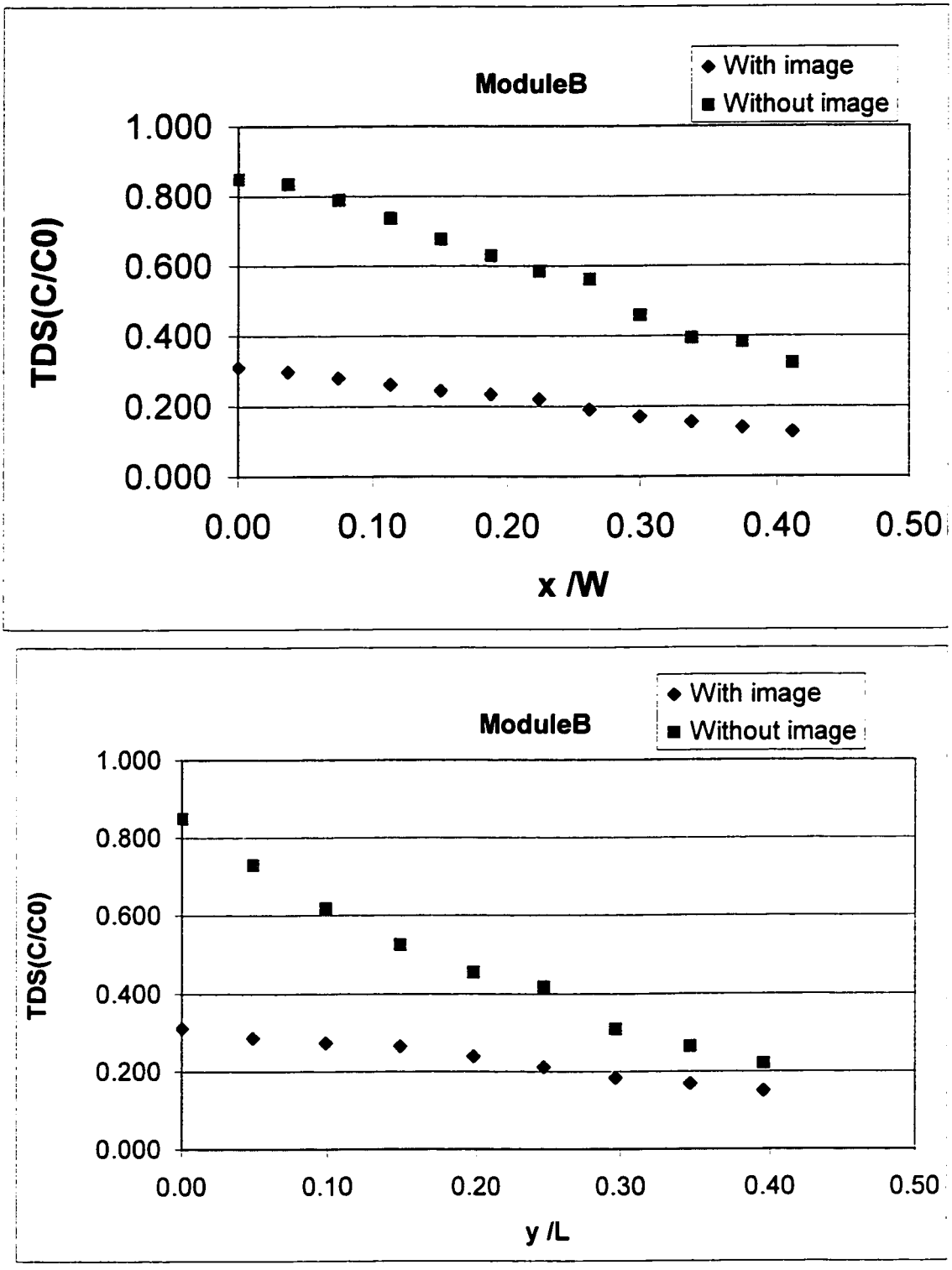

Figure 6.3 Module B Variation of TDS (C/C_0) along the boundary

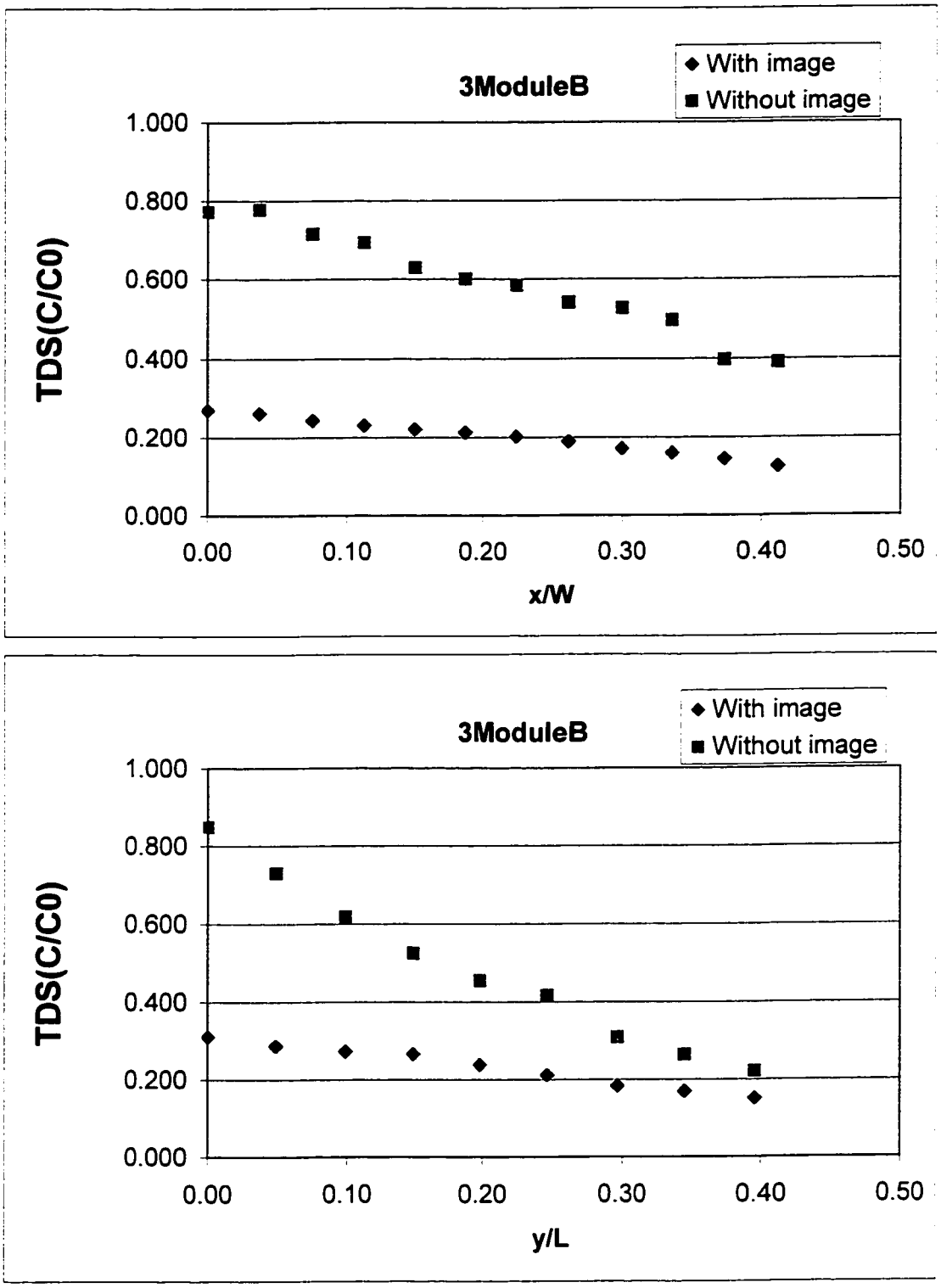

Figure 6.4 3 Module B Variation of TDS (C/C_0) along the boundary

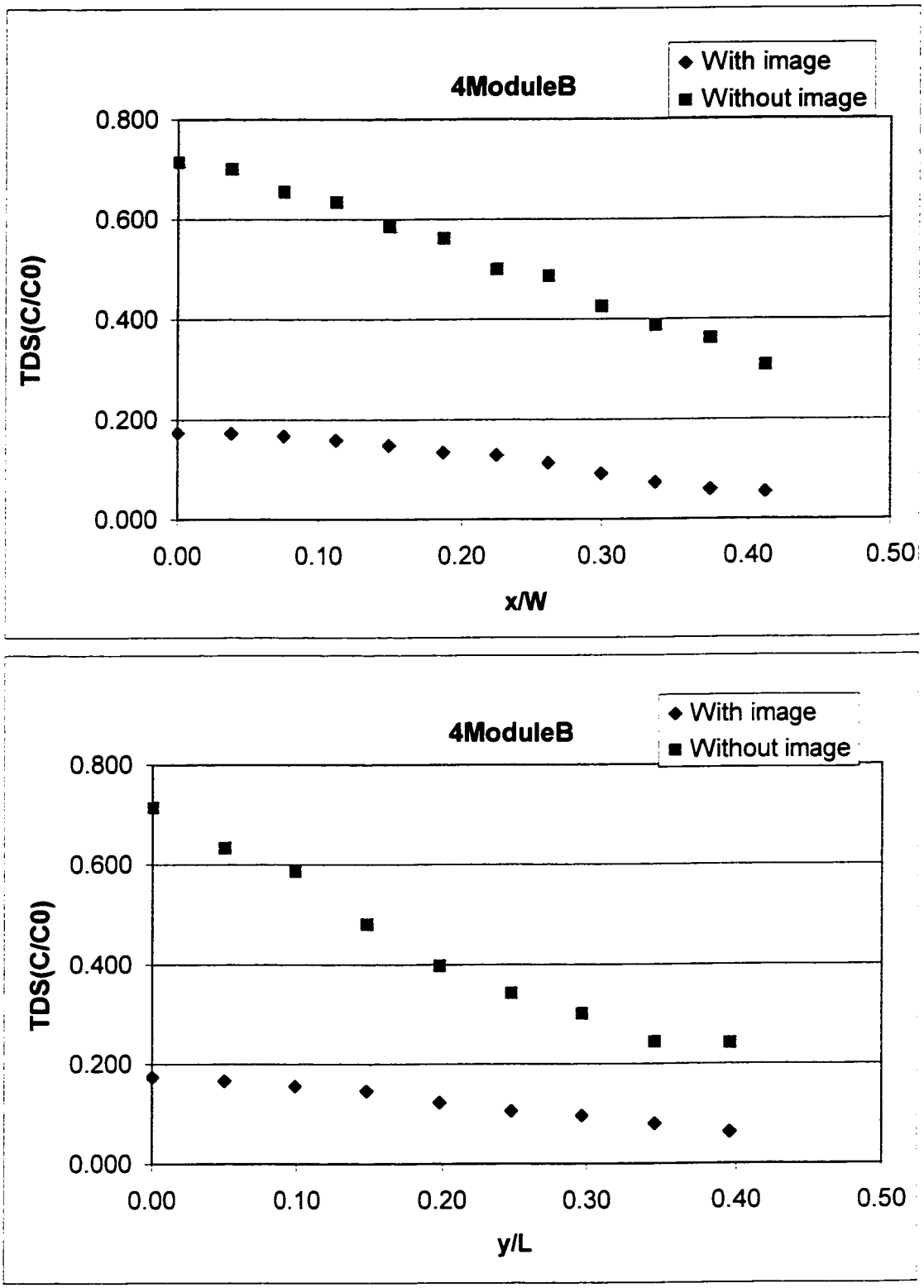

Figure 6.5 4 Module B Variation of TDS (C/C_0) along the boundary

6.4.2 Number of modules

The number of module B and the corresponding C/C_0 values are shown in Figure 6.6 . Here, C_0 is the concentration (TDS) of salt solution injected and C is the median concentration (TDS) of samples that were taken outside defined boundary(ABCD) for each module- Module B, 3 Module B and 4Module B, sampling points were S21,22,27,28. As we can find from figure 5.8 – 5.10, those samples were taken outside boundary ABCD from same locations for each module.

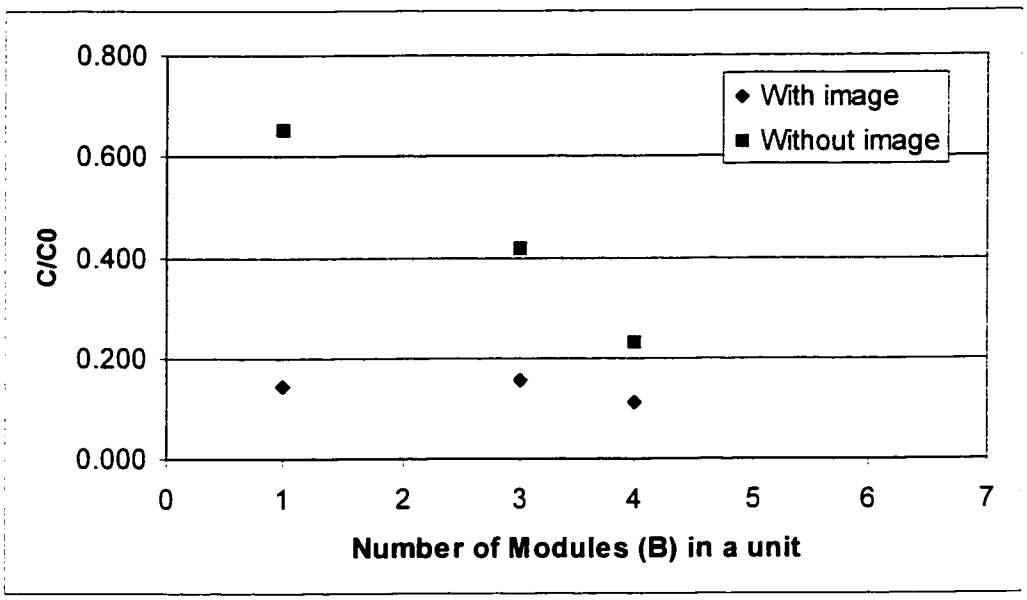

Figure 6.6 C/C_0 Vs number of modules

6.5 Analysis

6.5.1 Boundary

As shown in Figure 6.1 ,6.2,6.3,6.4 and 6.5, in the experiments, applying the image wells outside the boundary ABCD distinctly decreases the salt solution concentration along the boundary. Moreover, the concentration can be further decreased by increasing the image wells(or modules) . This is due to the follows,

1. The introducing of image wells into the system provides a hydraulic barrier that confines the movement of injected salt solution;
2. The injected water from image wells outside boundary flows along and across the boundary and this dilutes the salt solution.

The modules with image wells and corresponding boundary conditions are showed in Figure 6.7.

6.5.2 Leakage calculation for module B(s) with image wells

To evaluate the leakage in moduleB(s) experiments with image wells, calculations were performed based on measured TDS and flow rate of each sampling points(same as 6.4.2, data were provided in Appendix B). The calculation can be performed using the following equation,

$$L = \frac{\sum_{i=1}^{n} C_i Q_i}{\sum_{j=1}^{m} C_j Q_j} + E_{ij} \qquad (6.4)$$

where

L = leakage as a fraction of total mass input,

C_i = TDS of samples from discharge wells outside boundary

Q_i = flow rate of discharge wells outside boundary

C_j = TDS of salt solution

Q_j = flow rate of salt solution injection wells inside boundary

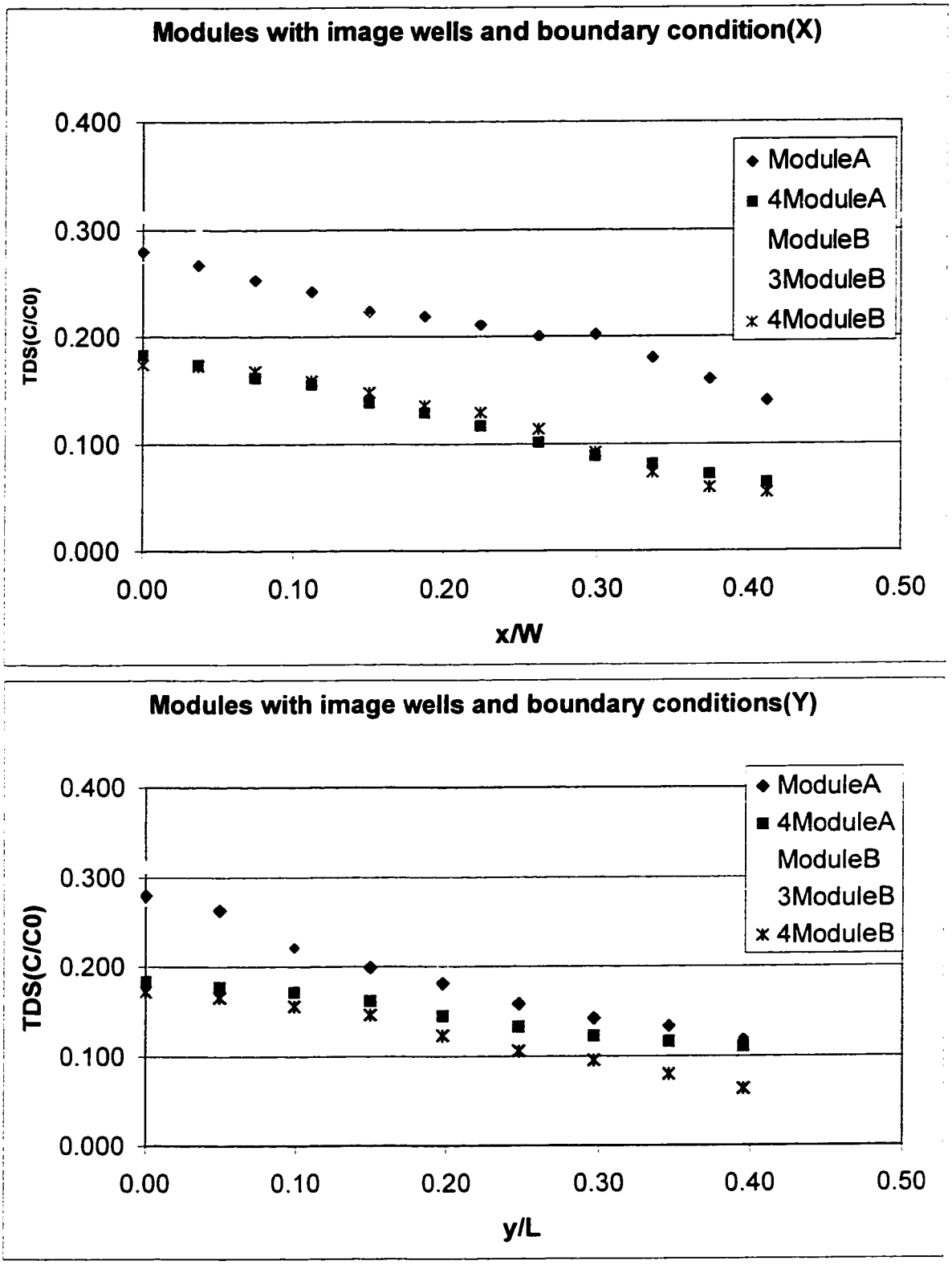

Figure 6.7 Modules with image wells and Variation of TDS (C/C_0) along the boundary

E_{ij} = leakage from other positions than the sampling points

As shown in Figure 6.7, in experiments of moduleB(s) with image wells, the TDS value(C/C_0) along the boundary follows the sequence ,

ModuleB > 3ModuleB>4ModuleB

The E_{ij} value will follow the same sequence. This matches the theoretical prediction of more modules results less leakage. Herein one can use first item of right side of equation6.4 as an approximate approach to calculate the leakage outside the defined boundary. Figure 6.8 show the relation of theoretical calculation value for leakage ($\Delta Q/Q$) and leakage calculation which is done by above equation from experimental results.

6.6 Source of Error

The errors derives from two main sources in this study, the first one occurs because of limitation of measurements. All measurements contributes to some extent of errors. The second source of errors is attributed to the theoretical assumptions made in the module development.

In Chapter3 and Chapter4, it is stated that Darcy's law is valid and hydraulic-head gradients are the only significant driving mechanism for the fluid flow and that the

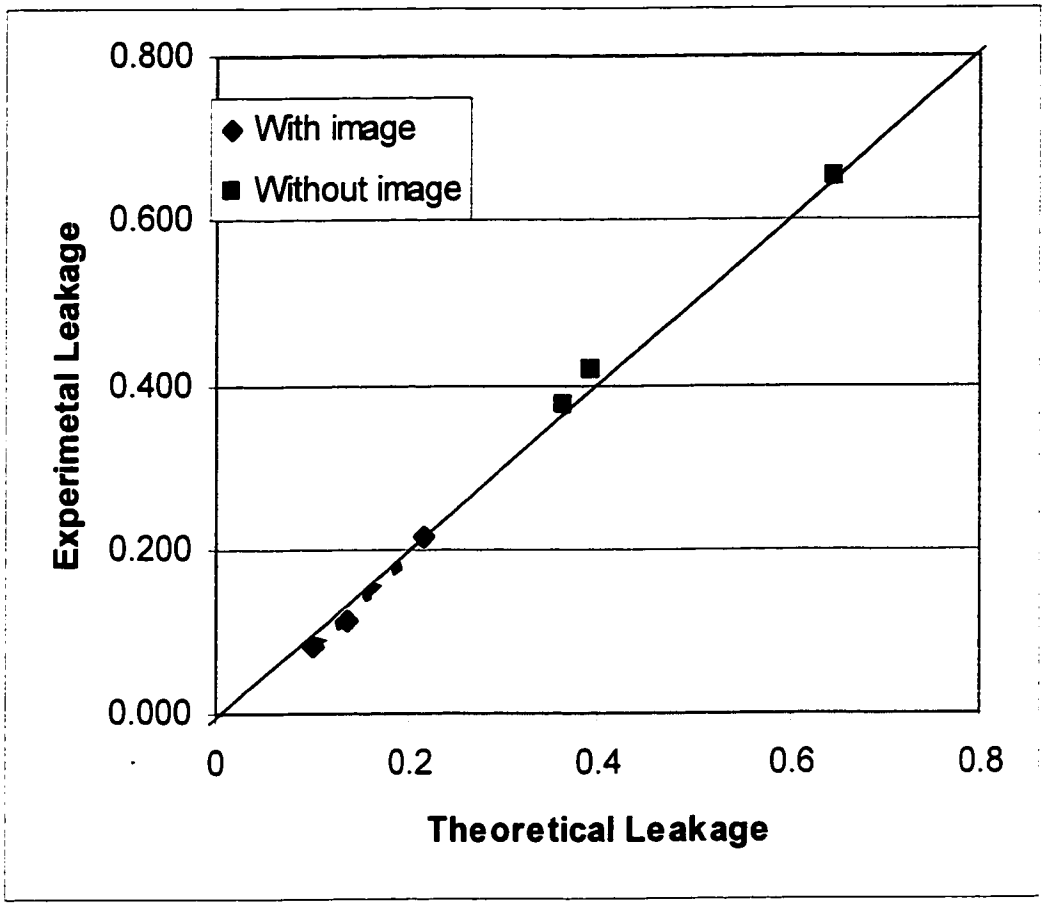

Figure 6.8 Theoretical results Vs Experimental results

gradients of fluid density, viscosity and ionic & molecular diffusion are negligible. Because of scale limitation in the lab demonstration unit-sandbox, the solid boundary does make an effect on the above factors which were assumed to extend to infinity in the theoretical calculation. This is less significant in those modules with image wells. Theoretical flow is assumed to occurs from a line source. In reality , the well has a finite thickness.

In the immediate vicinity of the wells, Darcy's law is not strictly valid as the Reynolds number is large. Hence, this may introduce some errors. However, this region is a very small fraction of the total region of interest

In field conditions, the presence of organic material, inhomogeneity of contaminant distribution, inhomogeneity in soil conditions, deviation from two dimensional flow conditions can alter the predicted flow behaviors. Ideally, as stated earlier, the presence of a nearly impermeable lower of soil/rock layer ensures that flow is mainly in the lateral distributions. The presence of some organic can distort the results due to high adsorption rates of chemicals.

CHAPTER SEVEN

Summary, Conclusions and Recommendations

The studies conducted to examine the effectiveness of applying hydrodynamic barrier for improving the containment efficiency of chemical enhanced pump and treat system by means of both theoretical modeling and lab experiments. The model and the experimental design developed for the present study provides a basic analytical tool for the real world problems. The conclusion of the present study can be summarized as follows:

- The mathematical models developed indicated that the hydraulic barriers are effective in reducing leakage of chemicals from targeted site duringpump and treat operations;
- Test results qualitatively confirmed the fact that hydraulic barriers do reduce the leakage considerably ;
- For large sites, dummy end units of pure water well system modules such as 4 modules B or its variations can reduce the leakage even further.
- The effectiveness of the proposed system in the field is closely related to the assumptions such as the presence of impermeable lower layer and the homogeneity of pollution distribution in the site ;
- Hydraulic barriers are easy to construct and dismantle;
- Image wells can be taken as monitoring wells of the clear up operations.

When applying the model developed in this study for a real world problem. one should be carefully to review all assumptions which were made.

For future work, a few recommendations are given below,

1. This study will be useful to a three-dimensional model since the actual site conditions tend to be closer to three-dimensional conditions;
2. Actual chemicals such as surfactants may be used to study the effectiveness of image wells in the pump and treat schemes used for decontamination of soil and groundwater;
3. The effect of non- homogeneity of contaminant(s) may be studied by using soil artificially contaminated to reflect non- homogeneity;
4. Other module systems can be studied for their effectiveness;

References

Andrew , Duffield, 2001. "Surfactant enhanced mobilisation of non-aqueous phase liquids ." Thesis (M.A.Sc.)--Dept. of Building, Civil, and Environmental Engineering, Concordia University.

Bear, J., 1979. "Hydraulics of groundwater", Mc Graw-Hill, N.Y.

Bedient, P.B., Rifai, H.S. and Newell, C.J., 1994. "Groundwater contamination", Prentice Hall, NY.

Borden, R.C., et al., " Modeling Ground water Transport at Conroe Creosote Waste Site." Proceedings of the Second International Conference on Ground Water Quality Research, OK, 1984, PP. 88-90

Carl D. Palmer and William Fish, 1992. "Chemical Enhancements to Pump-and-Treat Remediation." EPA/540/S-92/001

Cohen, R.M., A.H. Vincent, J.W. Mercer, C.R. Faust, and C.P. Spalding. 1994. "Methods for Monitoring Pump-and-Treat Performance." EPA/600/R-94/123. R.S. Kerr Environmental Research Laboratory, Ada, OK. 102 pp.

Dwyer, B.P. 1998. "Treatment of Mixed Contamination in Complex Hydrogeologic Settings." Sandia National Laboratories.

Gorelick, S.M., R.A. Freeze, D. Donohue, and J.F. Keely. 1993. "Groundwater Contamination: Optimal Capture and Containment." Lewis Publishers: Boca Raton, FL. 416 pp.

Gupta, H.S., 1993. "Modeling the effectiveness of barriers for improving the hydraulic efficiency of a pump and treat system utilizing chemical agents"- Thesis submitted in partial fulfillment for the M.Sc. degree at the University of Oklahoma.

Heiser, J.H. and B. Dwyer. 1997. "Summary Report on Close-Coupled Subsurface Barrier Technology Initial Field Trials to Full-Scale Demonstration." Brookhaven National Laboratory, BNL-52531.

Keeley, J.F., 1984. "Optimizing pumping strategies for contaminant studies and remedial actions", Fourth national symposium on aquifer restoration and groundwater monitoring, Columbus.

Konikow, L.F., and Bredehoeft, J.D., 1978. "Computer Model of Two-Dimensional Solute Transport and Dispersion in Groundwater", Techniques of Water Resources Investigations, U.S. Geological Survey, Chapter C2, Book7, U.S. Government Printing Office, Washington, D.C., PP1-20.

Knox, R.C., 1983. "Effectiveness of impermeable barriers for retardation of pollutant migration", National conference on management of uncontrolled hazardous waste sites. Washington D.C..

Lauryn Strbak , 2000. "In situ flushing with surfactants and cosolvents," Advanced Applied Technology Development Facility (AATDF) at Rice University

http://www.clu-in.org

Leslie Pearlman, 1999. "Subsurface Containment and Monitoring Systems: Barriers and Beyond." National Network of Environmental Management Studies Fellow for U.S. Environmental Protection Agency.

Mercer, J.W., Skipp D. and Giffin D. 1990. "Basics of pump-and-treat ground-water remediation technology." EPA – 600/8 – 90/003, USEPA Office of research and development, Ada, OK.

Mutch, R.D., R.E. Ash, and J.R. Caputi. 1997. "Contain Contaminated Groundwater." Chemical Engineering, Vol. 104, No. 5, pp. 114-119.

Ozbilgin, M. and Powers, M.A., 1984. "Hydrodynamic isolation in hazardous waste containment", Fourth national symposium on aquifer restoration and groundwater monitoring, Columbus.

Palmer, C.D. and Fish, W., 1992. "Chemical enhancements to pump and treat remediation". EPA Groundwater issue, Report No. EPA/540/S-92/001.

Remson, I., Hornberger, G.M., and Molz, F.J., 1971. " Number Methods in Subsurface Hydrology." John Wiley and Sons, New York, NY.

Richard A. Gordon.1996. "Waging The War Against DNAPLs." Applied Science & Technology, Inc. (ASTI).

Rumer, R.R. and M.E. Ryan, eds. 1995. "Barrier Containment Technologies for Environmental Remediation Applications." Product of the International Containment Technology Workshop. John Wiley and Sons, Inc., New York.

Rumer, R.R. and J.K. Mitchell, eds. 1996. "Assessment of Barrier Containment Technologies A Comprehensive Treatment for Environmental Remedial Application." Product of the International Containment Technology Workshop. National Technical Information Service, PB96-180583.

Sabatini, D.A., Knox, R.C and Harwell, J.H., 1995. "Surfactant enhanced subsurface remediation". Am. Chem. Society.

Smyth, D.J.A., J.A. Cherry, and R.J. Jowett. 1995. "Sealable Joint Steel Sheet Piling (Waterloo Barrier™) for Groundwater Pollution Control." Presented at the International Containment Technology Workshop, Baltimore, Md.

Trescott, P.C., Pinder, G.F., and Larson, S.P., 1976. " Finite Difference Model for Aquifer Simulation in Two-Dimensions with Results of Numerical Experiments.", Techniques of Water Resources Investigation Book , U.S. Geological Survey, ChapterC1.

Valentine, H.R., 1969. "Applied hydrodynamics". – Butterworths.

Wilson, J.L., 1984. "Double-cell hydraulic containment of a pollutant plume", Fourth national symposium on aquifer restoration and groundwater monitoring, Columbus.

Advanced Applied Technology Development Facility (AATDF). Technology Practices Manual for Surfactants and Cosolvents. Rice University. Houston, Texas

Sullivan, T.M., J. Heiser, A. Gard, and G. Senum. 1998. "Monitoring Subsurface Barrier Integrity Using Perfluorocarbon Tracers." Journal of Environmental Engineering, Vol. 124, No. 6, pp. 490-497.

Global Environment and Technology Foundation (GETF). 1996. "Market Assessment Protective Underground Barrier Technologies." prepared for the U.S. Department of Energy.

Golder Associates Inc., 1994. "Preliminary Results of Permeation Tests using Montan Wax and Sodium Silicate Barrier Materials in Unconsolidated Soils at the Mixed Waste Landfill Integrated Demonstration Site (MWLID)." Report number 913-1248.600b. Groundwater Control Inc.

U.S. Environmental Protection Agency. 1998. "Evaluation of Subsurface Engineered Barriers at Waste Sites." EPA 542/R-98/005

U.S. Environmental Protection Agency. 1987. "Construction Quality Control and Post-Construction Performance Verification for the Gilson Road Hazardous Waste Site Cutoff Wall." EPA 600/2-87/065.

U.S. Environmental Protection Agency. 1993. "Quality Assurance and Quality Control for Waste Containment Facilities." EPA 600/R-93/182.

U.S. Environmental Protection Agency. 1992. "Construction Quality Management for Remedial Action and Remedial Design Waste Containment Systems." EPA 540/R-92/073.

U.S. Environmental Protection Agency. 1987. "Construction Quality Control and Post-Construction Performance Verification for the Gilson Road Hazardous Waste Site Cutoff Wall." EPA 600/2-87/065.

APPENDIX A :

Sample calculation

Partial calculation of leakage in 4 module A. Paste from Excel file.

Param.	W =	813	No. rows =	6	c =	35		
	L =	610	No.col. n =	6				
	Real W =	8	No. wells=	32				
			Aij	36				
						LEAK - v	y = c =	29.5
							x1 =	x2 =
			Sign				10	100.2
Aij	Xi	Yi	Sc/Sk	F/final	y-Yi		Ix1	Ix2
A11	0	669	0	0	-639.5		0	0
A12	59	669	1	15.9155	-639.5		1.217105	-1.02395
A13	406.5	669	-1	-15.9155	-639.5		-8.83321	-7.10915
A14	465.5	669	-1	-15.9155	-639.5		-9.85037	-8.26006
A15	813	669	1	15.9155	-639.5		14.29628	13.36184
A16	872	669	0	0	-639.5		0	0
A21	0	610	1	15.9155	-580.5		-0.27414	-2.72037
A22	59	610	1	15.9155	-580.5		1.34025	-1.12768
A23	406.5	610	-1	-15.9155	-580.5		-9.53731	-7.72731
A24	465.5	610	-1	-15.9155	-580.5		-10.5889	-8.93934
A25	813	610	1	15.9155	-580.5		15.03787	14.12246
A26	872	610	1	15.9155	-580.5		15.56732	14.73661
A31	0	364	-1	-15.9155	-334.5		0.475658	4.632132
A32	59	364	-1	-15.9155	-334.5		-2.31495	1.950471
A33	406.5	364	1	15.9155	-334.5		13.84666	11.80005
A34	465.5	364	1	15.9155	-334.5		14.9189	13.20003
A35	813	364	-1	-15.9155	-334.5		-18.7181	-18.0168
A36	872	364	-1	-15.9155	-334.5		-19.1087	-18.4911
A41	0	305	-1	-15.9155	-275.5		0.577442	5.551793
A42	59	305	-1	-15.9155	-275.5		-2.80141	2.362595
A43	406.5	305	1	15.9155	-275.5		15.33536	13.34177
A44	465.5	305	1	15.9155	-275.5		16.34256	14.71593
A45	813	305	-1	-15.9155	-275.5		-19.7399	-19.1301
A46	872	305	-1	-15.9155	-275.5		-20.0766	-19.5432
A51	0	59	1	15.9155	-29.5		-5.20161	-20.4431
A52	59	59	1	15.9155	-29.5		16.3751	-15.1102
A53	406.5	59	-1	-15.9155	-29.5		-23.8181	-23.4719
A54	465.5	59	-1	-15.9155	-29.5		-23.9707	-23.7175
A55	813	59	1	15.9155	-29.5		24.41558	24.3417
A56	872	59	1	15.9155	-29.5		24.45555	24.39198
A61	0	0	0	0	29.5		0	0
A62	59	0	1	15.9155	29.5		-16.3751	15.11017
A63	406.5	0	-1	-15.9155	29.5		23.81806	23.47189
A64	465.5	0	-1	-15.9155	29.5		23.9707	23.71753
A65	813	0	1	15.9155	29.5		-24.4156	-24.3417
A66	872	0	0	0	29.5		0	0
							6.365708	**1.635549**
							-4.73016	

= 15.9155* $\tan^{-1}$ ((10-59)/-639.5)

= 15.9155* $\tan^{-1}$ ((100.2-59) /-639.5)

Sample calculation of leakage in module B – with image wells. Data used here can be found in Appendix B –3 .

Leakage measured from points (S21,22,27,28) outside targeted site ABCD,

Leakage = 897 ppm * 0.182l/min + 903 ppm* 0.176l/min + 921ppm * 0.179 l/min + 935 ppm * 0.181l/min

= 656.3 mg/min

Total salt injected to the unit

= 5100ppm * 0.6l/min =3060 mg/min

Leakage in percentage

= (656.3 mg/min / 3060 mg/min) * 100%

= 21.45 %

APPENDIX B :

Experimental results

Module A experiment data sheet

Trial No.1 T = 20 °C Twater = 20°C

Number of real wells: 2 source + 2 sink

Number of image wells: 4 source + 4 sink

Total water flow rate = 1L/min

Total salt solution flow rate = 0.5L/min

Point	Coordinate				Sampling Vol.(ml)	TDS(PPM)			
	x(mm)	X/W	y(mm)	Y/L		Without image	C/C0	With image	C/C0
S1	0	0.00	241	0.40	15	975	0.191	613	0.120
S2	0	0.00	211	0.35	15	1014	0.199	679	0.133
S3	0	0.00	181	0.30	15	1196	0.235	724	0.142
S4	0	0.00	151	0.25	15	1967	0.386	806	0.158
S5	0	0.00	121	0.20	15	2460	0.482	923	0.181
S6	0	0.00	90	0.15	15	2780	0.545	1014	0.199
S7	0	0.00	60	0.10	15	3470	0.680	1134	0.222
S8	0	0.00	30	0.05	15	3930	0.771	1341	0.263
S9	0	0.00	0	0.00	15	4460	0.875	1426	0.280
S10	30	0.04	0	0.00	15	4230	0.829	1362	0.267
S11	60	0.07	0	0.00	15	3870	0.759	1287	0.252
S12	90	0.11	0	0.00	15	3590	0.704	1235	0.242
S13	121	0.15	0	0.00	15	3240	0.635	1135	0.223
S14	151	0.19	0	0.00	15	2980	0.584	1112	0.218
S15	181	0.22	0	0.00	15	2860	0.561	1079	0.212
S16	211	0.26	0	0.00	15	2530	0.496	1021	0.200
S17	241	0.30	0	0.00	15	2120	0.416	1031	0.202
S18	271	0.34	0	0.00	15	1576	0.309	920	0.180
S19	302	0.37	0	0.00	15	1564	0.307	812	0.159
S20	332	0.41	0	0.00	15	1236	0.242	711	0.139
S21	296	0.37	-30	-0.05	15	3330	0.653	976	0.191
S22	355	0.44	-30	-0.05	15	3470	0.680	1107	0.217
S23	621	0.77	-30	-0.05	15	2650	0.520	1378	0.270
S24	681	0.85	30	0.05	15	2730	0.535	1458	0.286
S25	-30	-0.04	452	0.74	15	2710	0.531	1560	0.306
S26	30	0.04	513	0.84	15	2540	0.498	1654	0.324
S27	296	0.37	513	0.84	15	3270	0.641	1257	0.246
S28	355	0.44	513	0.84	15	3340	0.655	1143	0.224
S29	621	0.77	30	0.05	15	2930	0.575	2750	0.539
S30	30	0.04	452	0.74	15	2890	0.567	2470	0.484
Tap water	na		na		15	190			
Salt solution	na		na		15	5100			

4 Module A experiment data sheet

Trial No.1 T = 20 °C Twater = 20°C

Number of real wells: 8 source + 8 sink

Number of image wells: 8 source + 8 sink

Total water flow rate = 1.2L/min,

Total salt solution flow rate = 1.2L/min

Point	Coordinate				Sampling Volume(ml)	TDS(PPM)			
	x(mm)	X/W	y(mm)	Y/L		Without image	C/C0	Wth image	C/C0
S1	0	0.00	241	0.40	15	877	0.172	565	0.111
S2	0	0.00	211	0.35	15	1035	0.203	592	0.116
S3	0	0.00	181	0.30	15	1265	0.248	622	0.122
S4	0	0.00	151	0.25	15	1768	0.347	675	0.132
S5	0	0.00	121	0.20	15	2150	0.422	738	0.145
S6	0	0.00	90	0.15	15	2750	0.539	823	0.161
S7	0	0.00	60	0.10	15	3160	0.620	873	0.171
S8	0	0.00	30	0.05	15	3690	0.724	902	0.177
S9	0	0.00	0	0.00	15	4280	0.839	934	0.183
S10	30	0.04	0	0.00	15	4330	0.849	882	0.173
S11	60	0.07	0	0.00	15	4220	0.827	823	0.161
S12	90	0.11	0	0.00	15	3970	0.778	794	0.156
S13	121	0.15	0	0.00	15	3650	0.716	703	0.138
S14	151	0.19	0	0.00	15	3320	0.651	657	0.129
S15	181	0.22	0	0.00	15	2820	0.553	595	0.117
S16	211	0.26	0	0.00	15	2470	0.484	516	0.101
S17	241	0.30	0	0.00	15	2230	0.437	451	0.088
S18	271	0.34	0	0.00	15	2060	0.404	415	0.081
S19	302	0.37	0	0.00	15	1460	0.286	367	0.072
S20	332	0.41	0	0.00	15	230	0.045	322	0.063
S21	296	0.37	-30	-0.05	15	1867	0.366	451	0.088
S22	355	0.44	-30	-0.05	15	1696	0.333	460	0.090
S23	-30	-0.04	211	0.35	15	1546	0.303	435	0.085
S24	-30	-0.04	271	0.45	15	1761	0.345	442	0.087
S25	-30	-0.04	211	0.35	15	2542	0.498	471	0.092
S26	30	0.04	271	0.45	15	2653	0.520	475	0.093
S27	296	0.37	271	0.45	15	1341	0.263	448	0.088
S28	355	0.44	271	0.45	15	1267	0.248	451	0.088
S29	-30	-0.04	211	0.35	15	3320	0.651	253	0.050
S30	30	0.04	271	0.45	15	3410	0.669	248	0.049
S31	296	0.37	30	0.05	15	3560	0.698	238	0.047
S32	355	0.44	30	0.05	15	3580	0.702	227	0.045
S33	621	0.77	211	0.35	15	3170	0.622	239	0.047
S34	621	0.77	271	0.45	15	3140	0.616	242	0.047
S35	296	0.37	452	0.74	15	3250	0.637	267	0.052
S36	355	0.44	452	0.74	15	3270	0.641	279	0.055
Tap water	na	na	na	na	15	190			
Salt solution	na	na	na	na	15	5100	=C0		

Module B experiment data sheet

Trial No.1 T = 20 °C Twater = 20°C

Number of real wells: 4 source + 4 sink

Number of image wells: 8 source + 4 sink

Total water flow rate = 1.2L/min

Total salt solution flow rate = 0.6L/min

Point	Coordinate				Sampling Vol.(ml)	TDS(PPM)		Flow rate(L/min)	TDS(PPM)		Flowrate (L/min)
	x(mm)	X/W	y(mm)	Y/L		Without image	C/C0	na	With image	C/C0	na
S1	0	0.00	241	0.40	15	1126	0.221	na	772	0.151	na
S2	0	0.00	211	0.35	15	1353	0.265	na	863	0.169	na
S3	0	0.00	181	0.30	15	1579	0.310	na	938	0.184	na
S4	0	0.00	151	0.25	15	2130	0.418	na	1076	0.211	na
S5	0	0.00	121	0.20	15	2320	0.455	na	1217	0.239	na
S6	0	0.00	90	0.15	15	2680	0.525	na	1354	0.265	na
S7	0	0.00	60	0.10	15	3150	0.618	na	1395	0.274	na
S8	0	0.00	30	0.05	15	3720	0.729	na	1463	0.287	na
S9	0	0.00	0	0.00	15	4330	0.849	na	1589	0.312	na
S10	30	0.04	0	0.00	15	4260	0.835	na	1524	0.299	na
S11	60	0.07	0	0.00	15	4020	0.788	na	1432	0.281	na
S12	90	0.11	0	0.00	15	3760	0.737	na	1337	0.262	na
S13	121	0.15	0	0.00	15	3450	0.676	na	1246	0.244	na
S14	151	0.19	0	0.00	15	3210	0.629	na	1198	0.235	na
S15	181	0.22	0	0.00	15	2980	0.584	na	1125	0.221	na
S16	211	0.26	0	0.00	15	2860	0.561	na	973	0.191	na
S17	241	0.30	0	0.00	15	2340	0.459	na	875	0.172	na
S18	271	0.34	0	0.00	15	2010	0.394	na	792	0.155	na
S19	302	0.37	0	0.00	15	1956	0.384	na	714	0.140	na
S20	332	0.41	0	0.00	15	1650	0.324	na	652	0.128	na
S21	681	0.85	211	0.35	15	3020	0.592	na	897	0.139	0.182
S22	681	0.85	271	0.45	15	3230	0.633	na	903	0.142	0.176
S23	621	0.77	211	0.35	15	4830	0.947	0.15	1335	0.262	na
S24	621	0.77	271	0.45	15	4760	0.933	0.15	1387	0.272	na
S25	30	0.04	211	0.35	15	4770	0.935	0.15	1365	0.268	na
S26	30	0.04	271	0.45	15	4840	0.949	0.15	1312	0.257	na
S27	-30	-0.04	211	0.35	15	3640	0.714	na	921	0.142	0.179
S28	-30	-0.04	271	0.45	15	3410	0.669	na	935	0.146	0.181
Tap water	na	na	na	na	15	**190**					
Salt solution	na	na	na	na	15	**5100**					

3Module B experiment data sheet

Trial No.1 T = 20 °C Twater = 20°C

Number of real wells: 12 source + 12 sink

Number of image wells: 16 source + 4 sink

Total water flow rate = 1.6L/min

Total salt solution flow rate = 1.2L/min

Point	Coordinate				Sampling Vol.(ml)	TDS(PPM)		Flowrate(L/min)	TDS(PPM)		Flowrate(L/min)
	x(mm)	X/W	y(mm)	Y/L		Without image	C/C0	na	With image	C/C0	na
S1	0	0.00	241	0.40	15	1743	0.342	na	645	0.126	na
S2	0	0.00	211	0.35	15	1824	0.358	na	723	0.142	na
S3	0	0.00	181	0.30	15	1932	0.379	na	814	0.160	na
S4	0	0.00	151	0.25	15	2040	0.400	na	878	0.172	na
S5	0	0.00	121	0.20	15	2230	0.437	na	988	0.194	na
S6	0	0.00	90	0.15	15	2510	0.492	na	1110	0.218	na
S7	0	0.00	60	0.10	15	1840	0.361	na	1164	0.228	na
S8	0	0.00	30	0.05	15	3420	0.671	na	1275	0.250	na
S9	0	0.00	0	0.00	15	3940	0.773	na	1373	0.269	na
S10	30	0.04	0	0.00	15	3970	0.778	na	1328	0.260	na
S11	60	0.07	0	0.00	15	3650	0.716	na	1235	0.242	na
S12	90	0.11	0	0.00	15	3540	0.694	na	1176	0.231	na
S13	121	0.15	0	0.00	15	3210	0.629	na	1124	0.220	na
S14	151	0.19	0	0.00	15	3060	0.600	na	1085	0.213	na
S15	181	0.22	0	0.00	15	2980	0.584	na	1024	0.201	na
S16	211	0.26	0	0.00	15	2760	0.541	na	963	0.189	na
S17	241	0.30	0	0.00	15	2690	0.527	na	872	0.171	na
S18	271	0.34	0	0.00	15	2530	0.496	na	812	0.159	na
S19	302	0.37	0	0.00	15	2020	0.396	na	735	0.144	na
S20	332	0.41	0	0.00	15	1987	0.390	na	639	0.125	na
S21	681	0.85	211	0.35	15	2120	0.416	na	975	0.154	0.185
S22	681	0.85	271	0.45	15	2030	0.398	na	951	0.153	0.183
S23	621	0.77	211	0.35	15	4896	0.960	0.1	1735	0.340	na
S24	621	0.77	271	0.45	15	4966	0.974	0.1	1721	0.337	na
S25	30	0.04	211	0.35	15	4834	0.948	0.1	1654	0.324	na
S26	30	0.04	271	0.45	15	4865	0.954	0.1	678	0.133	na
S27	-30	-0.04	211	0.35	15	2200	0.431	na	977	0.156	0.181
S28	-30	-0.04	271	0.45	15	2170	0.425	na	962	0.161	0.180
Tap water	na	na	na	na	15	**190**					
Salt solution	na	na	na	na	15	**5100**					

4 Module B experiment data sheet

Trial No.1 T = 20 °C Twater = 20°C

Number of real wells: 16 source + 16 sink

Number of image wells: 20 source + 4 sink

Total water flow rate = 1.6L/min

Total salt solution flow rate = 1.2L/min

Point	Coordinate				Sampling Vol.(ml)	TDS(PPM)		Flowrate(L/min)	TDS(PPM)		Flowrate(L/min)
	x(mm)	X/W	y(mm)	Y/L		Without image	C/C0	na	With image	C/C0	na
S1	0	0.00	241	0.40	15	1231	0.241	na	322	0.063	na
S2	0	0.00	211	0.35	15	1243	0.244	na	407	0.080	na
S3	0	0.00	181	0.30	15	1536	0.301	na	486	0.095	na
S4	0	0.00	151	0.25	15	1747	0.343	na	537	0.105	na
S5	0	0.00	121	0.20	15	2030	0.398	na	626	0.123	na
S6	0	0.00	90	0.15	15	2450	0.480	na	745	0.146	na
S7	0	0.00	60	0.10	15	2990	0.586	na	794	0.156	na
S8	0	0.00	30	0.05	15	3230	0.633	na	845	0.166	na
S9	0	0.00	0	0.00	15	3640	0.714	na	883	0.173	na
S10	30	0.04	0	0.00	15	3570	0.700	na	875	0.172	na
S11	60	0.07	0	0.00	15	3340	0.655	na	852	0.167	na
S12	90	0.11	0	0.00	15	3230	0.633	na	807	0.158	na
S13	121	0.15	0	0.00	15	2980	0.584	na	751	0.147	na
S14	151	0.19	0	0.00	15	2860	0.561	na	684	0.134	na
S15	181	0.22	0	0.00	15	2550	0.500	na	657	0.129	na
S16	211	0.26	0	0.00	15	2480	0.486	na	576	0.113	na
S17	241	0.30	0	0.00	15	2170	0.425	na	465	0.091	na
S18	271	0.34	0	0.00	15	1974	0.387	na	371	0.073	na
S19	302	0.37	0	0.00	15	1843	0.361	na	303	0.059	na
S20	332	0.41	0	0.00	15	1567	0.307	na	274	0.054	na
S21	681	0.85	211	0.35	15	1321	0.259	na	903	0.115	0.140
S22	681	0.85	271	0.45	15	1247	0.245	na	883	0.120	0.143
S23	621	0.77	211	0.35	15	4942	0.969	0.15	1347	0.264	na
S24	621	0.77	271	0.45	15	4811	0.943	0.15	1370	0.269	na
S25	30	0.04	211	0.35	15	4837	0.948	0.15	1404	0.275	na
S26	30	0.04	271	0.45	15	4904	0.962	0.15	1410	0.276	na
S27	-30	-0.04	211	0.35	15	1023	0.201	na	875	0.105	0.141
S28	-30	-0.04	271	0.45	15	1131	0.222	na	907	0.102	0.141
Tap water	na	na	na	na	15	**190**					
Salt solution	na	na	na	na	15	**5100**					